

**The role of mTORC2 in mammary morphogenesis
and HER2-mediated tumorigenesis**

By

Meghan Morrison

Dissertation

Submitted to the Faculty of the Graduate
School of Vanderbilt University in partial
fulfillment of the requirements for the
degree of

DOCTOR OF PHILOSOPHY

in

Cancer Biology

August, 2015

Nashville, Tennessee

Approved:

Dr. Robert Matusik, Chair

Dr. Harold Moses

Dr. Jin Chen

Dr. Rebecca Cook, Advisor

I dedicate this to my ultimate source of inspiration - my favorite person, Greg Joly.

In loving memory of Arthur William Hunt Jr.

ACKNOWLEDGEMENTS

I owe my training, my success and my sanity throughout graduate school to more people than I can list here, but I will try anyway. First, I want to thank my mentor, Dr. Rebecca Cook. Until I joined Rebecca's laboratory, I had no idea one person (much less a boss) could be so intelligent, strong, dedicated, hardworking and simultaneously kind-hearted, generous and incredibly funny. The training I have received from Rebecca has been multifaceted. She taught me to be a thorough, dedicated and conscientious scientist. She taught me the meaning of "nice science" and how anything is possible with hard work and passion. She taught me that you can do great research and still maintain a great sense of humor and compassion. Her passion for science and life has been a source of inspiration for me. Her dance parties kept me going. For being an amazing scientist, mentor and person, I thank her.

I would also like to thank my committee members, Dr. Robert Matusik, Dr. Harold Moses and Dr. Jin Chen, for their advice and critiques, which have made me a stronger scientist. They helped me learn to think more critically and learn how to ask important research questions. I have been incredibly lucky to have these exceptionally intelligent scientists as part of my training. They were a pleasure to work with.

Additionally, my research would not have been possible without those who contributed to my funding and financial support, including my F31 pre-doctoral fellowship from the National Institutes of Health (NIH), training and funds from the Vanderbilt Program for Molecular Medicine (VPMM), and funds from the Vanderbilt Institute for Clinical and Translational Research (VICTR).

Of course, I will never be able to thank my amazing lab members (past and present) enough for accepting me, teaching me, supporting me and always laughing with me. Christian Young, Jamie Stanford, Andrew Williams, David Vaught, Michelle Williams, and Donna Hicks have been the greatest lab mates imaginable. I want to thank Christian for his perfect balance of humor and seriousness, his editing skills and scientific input, and for thoroughly training me upon joining the Cook Lab. I am grateful for Jamie, for her patience and her wisdom. She has been the backbone of our lab and a joy to be around. I want to thank Andrew Williams for making the lab a fun place to be. He always agreed (sometimes reluctantly) to accompany me on coffee breaks or to just take a walk when I needed some fresh air, or just needed to talk, and it is greatly appreciated. I would like to acknowledge David for all of his guidance, for making me laugh nonstop for four years, for singing with me, for his great taste in music and for enduring my various musical selections (and even growing to like them over the years). I want to thank Michelle for being a great friend, a sounding board (on both science- and non-science- related topics), and the best coffee and conference buddy I can imagine. Finally, I want to thank Donna for being the absolute best and coolest lab manager and person. She is a rock and I will never be able to express how much I have appreciated her help, her hard work for the lab and her sense of humor. The Cook Lab members have made coming into work an absolute joy, and I couldn't imagine a better group of people to work so closely with.

A number of people outside of the Cook Lab contributed greatly to my training. I would like to thank the Skala Lab, the Chen Lab and the Duvall Lab for their technical and intellectual guidance.

I give many thanks to Violeta Sanchez for her amazing IHC skills. I would like to thank Dana Brantley-Sieders, my favorite collaborator, for her for hard work, for her insight and for continually driving our projects forward. Dana's positive attitude, sunny personality and jokes always made science so much fun. She is a super woman and has been an absolute pleasure to work with.

I would also like to thank Dr. Carlos Arteaga and all the members of his laboratory, both past and present. The experience of attending and presenting at his lab meeting has been invaluable. During this time, I learned to interact with clinicians and learned how to consider research questions in ways that will have the greatest impact on patients. The members of the Arteaga lab have always been helpful, generous and a pleasure to be around, and for that, I am grateful.

There is no doubt that I would not have been able to successfully and happily complete graduate school without the love and support of my friends. I want to thank Lehanna Sanders and Andrew Williams, two of my closest friends whom I love dearly. They have been a constant source of fun and laughter and have always been there to offer love and support. I want to thank Michelle Williams, Mallory Hacker, Henry Horne, Brent, Valary and Stacy Joly. Happy hours and movie nights with them have been integral to my success and sanity in graduate school. I also want to thank my best friend, Crystal King, for always checking in and being there. Even though our schedules have made it difficult to see each other regularly, her calls, texts and hugs mean the world to me. I am also fortunate to have many more friends than I am able to list here, and I am grateful for every single one of them.

Last, but definitely not least, I want to thank my family. Joan Hunt-Henderson, Jeff Henderson, Beth Hunt, and Fred Love have been my endless source of love, support and inspiration. Even though they didn't always quite understand my research, they continued to stay interested and engaged. I want to thank them for supporting and valuing my continuing education and for always being my advocate. I also want to thank Chloe Morrison, my sister and best friend. She is my go-to person for anything and everything. She is open, loving, generous and supportive, and I am so incredibly fortunate to know her. I want to thank Arthur Hunt for being my role model and for always loving and supporting me. I want to extend many thanks to Pat, Walt, Stacy, Brent and Valary Joly for welcoming me into their family. Visiting them in Chattanooga over the past few years has been my sanctuary, and I am so incredibly lucky to be a part of such a loving, funny, supportive and selfless family. And finally, thank you to Greg Joly. Every day since we met has been better and brighter. He is a constant and endless source of love, laughter and inspiration. His patience and sense of humor kept me sane throughout this process. He believes in me and always pushes me to work harder and to believe in my work and myself. For him, I am infinitely grateful.

TABLE OF CONTENTS

	Page
DEDICATION.....	ii
ACKNOWLEDGEMENTS	iii
LIST OF TABLES.....	ix
LIST OF FIGURES	x
LIST OF ABBREVIATIONS.....	xii
Chapter	
I. Introduction	1
Overview	1
The mTOR pathway	4
mTORC1: activation and main functions.....	8
Signaling downstream of mTORC.....	11
mTORC2: assembly and upstream regulators	13
mTOR signaling in development	15
Mammary gland development.....	17
PI3K-Akt-mTOR components in mammary gland development	20
Dysregulation of PI3K-Akt- mTOR pathway in breast cancer	21
Signaling effectors downstream of mTORC2: important roles in breast Cancer.....	22
A necessary role for mTORC2 in cancer.....	24
Targeting the PI3K-Akt-mTOR pathway in breast cancer.....	26
II. mTOR Directs Breast Morphogenesis through a Rictor-Dependent PKC α - RAC1 Signaling Axis that is Independent.....	32
Abstract.....	32
Introduction	33
Materials and Methods.....	35
Results	40
Discussion	73
III. Rictor/mTORC2 Drives Progression and Therapeutic Resistance of HER2- Amplified Breast Cancers	80

Abstract.....	80
Introduction	81
Materials and Methods.....	84
Results	89
Discussion.....	125
IV. Conclusions and Future Directions	131
REFERENCES	142

LIST OF TABLES

Table	Page
1. Drugs targeting the PI3K-Akt-mTOR pathway currently in clinical trials for breast cancer.....	29
2. Upregulation of mTORC2 pathway components overlaps with HER2/PI3K pathway alterations.....	92
3. Rictor and Raptor protein analysis in a human tissue microarray (TMA).....	93

LIST OF FIGURES

Figure	Page
1. Alterations in the HER2-PI3K-Akt pathway in clinical breast tumors.....	3
2. mTOR exists in two structurally and functionally distinct complexes, mTORC1 and mTORC2.....	5
3. Schematic representation of mTORC1 and mTORC2.....	7
4. Structure of the mTOR complexes	9
5. mTOR is a HER2/PI3K effector and regulates cellular functions in development and disease.....	12
6. Schematic representation of the structure of mammary epithelium in different stages of differentiation.....	18
7. Mammary gland development during puberty, pregnancy and lactation...	19
8. Targeting the PI3K-Akt-mTOR pathway in breast cancer.....	28
9. Loss of Rictor disrupts mammary branching morphogenesis in vivo...	41-42
10. Loss of Rictor decreases proliferation and survival of MECs in vivo.....	44
11. Impaired survival and morphogenesis of mammary epithelial structures upon loss of Rictor ex vivo.....	46-47
12. Loss of Rictor impairs branching and lumen formation in organoid culture.....	49
13. Akt activation is insufficient to rescue Rictor-deficient MEC survival, branch formation and invasion.....	52-53
14. Akt activation is insufficient to rescue Rictor-deficient MEC branching ex vivo.....	55
15. Loss of PKC α -mediated Rac activation in the absence of Rictor.....	57-58
16. Rictor-mediated Rac activity is necessary and sufficient for mammary branching morphogenesis ex vivo.....	61-62
17. Rictor-mediated PKC α activation controls acinar formation and motility of human and mouse MECs.....	64

18.	mTOR inhibition with rapamycin decreases MEC survival, motility and acinar formation, which are rescued by enforced Rac activity.....	66-67
19.	Unlike mTORC2, mTORC1 is dispensable for MEC survival and branching morphogenesis.....	69-70
20.	Unlike mTORC2, mTORC1 is dispensable for MEC survival in vivo.....	72
21.	Rictor expression is elevated in human breast cancer.....	91
22.	Loss of Rictor delays HER2-driven tumor formation.....	95-96
23.	Loss of Rictor or Raptor decreases HER2-induced focal neoplasias.....	98
24.	Rictor loss decreases growth and Akt S473 phosphorylation in established <i>HER2</i> -amplified breast cancer cells.....	101-102
25.	Genetic ablation of Rictor decreases growth and survival of HER2-positive breast cancer cells.....	103
26.	Rictor/mTORC2 signaling drives Akt-mediated survival of <i>HER2</i> -amplified breast cancer cells.....	106-107
27.	Rictor-mediated Akt activity is necessary and sufficient for breast cancer cell survival.....	108
28.	Rictor suppresses RhoGDI2 to activate Rac1 and control migration of HER2-positive breast cancer cells.....	111-112
29.	Rictor-mediated Rac1 activity is necessary for breast cancer cell migration.....	113
30.	Akt or PKC α is insufficient to rescue Rictor-mediated defects in cell migration or invasion.....	115
31.	Rictor/mTORC2 loss sensitizes <i>HER2</i> -amplified breast cancer cells to lapatinib-mediated cell killing.....	118-119
32.	Loss of Rictor/mTORC2 sensitizes parental and resistant cells to lapatinib in vitro.....	121-122
33.	Loss of Rictor/mTORC2 or Rac1 sensitizes resistant cells to cell-killing effects of lapatinib in vitro.....	124

ABBREVIATIONS

2D – 2-dimensional

3D – 3-dimensional

4EBP1 - EIF4E-binding protein 1

AD – Adenoviral

ADP – Adenosine diphosphate

AJ – Adherens junction

AKT/PKB – Protein kinase B

AMPK - AMP-activated protein kinase

ATP – Adenosine triphosphate

BCA - Bicinchoninic acid assay

BCL2 – B-cell lymphoma 2

BRDU - Bromodeoxyuridine

CA – Constitutively active

CK – Cytokeratin

DAPI - 4',6-diamidino-2-phenylindole

DCIS – Ductal carcinoma in situ

DEPTOR - DEP domain containing MTOR-interacting protein

DMEM - Dulbecco's Modified Eagle Medium

DNA – Deoxyribonucleic acid

EGFR – Epidermal growth factor receptor

EIF4E - Eukaryotic translation initiation factor 4E

EMT – Epithelial to mesenchymal transition

ER – Estrogen receptor

ERBB2/HER2 - V-erb-b2 erythroblastic leukemia viral oncogene homolog 2

ERK – Extracellular signal-related kinase

ESC's – Embryonic stem cells

FASN – Fatty acid synthase

FITC - Fluorescein isothiocyanate

FKBP1 - FK506-binding protein

FL – Floxed

FOXO1/3 – Forkhead transcription factors

FRAP - FKBP-12-rapamycin associated protein

FRB - FKBP12-Rapamycin Binding domain

GAP – GTP-ase-activating protein

GFP – Green fluorescent protein

GK – Glucokinase

GLUT1 – Glucose transporter 1

GSK3B – Glycogen synthase kinase 3 beta

GST- PAK-PBD – Glutathione s transferase p21-activated kinase protein binding domain

GTPASE – GTP hydrolase

HELA – Henrietta lacks (cell line derived from the tumor of Henrietta Lacks)

HDAC – Histone deacetylase

HM – Hydrophobic motif

HRP – Horseradish peroxidase

IBC – Invasive breast cancer

IF – Immunofluorescence

IGF1 – Insulin growth factor 1

IGFR – Insulin growth factor receptor

IHC – Immunohistochemistry

ILK – Integrin linked kinase

IRES – Internal ribosome entry site

IRS1 – Insulin receptor substrate 1

LACZ – Lac operon Z

LC-MS – Liquid chromatography mass spectrometry

MAPKAP1 - Mitogen-activated protein kinase associated protein 1

MEC – Mammary epithelial cell

MGKO – Mammary gland knockout

MLST8 - Mammalian lethal with SEC13 protein 8

MMTV – Mouse mammary tumor virus

MTOR- Mammalian target of rapamycin

MTORC1 – MTOR complex 1

MTORC2 – MTOR complex 2

MYR – Myristoylated

NIC – Neu-Ires-Cre

NIH – National institutes of health

P120 – P120 catenin

P53 – Tumor protein 53

PDK1 – Protein-dependent kinase 1

PH – Plextrin homology

PI3K - Phosphoinositide 3-kinase

PKB/AKT - Protein kinase B also known as Akt

PKC – Protein kinase C

PMEC – Primary mammary epithelial cell

PMO – Primary mammary organoid

PRAS40 - Proline-rich Akt substrate of 40 kDa

PROTOR – Protein observed with Rictor – 1

PTEN - Phosphatase and tensin homolog

RAB11- Ras-related protein Rab11

RAC1 - Ras-related C3 botulinum toxin substrate 1

RAG – Recombination activating gene

RAPTOR - Regulatory-associated protein of *mTOR*

RAS – Rat sarcoma

RFP – Red fluorescent protein

RHEB – Ras homologue enriched in brain

RHOGDI2 - Rho GDP-dissociation inhibitor 2

RICTOR – Rapamycin-insensitive companion of mTOR

RTK – Receptor tyrosine kinase

S6 - Ribosomal protein S6

S6K – Ribosomal protein p70-protein kinase

SDS-PAGE - Sodium dodecyl sulfate polyacrilimide gel electrophoresis

SGK1 – Serum glucocorticoid kinase 1

SHRNA – Short hairpin ribonucleic acid

SIRNA – Small-interfering ribonucleic acid

SREBP – Sterol regulatory element binding protein

TBS – Tris buffered saline

TBST – Tris buffered saline plus tween

TEB – Terminal end bud

TM – Turn motif

TSC1/2 - Tuberous sclerosis proteins

VPMM – Vanderbilt Program in Molecular Medicine

V-ATPASE – Vacuolar adenosine triphosphate hydrolase

VICTR – Vanderbilt institute for clinical and translational research

WNT – Wingless

WT – Wildtype

ZFN – Zinc finger nuclease

ZO-1 – Zona occludens

CHAPTER I

INTRODUCTION

Overview

mTOR is a serine/threonine kinase that integrates a wide array of cellular processes, which contribute to mammary gland development and disease. mTOR operates downstream and within the PI3K/Akt signaling pathway, functioning in two distinct complexes, mTORC1 and mTORC2, whose activity and substrate specificity are regulated by complex-specific cofactors. Specifically, mTORC1 requires the cofactor Raptor to perform the essential roles of mTORC1 in regulating growth and metabolism. Relatively less is known about mTORC2, although its role in cell survival, polarity and cytoskeletal dynamics requires its cofactor, Rictor. Importantly, mTORC2 phosphorylates Akt at Serine-473. Akt is a critical signaling effector that lies at the apex of several potentially oncogenic signaling pathways controlling cell survival, motility, proliferation, and metabolism. Akt is activated in response to phosphorylation. Interestingly, Akt is phosphorylated at two distinct sites, Serine 473 (by mTORC2) and Threonine 308 (in response to PI3K signaling). Once activated by mTORC2, Akt signaling activates mTORC1, thus placing mTOR at locations both *upstream* and *downstream* of Akt in the PI3K/Akt pathway. Abundant evidence demonstrates that mTORC2 has numerous substrates unrelated to the PI3K/Akt pathway, although the function of mTORC2 in breast cancer is not yet fully understood.

The PI3K/Akt/mTOR is aberrantly activated in 60% of breast cancers, frequently in response to *HER2* amplification. 20% of all breast tumors bear *HER2* gene amplification **(Figure 1)**. PI3K/Akt signaling is required for HER2-mediated transformation and promotes resistance to HER2 inhibitors, thus defining *HER2*-amplified breast tumors as PI3K-dependent. Since nearly 100% of metastatic HER2-positive breast cancers acquire resistance to HER2 inhibitors, a desperate need for new therapeutic targets in *HER2*- amplified breast cancers is evident. Preclinical studies demonstrated that everolimus, an mTORC1 inhibitor that can inhibit mTORC2 through indirect mechanisms in some cell types, sensitized *HER2*-amplified tumors to Herceptin. In these studies, everolimus inhibited both mTORC1 and mTORC2. Although ATP competitive mTORC1/2 inhibitors effectively prevent mTORC2 activity, the negative consequences of mTORC1 inhibition [compensatory activation of PI3K signaling, immunosuppression] may limit their therapeutic potential. Thus, while the role of mTOR in *HER2*-amplified breast cancer is evident, a knowledge gap remains regarding the specific role and therapeutic potential of mTORC2 in *HER2*-amplified, PI3K-dependent breast cancers. Additionally, because breast tumor cells hijack many signaling pathways required for normal tissue processes, understanding the distinct roles of mTORC1 and mTORC2 in mammary morphogenesis is necessary.

Data from my thesis work is the first to show that Rictor/mTORC2 is required for both normal and HER2-transformed mammary epithelial cells (MECs), though, interestingly, the Rictor-dependent pathways that regulate normal MEC versus tumor cell functions are distinct.

Case Set: All Tumors: All tumor samples (825 samples)

Altered in 478 (58%) of cases

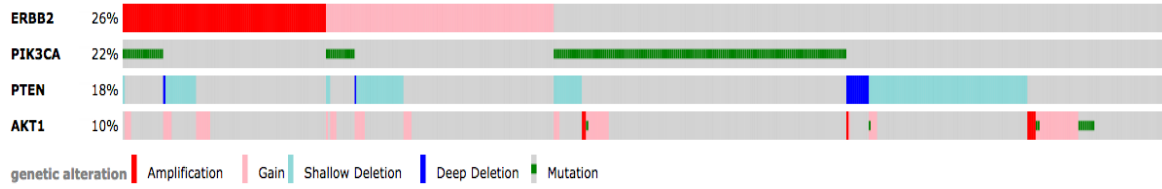


Figure 1. Alterations in the HER2-PI3K-Akt pathway in clinical breast tumors. HER2-PI3K-mTOR pathway aberrations were assessed in TCGA-curated breast cancers.

We found that Rictor/mTORC2 activates Akt to drive survival of *HER2*-amplified breast tumor cells. Interestingly, Akt was not sufficient to restore migration/invasion of Rictor-deficient *HER2*-amplified breast cancer cells. Instead, tumor cells downregulate RhoGDI2, a Rac1 inhibitor, in order to drive Rictor-mediated Rac1-dependent cell migration and metastasis. In contrast, untransformed MECs use an mTORC2-PKC α -Rac1 signaling pathway that is Akt-independent. Our data uncovers a previously unreported role for Rictor/mTORC2 in mammary morphogenesis and *HER2*-mediated tumorigenesis and suggests that mTORC2-specific inhibitors, or Rac inhibitors, may improve *HER2*-positive tumor cell killing in combination with clinically prescribed *HER2* inhibitors.

The mTOR pathway

Mechanistic target of rapamycin (mTOR) is an intracellular serine/threonine protein kinase, first discovered as the target of the naturally derived compound, rapamycin or sirolimus, which initially gained attention for its wide anti-proliferative properties. Studies in yeast identified TOR1 and TOR2, two TOR enzymes encoded by distinct genes, as mediators of these rapamycin-induced effects [5]. Observations that rapamycin did not inhibit all mTOR functions in mammalian cells ultimately led to the discovery that mTOR exists in two structurally and functionally distinct complexes, mTOR complex 1 (mTORC1) and mTOR complex 2 (mTORC2) (**Figure 2**) [6]. Each mTOR complex is defined by **1)** complex-specific co-factors, **2)** varying sensitivity to rapamycin, **3)** distinct signaling inputs, and **4)** distinct substrates that regulate diverse cellular processes.

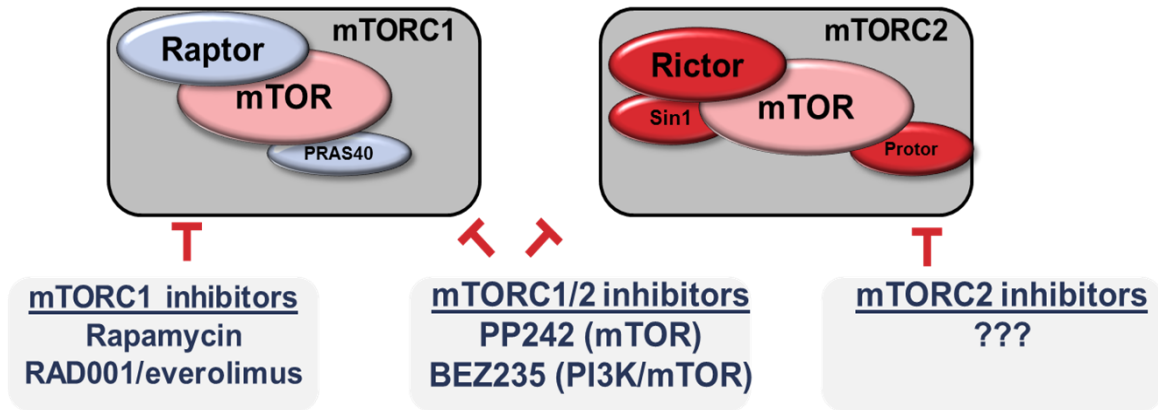


Figure 2. mTOR exists in two structurally and functionally distinct complexes, mTORC1 and mTORC2. Raptor is a required cofactor for mTORC1, while Rictor and Sin1 are cofactors required for mTORC2. mTORC1 inhibitors and dual mTORC1/2 inhibitors exist but mTORC2-specific inhibitors do not currently exist.

Both mTOR complexes are large - mTORC1 is comprised of six known subunits and mTORC2 is comprised of seven. Each complex shares several components including the catalytic mTOR subunit, the mammalian lethal of sec13 (mLST8) protein, and the DEP-containing mTOR-interacting protein (DEPTOR). In contrast, regulatory associated protein of mechanistic target of rapamycin (Raptor) and proline-rich Akt substrate 40 kDA (Pras40) are mTORC1-specific whereas rapamycin-insensitive companion of mTOR (Rictor), mammalian stress-activated map kinase-interacting protein (mSin1) and protein observed with Rictor 1/2 (Protor 1/2) are mTORC2-specific components (**Figure 3**) [reviewed in [7]].

Once rapamycin was identified as an mTORC1 inhibitor, it was quickly determined that its mTORC1 inhibitory effects were due to formation of a gain-of-function complex with the small, intracellular FK506-binding protein (FKBP12) however precisely how this complex inhibits mTORC1 is still not fully understood (**Figure 4**) [8, 9]. Adding to this complexity, recent studies show that prolonged rapamycin treatment can inhibit mTORC2 in a cell type-dependent context, although this mechanism remains unclear. For example, prolonged (24 hours) but not acute (1 hour) rapamycin treatment in PC3 or HeLa cells decreased Rictor-mTOR interaction and downstream signaling [10]. Therefore, while it is clear that rapamycin can inhibit growth of cancer cells *in vitro* and *in vivo*, the distinct contributions of mTORC1 and mTORC2 in inhibiting these processes is still unclear.

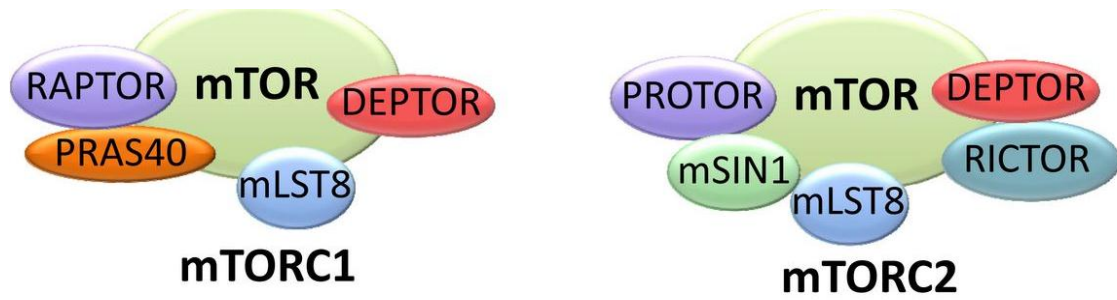


Figure 3. Schematic representation of mTORC1 and mTORC2. Common cofactors include DEPTOR and mLST8. From [3].

mTORC1: activation and main functions

mTORC1 is the better characterized mTOR complex. As a main function, mTORC1 integrates signals from intracellular and extracellular cues including growth factors, stress, oxygen and amino acids to control important cellular processes like protein and lipid synthesis, cell growth and autophagy. The signaling pathways directly upstream of mTORC1 have been well described and include the tuberous sclerosis (TSC) 1/2 complex, a major upstream regulator of mTORC1 that functions as a GTP-ase activating protein (GAP) for the Ras homolog enriched in brain (Rheb) GTP-ase. GTP-loaded Rheb directly interacts with mTORC1 and stimulates its kinase activity, while TSC1/2 negatively regulates mTORC1 by converting Rheb into its GDP-bound, inactive state. TSC1/2 directly integrates many of the upstream signals to mTORC1, like insulin and insulin-growth factor 1 (IGF1) that stimulate PI3-kinase and Ras pathways. PI3K and Ras effectors like protein kinase B (Akt/PKB) and extracellular-signal-related kinase (Erk) directly phosphorylate TSC1/2 to inactivate it and subsequently activate mTORC1. Additionally, the canonical Wnt pathway, a major regulator of cell growth, proliferation, polarity, differentiation, and development, inhibits glycogen synthase kinase 3 β (GSK3- β), which normally phosphorylates and promotes Akt TSC2 activity, resulting in activation of mTORC1 [11].

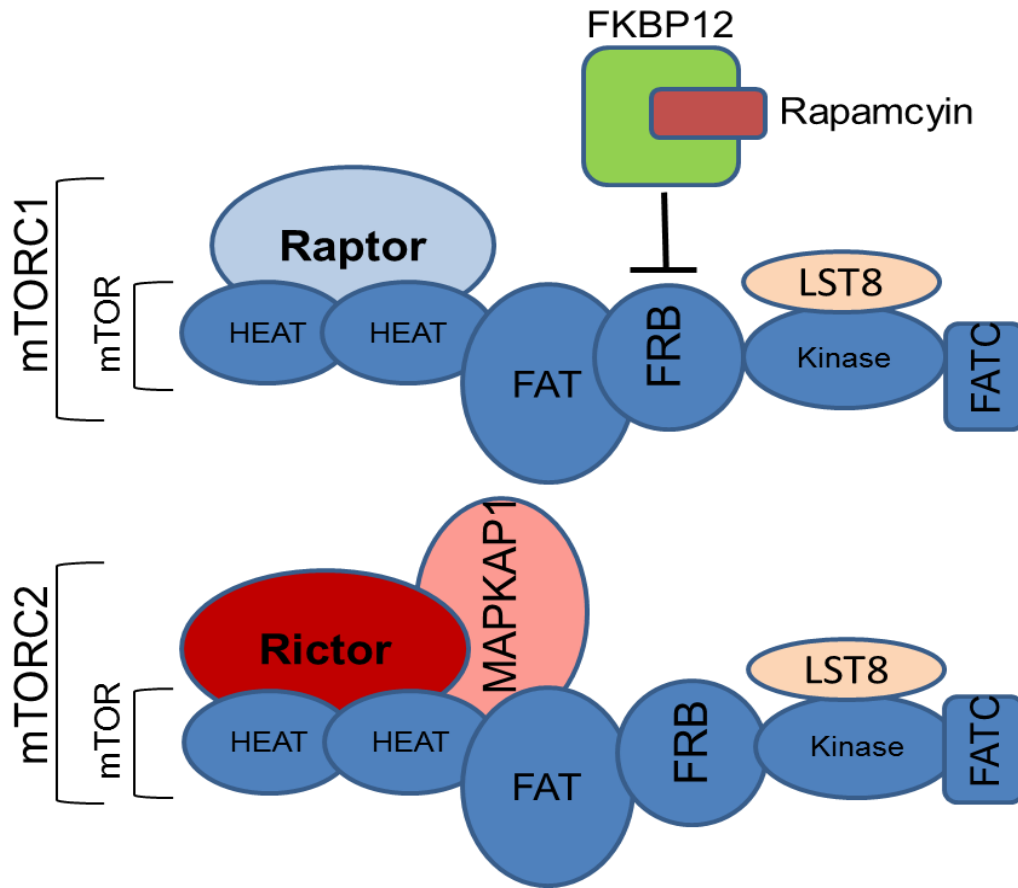


Figure 4. Structure of the mTOR complexes. mTOR is a large kinase that contains a carboxy-terminal serine/threonine protein kinase domain, a FAT domain and a C-terminal FAT (FATC) domain that is thought to play a role in its structure and stability. Mammalian LST8 associates with the kinase domain of mTOR and is thought to facilitate mTOR signalling. mTOR and LST8, together with RAPTOR form mTORC1. RAPTOR is essential for mTORC1 activity and is proposed to interact with mTOR through shared HEAT domains. Rapamycin binds to FKBP12 to form a drug–receptor complex that specifically and effectively blocks the activity of mTORC1. The rapamycin–FKBP12 complex binds next to the kinase region of mTOR in the FKBP12–rapamycin-binding (FRB) domain and disrupts the *in vitro* and *in vivo* activity of the complex, potentially by disrupting the interaction between RAPTOR and mTOR. mTORC2 also contains LST8 but specifically associates with RICTOR and MAPKAP1 (also known as SIN1). Unlike mTORC1, mTORC2 is resistant to direct inhibition by rapamycin. It is unknown what prevents the interaction between the rapamycin–FKBP12 complex and the FRB domain on mTORC2.

In contrast, hypoxia and DNA damage can inhibit mTORC1 [12]. For example, in response to low oxygen levels, adenosine monophosphate-activated protein kinase (AMPK) phosphorylates TSC2 and increases its GAP activity towards Rheb to suppress mTORC1 function. AMPK can also directly inhibit mTORC1 through phosphorylation of Raptor and subsequent allosteric inhibition of mTORC1. DNA damage also signals to mTORC1 through multiple p53-dependent mechanisms. Specifically, DNA damage induces expression of TSC1 and phosphatase and tensin homolog deleted on chromosome 10 (PTEN) resulting in downregulation PI3K-mTOR signaling [13].

Notably, amino acids, like leucine and arginine, play an important role in mTORC1 activation and their presence is required for activation of mTORC1. Because of this, research efforts have been focused on elucidating the specific amino acid sensors on mTORC1. Several groups have identified that amino acid-dependent activation of mTORC1 requires the Rag GTPases, of which there are four: RagA, B, C and D [14]. Rag A or B forms a heterodimer with either Rag C or D each of which have opposite nucleotide loading state so that when Rag A/C is in the GTP-bound state, Rag B/D is in the GDP-bound state and vice versa. Amino acids promote the loading of GTP on Rag A/B, which enables the heterodimer to interact with Raptor, resulting in translocation of mTORC1 to the lysosomal surface where the Rag GTPases dock on a complex called the Ragulator. Like the Rags, the Ragulator is essential for amino acid signaling to mTORC1. Recent work proposes an inside-out model of amino acid sensing in which the accumulation of amino acids in the lysosomal lumen leads to initiation of signaling.

These processes are thought to require the vacuolar H⁺-adenosine triphosphate ATPase (v-ATPase) as depletion of necessary v-ATPase subunits blocks amino-acid-induced lysosomal localization of mTORC1 and downstream signaling. Additionally, the v-ATPase and the Ragulator directly interacted at the lysosomal surface, further implicating v-ATPase in integration of amino-acid-stimulated mTORC1 signaling [15].

Signaling downstream of mTORC1

Control of protein synthesis is a main function of mTORC1 and the effectors involved have been well characterized. First, mTORC1 directly phosphorylates eukaryotic translation initiation factor 4E (eIF4E)-binding protein 1 (4E-BP1) (**Figure 5**) which results in exclusion from the negative regulator of cap-dependent translation, eIF4E. This allows activated 4EBP1 to directly interact as part of the eIF4F complex, which is necessary for the initiation of cap-dependent translation. Additionally, direct phosphorylation and activation of S6 kinase 1(S6K1) by mTORC1 results in increased mRNA production and enhanced translational elongation and initiation. The role of mTORC1 in the regulation of mRNA translation has been confirmed using mTORC1-specific inhibitors in cell culture, showing a significant reduction in overall rates of protein synthesis upon treatment with mTORC1 inhibitors. mTORC1 can also control the rates of lipid synthesis, a process necessary for the formation of cell membranes. These mTORC1-specific functions are, at least partially, through sterol regulatory element binding protein 1/2 (SREBP 1/2) transcription factors that control the transcription of a number of necessary lipogenic genes, including fatty acid synthase (FASN).

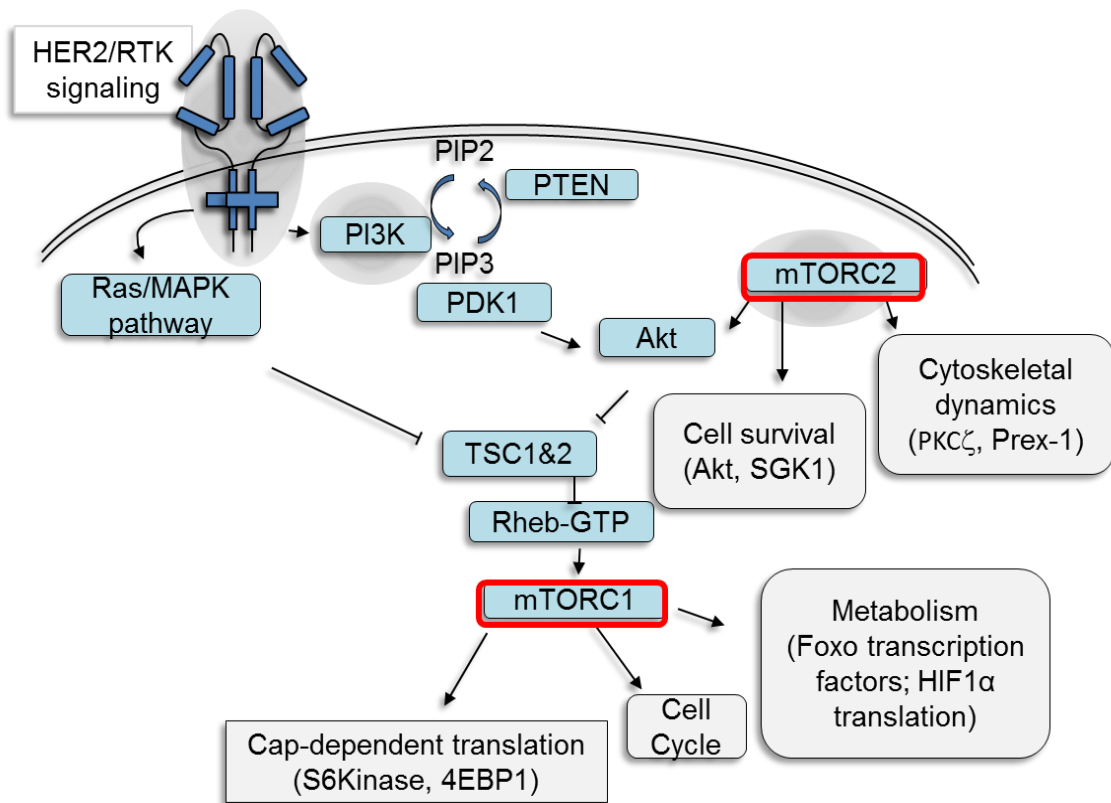


Figure 5. mTOR is a HER2/PI3K effector and regulates cellular functions in development and disease. mTOR exists in two complexes, Raptor-dependent mTORC1 and Rictor-dependent mTORC2. Signaling inputs for each complex are shown in blue and signaling outputs are shown in gray. mTORC1 and mTORC2 substrates are shown in parentheses.

mTORC2: assembly and upstream regulators

The core components of mTORC2 include mTOR, Rictor, Sin1, protor1/2 and mSLT8. The subunit Rictor is a necessary mTORC2 component, since Rictor loss decreases mTORC2 stability, activation and downstream signaling [16]. However, it should not be overlooked that mTOR-independent roles for Rictor have also been described. In one study, Rictor interacted with integrin-linked kinase (ILK) to phosphorylate Akt and control survival of breast and prostate cancer cells [17]. Therefore, it is possible that Rictor possesses additional undiscovered roles, by interacting with other kinases independently of mTOR. Similarly, Sin1 [18] and mLST8 [19] maintain the Rictor-mTOR interaction, which is necessary for mTORC2 signaling, as genetic Sin1 or mLST8 ablation in cells or in mice robustly compromises mTORC2 activity. Additionally, Sin1-null mouse embryonic fibroblasts (MEFs) display impaired Akt phosphorylation at Ser473 in response to serum or insulin, while Thr308 phosphorylation (the PDK1-substrate site) remains intact. Interestingly, loss of mTORC2-dependent Akt-S473 phosphorylation blocked Akt-mediated phosphorylation of FOXO1/3a, increasing stress-induced cell death despite intact Akt-T308 phosphorylation and mTORC1 activity [18].

The upstream factors that activate mTORC2 are not understood fully. Unlike mTORC1, mTORC2 is nutrient-insensitive, but does respond to growth factors (e.g., insulin), reportedly through PI3K-dependent and ribosome-dependent mechanisms. In HeLa cells, ribosomes (but not protein synthesis) are required for proper mTORC2 assembly and activation.

In HeLa cells, insulin-stimulated PI3K signaling increases mTORC2-ribosome interaction, while the mTORC2-ribosome interaction promotes Akt Ser473 phosphorylation in melanoma cells [20].

Phospho-proteomic studies have revealed at least 21 distinct phosphorylation sites on Rictor, uncovering an additional layer of mTORC2 regulation. The vast majority of these sites still possess unrevealed functions. However, liquid chromatography mass spectrometry (LC-MS) identified Rictor phosphorylation at Thr-1135 as a rapamycin-sensitive site phosphorylated directly by S6-Kinase (S6K) in response to mTORC1 signaling. Although a Thr-1135-to-Ala mutant did not affect mTORC2 integrity or *in vitro* kinase activity, a constitutively active Thr-1135 phospho-mimetic mutant increased P-Akt (S473) beyond what was seen with wild-type Rictor, showcasing another example of crosstalk between mTORC1 and mTORC2 [21].

Other studies demonstrated that S6K and Akt phosphorylate Sin1 at Thr-86 and Thr-398, respectively, resulting in Sin1 dissociation from mTORC2, complex instability, impaired Akt phosphorylation and activity, and profoundly decreased tumorigenesis. Importantly, the authors identified a cancer-derived Sin1 (*MAPKAP1*) mutation that impairs Sin1 phosphorylation, increasing mTORC2 stability and activity. Together, these findings suggest that mTORC1-S6K-Sin1 pathway mutations may increase mTORC2-Akt, thereby facilitating tumor progression [22]. Clearly, a dynamic interplay between Akt, mTORC1 and mTORC2 exists, warranting further efforts to understand the consequences of mTORC1 or dual mTORC1/2 inhibitors on feedback signaling through the PI3K/Akt/mTOR pathway.

mTOR signaling in development

As previously mentioned, the mTOR pathway integrates numerous signaling pathways to control many processes necessary for cellular function. As such, a vast amount of research has been dedicated to elucidating the role of mTOR in physiological processes in hopes that these findings could directly apply to pathological states. Classic models of gene targeting demonstrated that ablation of mTORC1 or mTORC2 cofactors leads to embryonic lethality, resulting in limited data generated from these studies [18, 19, 23]. However, generation of tissue-specific knockout models in mice provided further insight into the relative contributions of mTORC1 versus mTORC2 in tissue types. For example, mice with adipose-specific deletion of necessary mTORC1 cofactors have fewer and smaller adipocytes, resulting in less adipose tissue and resistance to obesity induced by high fat diet [24]. In contrast, loss of mTORC2 signaling in adipose tissue results in decreased activation of Akt S473 and increases lipolysis without affecting the number or size of adipocytes [25]. Muscle-specific loss of mTORC1 signaling causes decreased muscle mass, oxidative function and ultimately leads to early death in mice. In these mice, reduced oxidative metabolism was linked to decreased levels of transcriptional regulators of mitochondrial function [26]. Impaired mTORC2 signaling in muscle cells produces a different phenotype, with no effect on muscle structure but a mild decrease in glucose uptake. These results are interesting because while mTORC1's contribution to glucose metabolism has been well described, a role for mTORC2 in these processes is just becoming apparent.

Because the liver plays important roles in the regulation of glucose and lipogenesis in response to varying feeding and fasting states, it is not surprising that mTORC1 and mTORC2 are essential to hepatic regulation of whole body metabolism. Indeed, mTORC1 controls hepatic energy production in response to fasting [27]. Additionally, mTORC1 is required for anabolic processes during the fed state through its control of the transcription factor SREBP1c [28]. However, the complexity and crosstalk between key signaling molecules of the mTOR pathway is apparent as insulin-stimulated Akt can activate hepatic SREBP1 activity through both mTORC1-dependent and mTORC1-independent pathways [29]. Additionally, mTORC2 can also activate SREBP1 to control hepatic glycolysis and lipogenesis. In these studies, mTORC2-Akt signaling controlled SREBP1, which regulated lipogenesis, and glucokinase (GK) activity, which controlled glycolysis [30]. These data provide increasing evidence that mTORC2 may control key processes in cell metabolism, which previously have been only attributed to mTORC1 signaling.

In addition to the cell types already mentioned, essential roles for mTOR complexes have also been described in the pancreas where mTORC1-S6K signaling and mTORC2-Akt-Foxo signaling controls β -cell mass and function [31, 32]. Additionally, brain-specific mTORC1 loss suggests a role for mTORC1 signaling in control of energy balance in the hypothalamus [33], while the role for mTORC2 in these processes has yet to be clearly defined.

While the relative contributions of mTORC1 and mTORC2 have been described for many tissues, knowledge gaps remain. For example, the specific roles of mTORC1 and mTORC2 in mammary gland development have not yet been explored. This is discussed below and is the focus of our studies in Chapter I.

Mammary gland development

The post-natal mammary gland undergoes a complex series of events in which an extensively branched ductal network develops from a rudimentary epithelial bud (**Figure 6**) [34]. Pubertal changes trigger the onset of branching morphogenesis which is regulated by endocrine hormones and local paracrine interactions with mesenchymal stroma [35]. In response to hormonal and growth factor cues, mammary epithelial cells (MECs) within the terminal end buds (TEBs) rapidly [34, 35] proliferate and collectively invade surrounding stroma. Differentiation of epithelial progenitors in the TEB populates the ducts with mature luminal MECs, and apoptosis canalizes the lumen. TEB's undergo successive rounds of elongation, bifurcation and branching until a mature epithelial tree has formed within the virgin gland [34, 35]. The careful coordination of numerous molecular signaling pathways is required for the dynamic processes that occur during puberty in the mammary epithelium (**Figure 7**).

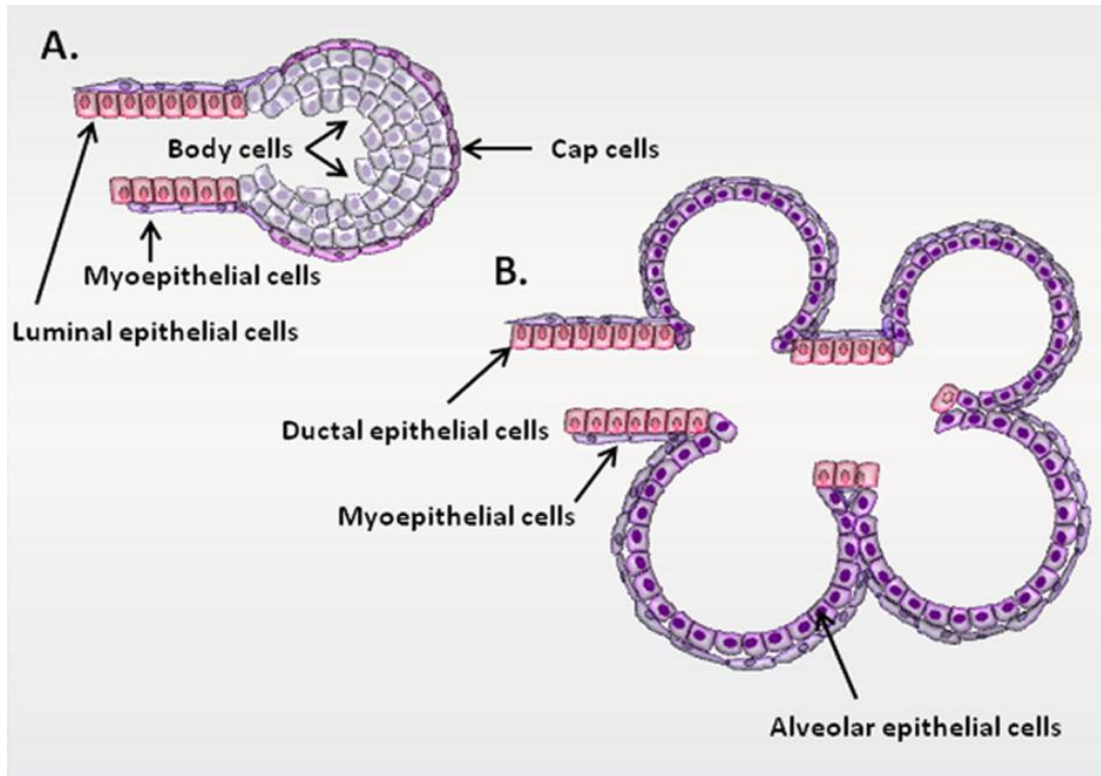


Figure 6. Schematic representation of the structure of mammary epithelium on different stages of differentiation. **A.** Prepubertal and pubertal mammary gland consists of ducts terminated by highly proliferative terminal end buds (TEBs) that comprise cap cells in direct contact with basal lamina, and body cells forming the bulk of the TEBs. **B.** During pregnancy, more extensive ductal branching and formation of alveolar structures, which are required for milk production, takes place. In functionally active mammary glands, alveoli are built by a single layer of milk-secreting luminal epithelial cells surrounded by myoepithelial cells, and basement membrane. Myoepithelial contractions release the milk into the ducts, and further to the nipple, whereas basement membrane provides cell contact with the extracellular environment. From [4].

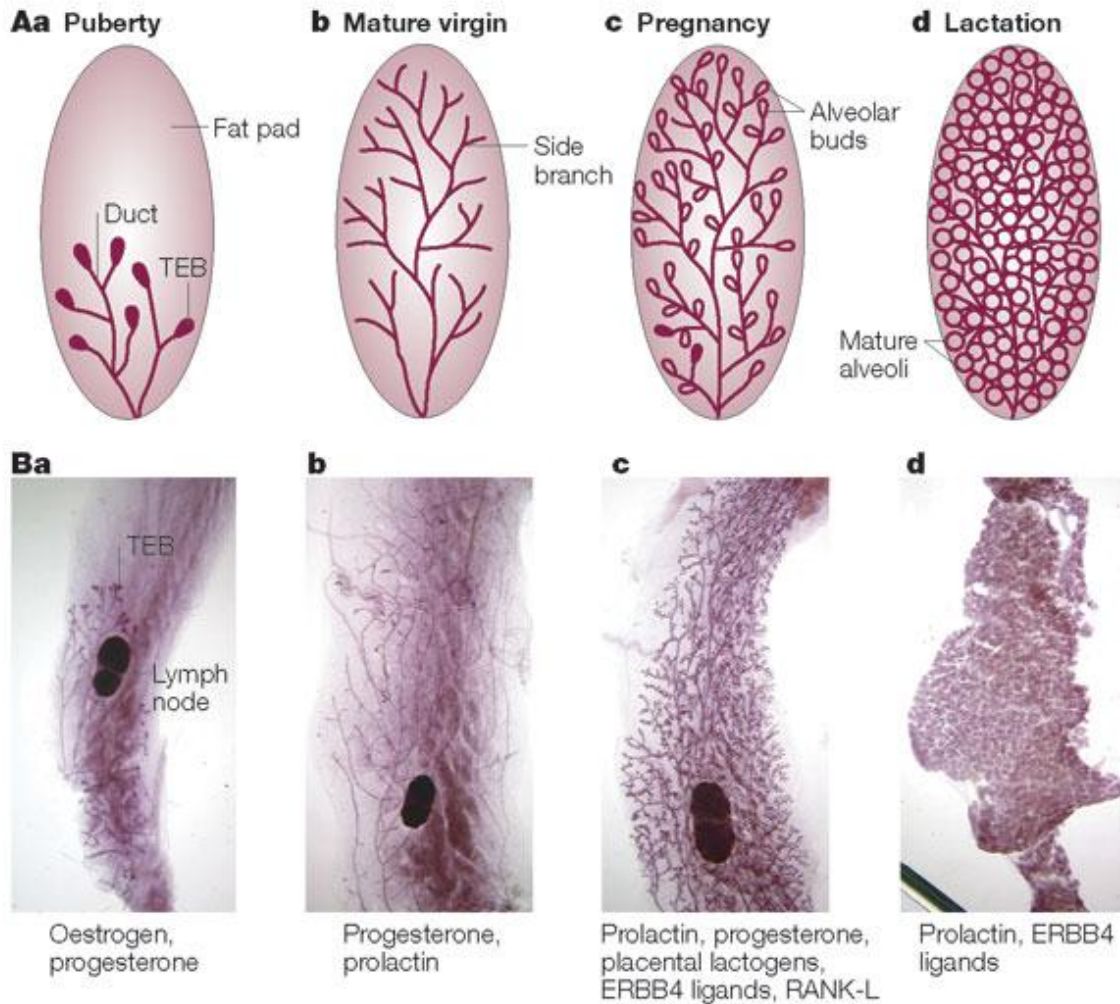


Figure 7. Mammary gland development during puberty, pregnancy and lactation.

A. Schematic presentation of the different stages of mammary gland development. (a-d) Rudimentary ductal design within the mammary fat pad is visible at birth, which grows at the same rate as the animal until the onset of puberty. (a) During puberty, cyclical hormone production accelerates ductal outgrowth causing club-shaped structures (TEB) where the highest levels of cell division occur to appear at ductal tips. (b) In mature virgin, the entire fat pad is filled with a regularly spaced system of primary and secondary ducts, with side branches that form and disappear in each oestrous cycle. (c) Hormonal changes that occur when pregnancy begins increase cell proliferation and the formation of alveolar buds. (d) During lactation, alveoli are fully matured and the luminal cells synthesize and secrete milk components in the lumen. Following lactation, the mammary gland will undergo massive apoptosis during involution to revert back to a mature virgin gland structure. **B.** Whole mount hematoxylin-stained mammary glands corresponding with each stage of development and highlighting the major hormone signals involved in each stage. From [2].

PI3K-Akt- mTOR pathway components in mammary gland development

The PI3K-Akt-mTOR pathway and its downstream effectors control important processes that are necessary for proper mammary gland development. Inasmuch, the use of transgenic mouse models has confirmed distinct roles for the Akt isoforms, Akt1, 2 and 3 in specific stages of mammary gland development. For example, Akt1 is required for efficient lactation to support offspring, partially due to inability of Glut1 to localize to the plasma membrane and reduced glucose uptake in Akt-deficient mice. Additionally, Akt1 knockout mice display reduced lipid synthesis and expression of lipogenic enzymes [36]. Conversely, forced expression of a constitutively active Akt1 results in defects in lactation and delayed involution due to decreased cell death [37, 38]. Alveolar-specific constitutive Akt activation resulted in aberrant accumulation of lipid droplets during pregnancy, and these mice produced small pups, presumably due to increased milk fat content/viscosity, which caused decreased suckling in pups [39].

Interestingly, several studies have revealed opposing roles for Akt1 and Akt2 in the developing mammary gland. Ablation of Akt1 results in delayed development and differentiation during pregnancy and lactation whereas Akt2 deficiency results in precocious differentiation. Likewise, although involution is accelerated in the absence of Akt1, it is delayed in Akt2-deficient mammary glands [40]. Phosphorylated Akt activates downstream substrates including the serine/threonine kinase mTOR and the forkhead family of transcription factors (FOXO). mTOR uses these substrates to regulate cellular metabolism, protein and lipid synthesis, cell survival, and cytoskeletal organization, processes that are required for proper mammary morphogenesis.

While mTOR regulates MEC growth [41, 42] and milk protein expression in cell lines [41, 43-45], mTOR-mediated regulation of mammary ductal morphogenesis remains under-investigated, partially due to the lack of specific inhibitors of each mTOR complex.

Dysregulation of PI3K- Akt- mTOR pathway in breast cancer

The PI3K-Akt-mTOR pathway is the most frequently altered pathway in breast cancer, with alterations occurring in approximately 60% of all breast cancers. These alterations often occur in response to HER2 overexpression or activation, which occurs in almost 25% of breast cancers. Activating mutations in *PIK3CA*, the gene encoding the p110 α catalytic subunit of PI3K, are also common, occurring in 36% of all breast cancers, most prevalently in luminal and *HER2*-amplified tumors. These mutations commonly reside in “hot spot” sites, H1047R and E545K, which confer increased PI3K catalytic activity resulting in cellular transformation and contribute to resistance to HER2-targeted therapies. Additionally, activating mutations in the *Akt1* gene are observed in approximately 36% of ER+ breast cancers. Amplifications and overexpression of *AKt1* have also been described, although in a much smaller subset of breast cancers. Finally, the tumor suppressor and negative regulator of PI3K signaling, PTEN, is mutated or lost in 7% of breast cancers, though almost exclusively in triple negative breast cancers (TNBCs). Loss of PTEN protein in tumors results in accumulation of PI(3,4,5)P₃ and in turn, phosphorylation and activation of Akt.

Several lines of evidence support PI3K pathway alterations as drivers of breast cancer formation. For example, active *PIK3CA* or *Akt1* mutants in human MECs results in growth factor independence, anchorage independent growth and tumor formation in mice. Importantly, PI3K/Akt pathway re-activation is a major driver of resistance to HER2-targeted therapies. For example, *PIK3CA* mutations can confer resistance to the anti-HER2 monoclonal antibody, trastuzumab, which can be overcome by combining trastuzumab with PI3K, Akt, or mTOR inhibitors.

Signaling effectors downstream of mTORC2: important roles in breast cancer

mTORC2 directly phosphorylates and activates the AGC kinases including Akt, SGK1 and PKC family members [46, 47]. Specifically, the mTOR components Rictor, Sin1 and mTOR are each required for carboxy-terminal phosphorylation of both the turn motif (TM) and hydrophobic motif (HM) of all conventional protein kinase Cs (PKCs) (including PKC α and PKC ϵ), Akt and the HM of serum- and glucocorticoid-induced protein kinase 1 (SGK1).

The serine/threonine protein kinase Akt is a major downstream signaling component of the PI3K pathway and upon activation controls cell survival, proliferation, migration and glucose metabolism. PI3K signaling recruits Akt to the inner plasma membrane, where Akt is phosphorylated at Thr-308 by phosphoinositide-dependent kinase 1 (PDK1) and at Ser473 by mTORC2. Akt exists in three isoforms: Akt1, 2 and 3. Akt 1 and 2 are ubiquitously expressed while Akt 3 expression is expressed in a cell-type dependent manner. Overexpression studies paired with genetic and pharmacological inhibition of Akt have provided insight into Akt's role in tumor cell survival, proliferation and tumorigenesis.

Akt's transforming properties were highlighted in early preclinical studies where overexpression of wildtype Akt2 transformed NIH3T3 fibroblasts; NIH3T3 cells expressing a constitutively active Akt1 construct (myr-Akt) formed colonies in soft agar, produced tumors in mice [48] and rescued apoptosis induced by PTEN [49]. Additionally, overexpression of Akt2, but not Akt 1 or 3, increased aggressiveness and metastatic properties in human breast cancer cell lines [50]. Transgenic mouse models have been beneficial in further dissecting the distinct roles of Akt in tumorigenesis. While mice with mammary-specific expression of Akt exhibited delayed postpartum involution, tumors did not develop [37], suggesting that an additional oncogenic hit might be necessary for overt tumorigenesis

Conversely, targeted deletion of Akt in PTEN null embryonic stem cells (ESCs) partially reduced tumorigenic properties [51]. Dominant negative forms of Akt block insulin-like growth factor 1 (IGF1)-induced cell survival, showcasing Akt's anti-apoptotic roles. Additionally, aberrant Akt activation has been widely described in clinical breast cancers, including *Akt1* mutations, which occur in breast cancers, albeit at low frequencies and *Akt1* amplifications, which correlate with poor survival outcome in breast cancer patients. More often, Akt is hyperactive due to genetic alterations in upstream activators such as *HER2* gene amplification and *PIK3CA* activating mutations occur in approximately 25% and 21% of breast cancers, respectively.

The PKC family of serine/threonine kinases controls several cellular processes, including proliferation, migration, and differentiation. PKC members are traditionally categorized into three classes termed “conventional”, “novel” and “atypical” [52] and are controlled via serine, threonine or tyrosine phosphorylation.

Notably, mTORC2-dependent phosphorylation of the PKC TM regulates maturity and stability of all conventional PKC isoforms, including PKC α .

PKC gene mutations are relatively rare, but increased PKC α expression and/or phosphorylation correlate with tumor aggressiveness and decreased survival in breast cancer patients. Experimental PKC α over-expression in breast cancer cells increased migration, leading to a more aggressive phenotype [53, 54]. Rictor-PKC ζ interactions control breast cancer cell migration and metastasis [55].

SGK plays important roles in growth factor-induced cell survival. SGK exists in three isoforms, SGK1, 2 and 3. Like Akt, SGK1 activation is triggered by two phosphorylation events: T-loop phosphorylation on Thr-256 by PDK1 and HM phosphorylation at Ser-244 by mTORC2, which is enhanced by stimulation with insulin and growth factors [56]. Previous reports have shown that SGK1 activation requires PI3K-PDK1 signaling, as PI3K inhibition suppresses SGK1 activity [57]. Elevated SGK1 expression has been described in clinical breast tumors [58] and in response to Akt inhibitors, suggesting overlapping roles for SGK1 and Akt in activating downstream effectors and compensation for Akt activity by SGK1 [59].

A necessary role for mTORC2 in cancer

One of the first described cellular functions of mTORC2 is control of cytoskeleton reorganization through regulation of Rho family of GTPases [6]. Additionally, mTORC2 regulates migration, proliferation and survival in various cell types including neutrophils, β -cells, endothelial cells, and primary mammary epithelial cells [31, 60-62]

Given the potent roles of cell survival and motility in tumor formation and progression, it is not surprising that mTORC2 has recently garnered interest for its potential role in cancer. Intriguing studies utilizing mouse models have revealed a necessary role for mTORC2 in the formation of PI3K-driven prostate cancer. Although Rictor was dispensable for normal prostate development, PI3K-driven prostate tumor formation was blocked upon Rictor loss [63]. In gliomas, Rictor overexpression promotes mTORC2 activity, tumor cell growth and motility [64], whereas genetic mTORC2 inhibition (i.e., stable Rictor knockdown) causes cell cycle arrest and decreased colon cancer growth [65].

Less is known regarding the distinct contributions of mTORC2 to breast cancer cells. Preclinical studies using breast cancer models have demonstrated that everolimus, an mTORC1 inhibitor that can inhibit mTORC2 through indirect mechanisms in some cell types, sensitizes *HER2*-amplified tumors to the *HER2* inhibitor, trastuzumab. In these studies, everolimus inhibited both mTORC1 and mTORC2. Although ATP competitive mTORC1/2 inhibitors effectively prevent mTORC2 activity, increasing evidence also suggests that targeting mTORC1, via mTORC1-specific inhibitors, may increase IRS1-to-PI3K signaling and mTORC2-mediated Akt phosphorylation, ultimately dampening tumor response and promoting therapeutic resistance [66]. Current clinical trials are investigating mTOR kinase inhibitors that block both mTORC1 and mTORC2 [67], but little is known about mTORC2 in breast cancer formation, progression, and therapeutic response, despite its known role in activation of Akt, a key signaling node in many breast cancers.

In vitro experiments have hinted at the importance of mTORC2 in breast cancer cells. Several lines of evidence suggest that cancer cells exploit Rictor-dependent mTOR signaling pathways to facilitate invasion and metastasis. For example, siRNA-mediated Rictor knockdown inhibited MCF7 and MDA-MB-231 breast cancer cell migration [55, 68]. Rictor knockdown inhibited transforming growth factor beta (TGF β)-mediated epithelial-to-mesenchymal transition (EMT) in breast cancer lines [69]. Additionally, Rictor can interact with PKC ζ to regulate breast cancer metastasis [55].

Importantly, there is increasing evidence indicating a critical role of Rictor in clinical breast tumors. For example, Rictor protein expression is elevated in invasive ductal carcinoma compared to normal tissue or ductal carcinoma *in situ* (DCIS) and this correlates positively with lymph node status [55].

Targeting the PI3K-Akt-mTOR pathway in breast cancer

As the PI3K-Akt-mTOR pathway is a central signaling pathway that regulates many critical aspects of cancer cell physiology, and because it is altered in 60% of breast cancers, intense research efforts have focused on developing and testing inhibitors of PI3K-Akt-mTOR pathway components for the treatment of breast cancer. Abundant evidence from preclinical studies confirms the efficacy of pathway inhibition on tumor growth and survival. Additionally, numerous studies confirm a role for the PI3K-Akt-mTOR pathway in acquiring resistance to targeted therapies, including HER2-inhibitors.

PI3K pathway inhibition can be achieved in numerous ways including at the level of growth factor receptors (through direct inhibition of receptor tyrosine kinases, HER2 with trastuzumab or EGFR/HER2 with lapatinib), PI3K (through PI3K inhibitors), Akt (allosteric and kinase inhibitors of Akt) and mTOR (both mTORC1-specific inhibitors, dual mTORC1/2 inhibitors, and dual PI3K/mTOR inhibitors) **(Figure 8) [1]**. Promising results from preclinical data highlighted above has led to clinical trials investigating these inhibitors for treatment of breast tumors **(Table 1)**. Given the prominent role of mTORC1 in cell cycle progression, intense research efforts have been invested in identifying mTORC1 inhibitors. Rapamycin (sirolimus) was the first available mTOR inhibitor and is approved for use as an immunosuppressant in transplant recipients. Improvements on rapamycin were made and the resulting next generation mTOR inhibitors, rapalogues, display better pharmacokinetic and pharmacologic properties. Several of these drugs are approved for use in cancers. For example, temsirolimus has been approved for the treatment of renal cell carcinoma and everolimus is now approved for treatment of patients with renal cell carcinoma, neuroendocrine tumors of the pancreas and in postmenopausal women with estrogen receptor (ER) positive breast cancer. Additionally, the BOLERO-2 trial, a randomized, phase III trial which evaluated everolimus and exemestane in postmenopausal women with hormonal positive breast cancer who progressed on aromatase inhibitors, showed that adding everolimus to standard chemotherapy significantly improved progression-free survival (PFS) in patients [70].

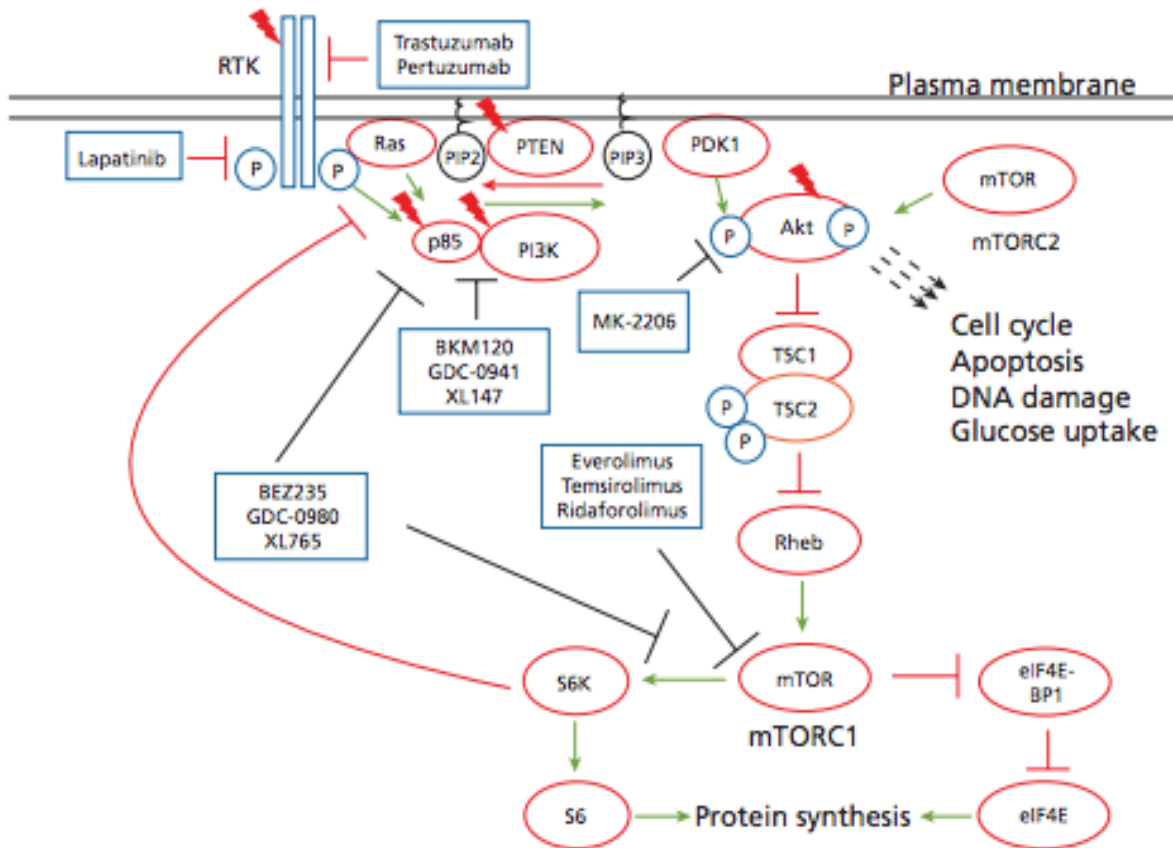


Figure 8. Targeting the PI3K-Akt-mTOR pathway in breast cancer.

Green arrows represent activation of positive regulation, red bars indicate inhibition. Red lightning bolts represent genes frequently mutated in human breast cancer. Blue rectangles depict drugs either approved or being assessed in clinical trials for breast cancer, and the targets they inhibit (black bars). For simplicity, other targets of Akt are not shown. P = phosphorylation. RTK = receptor tyrosine kinase. From [1].

Table 1. Drugs Targeting the PI3K-AKT-mTOR Pathway Currently in Clinical Trials for Breast Cancer			
Drug	Class	Study Population(s)	Common Toxicities
Everolimus (Rad001)	Allosteric mTOR inhibitor	Adjuvant HR+;locally advanced/metastatic, HER2+; advanced HER2-negative; neoadjuvant	Fatigue, stomatitis, diarrhea, rash
Temsirolimus	Allosteric mTOR inhibitor	HER2+ or TN	Fatigue, stomatitis, diarrhea, rash
Ridaforolimus (MK-8669)	Allosteric mTOR inhibitor	Advanced/metastatic HR+/HER2-	Fatigue, stomatitis, anorexia, diarrhea, nausea
AZD2014	mTOR (TORC1/2) kinase inhibitor	Advanced/metastatic HR+	Fatigue, stomatitis, anorexia, diarrhea, nausea
MK-2206	Allosteric Akt inhibitor	HR+ neoadjuvant and advanced; preoperative biomarkers, all subtypes; advanced HER2+	Rash, nausea, pruritus, hyperglycemia, diarrhea
AZD5363	Akt kinase inhibitor	Advanced/metastatic, all subtypes	Not reported
Triciribine	Akt inhibitor	Neoadjuvant; advanced HER2-	Hyperlipidemia, hyperglycemia, fatigue
GDC-0941	PI3-kinase inhibitor	Advanced/metastatic HR+, HER2+, TN	Fatigue, nausea, diarrhea, rash, transient hyperglycemia
BKM120	PI3-kinase inhibitor	Advanced/metastatic HR+ or TN; neoadjuvant HER2+; preoperative biomarker; advanced HER2+ resistant to trastuzumab	Fatigue, rash, nausea, mood alteration, hyperglycemia
BAY80-6946	PI3-kinase inhibitor	Advanced/metastatic	Not reported
XL147	PI3-kinase inhibitor	Advanced/metastatic HR+; advanced/metastatic HER2+ progressing on trastuzumab	Rash, hyperglycemia
BYL719	PI3-kinase/PIK3CA-specific inhibitor	Advanced/metastatic HR+	Hyperglycemia, nausea, vomiting, diarrhea, anorexia
XL765	Dual PI3-kinase/mTOR inhibitor	Advanced/metastatic HR+	Nausea, diarrhea, anorexia, rash, elevated LFTs
BEZ235	Dual PI3-kinase/mTOR inhibitor	HER2+;preoperative biomarker; advanced/metastatic HER2-	Nausea, vomiting, diarrhea, fatigue, anemia
GDC-0980	Dual PI3-kinase/mTOR inhibitor	Advanced/metastatic HR+	Nausea, fatigue, diarrhea

Table 1. Drugs targeting the PI3K-AKT-mTOR pathway currently in clinical trials for breast cancer. Adapted from [1].

Additional clinical trials have also demonstrated a significant improvement in patients with neoadjuvant everolimus plus letrozole [71] or the addition of everolimus to tamoxifen [72], suggesting that mTOR inhibition may play a significant role in hormonal-positive breast cancers. Unfortunately, the progression-free survival for these studies was still only 6 months, suggesting that patients developed resistance to the combination of endocrine therapy plus mTOR inhibition. More studies will be needed to identify which patients are most likely to benefit and what additional mechanisms of resistance may contribute to response.

As numerous preclinical studies have implicated the PI3K-Akt-mTOR pathway in resistance to treatment with the HER2-monoclonal antibody, trastuzumab, clinical trials adding everolimus to trastuzumab and cytotoxic therapy in patients with metastatic HER2-positive breast cancer are underway. In one trial, the addition of everolimus significantly improved progression-free survival, albeit by only a few months [73]. This study and others support the idea that mTOR inhibition may improve the response of patients with HER2-overexpressing tumors that are resistant to trastuzumab. More recently developed ATP-competitive mTOR kinase inhibitors that are designed to simultaneously block both mTORC1 and mTORC2 and are also being tested in clinical trials. INK128, an orally bioavailable and selective inhibitor of both mTORC1 and mTORC2, is being evaluated in phase I clinical trial of patients with advanced solid tumors. This trial is ongoing, but INK128 was well-tolerated at the doses and schedules tested and preliminary data showed anti-tumor data in some cancer types [74].

While multiple PI3K and Akt inhibitors are currently being tested in clinical trials, none are currently approved for treatment of breast cancer. These inhibitors have exhibited high dose-limiting toxicities, with adverse events including nausea, diarrhea, vomiting and fatigue. BKM120, an oral, selective pan class I PI3K inhibitor, has been used in phase I dose escalation studies for patients with advanced solid tumors. It was safe and well-tolerated in these studies and is now being tested in combination with chemotherapy and endocrine therapy to determine if this combination will overcome resistance to hormonal therapy. Selective p110 α inhibitors are being evaluated in phase I studies of metastatic solid tumors and dual PI3K/mTOR inhibitors like BEZ235 are being tested in phase I studies in the setting of metastatic breast cancer. These trials are ongoing (Reviewed in [75]).

Chapter II

MTOR DIRECTS BREAST MORPHOGENESIS THROUGH A RICTOR-DEPENDENT PKC α -RAC1 SIGNALING AXIS THAT IS AKT-INDEPENDENT

The work presented in this chapter is published in PLOS Genetics under the same title

Abstract

Akt phosphorylation is a major driver of cell survival, motility, and proliferation in development and disease, causing increased interest in upstream regulators of Akt like mTOR complex 2 (mTORC2). We used genetic disruption of *Rictor* to impair mTORC2 activity in mouse mammary epithelia, which decreased Akt phosphorylation, ductal length, secondary branching, cell motility, and cell survival. These effects were recapitulated with a pharmacological dual inhibitor of mTORC1/mTORC2, but not upon genetic disruption of mTORC1 function via *Raptor* deletion. Surprisingly, Akt re-activation was not sufficient to rescue cell survival or invasion, and modestly increased branching of mTORC2-impaired mammary epithelial cells (MECs) in culture and *in vivo*. However, another mTORC2 substrate, protein kinase C (PKC)- α , fully rescued mTORC2-impaired MEC branching, invasion, and survival, as well as branching morphogenesis *in vivo*. PKC α -mediated signaling through the small GTPase Rac1 was necessary for mTORC2-dependent mammary epithelial development during puberty, revealing a novel role for Rictor/mTORC2 in MEC survival and motility during branching morphogenesis through a PKC α /Rac1-dependent mechanism.

Introduction

Post-natal mammary epithelial morphogenesis is a complex process during which an extensively branched ductal network develops from a rudimentary epithelial bud [34]. Branching morphogenesis is most active during puberty and is regulated by endocrine hormones and local paracrine interactions with mesenchymal stroma [35]. In response to hormonal and growth factor cues, mammary epithelial cells (MECs) within the terminal end buds (TEBs), the club-shaped structures at the distal epithelial tips [34, 35], proliferate and collectively invade surrounding stroma. Differentiation of epithelial progenitors in the TEB populates the ducts with mature luminal MECs, and apoptosis canalizes the lumen. TEB bifurcation results from mechanical restraints at the TEB midline, forming new primary ducts. Side-branches sprout laterally from the trailing ducts as proliferative out-pouchings. Primary and side branching reiterates, filling the entire mammary fat pad [34, 35]. Many molecular signaling pathways carefully coordinate the dynamic processes that occur during puberty in the mammary epithelium.

The intracellular serine/threonine kinase mammalian target of rapamycin (mTOR) regulates cellular metabolism, protein and lipid synthesis, cell survival, and cytoskeletal organization, processes that are required for proper mammary morphogenesis. mTOR regulates these processes through phosphorylation of its target substrates, including translation initiation factor 4E (eIF4E)-binding protein 1 (4E-BP1), p70S6 kinase (S6K), Akt, SGK1, and protein kinase C- α (PKC α) [76].

mTOR functions in two distinct complexes, each defined by the specific co-factors in complex with mTOR kinase and by their relative sensitivity to rapamycin. The rapamycin-sensitive mTOR complex (mTORC)-1 requires the co-factor regulatory-associated protein of mammalian target of rapamycin (Raptor), whereas mTORC2 requires the co-factor rapamycin-insensitive companion of mammalian target of rapamycin (Rictor). Although mTORC2 is relatively insensitive to acute rapamycin treatment, more recent studies determined that prolonged rapamycin treatment can inhibit mTORC2 complex assembly [10, 77-79]. The intracellular serine/threonine kinase Akt is phosphorylated at S473 directly by mTORC2 and is key effector for many of the biological effects initiated by mTORC2. Akt is also linked to activation of mTORC1 downstream of PI3-kinase, making Akt a point of intersection between mTORC1, mTORC2, and their associated effectors [76].

Though mTOR regulates MEC growth in cell lines [41, 42] and milk protein expression [41, 43-45], mTOR-mediated regulation of mammary ductal morphogenesis remains under-investigated. The signaling complexity of mTOR, its pleiotropic functions, and a lack of mTORC2-specific inhibitors present a challenge to dissecting the relative roles of mTORC1 and mTORC2 in mammary development. Given the importance of mTOR in breast cancer progression and treatment, an understanding of mTORC1 and mTORC2 in untransformed MECs is needed. We assessed the impact of tissue-specific *Rictor* and *Raptor* ablation on mammary morphogenesis. *Rictor* loss impaired mTORC2 activity, reduced ductal lengthening and secondary branching, and reduced MEC proliferation and survival *in vivo* and *ex vivo*.

Surprisingly, genetic disruption of mTORC1 via *Raptor* ablation resulted in distinct and milder effects on the developing mammary ductal epithelium, revealing non-overlapping roles for mTORC1 and mTORC2 during mammary morphogenesis. Interestingly, we found that mTORC2 controls mammary morphogenesis through downstream effectors PKC α and Rac1, but not Akt.

Materials and Methods

Mice. All animals were housed under pathogen-free conditions, and experiments were performed in accordance with AAALAC guidelines and with Vanderbilt University Institutional Animal Care and Use Committee approval. *Rictor*^{FL/FL} mice (C57BL/6) were kindly provided by Dr. Mark Magnuson (Vanderbilt University) and have been previously described [23]. *Raptor*^{FL/FL} mice [[19], C57BL/6] were purchased from the Jackson Laboratories (Bar Harbor, ME). *MMTV-Cre* mice[[80] FVB] were purchased from the Jackson Laboratories. All analyses were performed on age-matched siblings resulting from F1 (1:1, FVB:C57BL/6) intercrosses.

PMEC and Organoid Cell Culture. Primary mammary organoids were generated from freshly collected, partially disaggregated mouse mammary glands using a modification of previously described methods [81]. Primary mouse mammary epithelial cells (PMECs) were harvested as described previously [82]. Organoids were immediately embedded in growth factor reduced Matrigel (BD Bioscience) at 50 organoids/100 μ l. Once polymerized, Matrigel-embedded cultures were overlain with Growth Media [DMEM:F12 supplemented with 5 μ g/ml porcine insulin (Sigma-Aldrich), 10 pg/ml each estrogen and progesterone (Sigma-Aldrich), 5 ng/ml human epidermal growth factor (R&D Systems), 100 I.U./ml penicillin-streptomycin (Life Technologies)].

PMECs were maintained in Growth Media. For some experiments, cells were maintained for 24 hour in Starvation Media [Growth Media supplemented with penicillin-streptomycin only] or treated with Fibroblast-Conditioned Media (DMEM:F12 supplemented 100 I.U./ml penicillin-streptomycin cultured with mouse mammary fibroblasts for 48 hours and passed through a 0.2 µm filter) for wound closure migration studies. Rapamycin (Sigma-Aldrich, 20 nM), In Solution Rac1 inhibitor (Calbiochem/Millipore, 20 µM), and adenoviral particles (Ad.Cre, Ad.LacZ, Ad.caRac1, Ad.Akt^{myr}, and Ad.PKCα, Vector Biolabs) were purchased. Freshly collected organoids were incubated with adenoviral particles (5 X 10⁸ particle forming units/ml) with constant rocking for 3-5 hours at 37°C, washed, and embedded in Matrigel.

Morphogenesis in organoids was scored by counting the number of branches/organoid in 10 or more organoids/culture condition. For structures that appeared more spherical and less branched (e.g. cultures treated with Ad.Cre or inhibitors), we counted bifurcations and/or small protrusions from ball-shaped structures as branches in order to be as rigorous and conservative in our quantifications as possible. Organoid size was scored using NIH Image J software to quantify pixel area in 10 or more organoids/culture condition.

MCF10A Cell Culture. MCF10A and MCF10A Rictor^{ZFN} were purchased from Sigma-Aldrich and cultured in Growth Medium [DMEM:F12 supplemented with 5% Horse Serum (Life Technologies), 10 µg/ml porcine insulin (Sigma-Aldrich), 20 ng/ml human epidermal growth factor (R&D Systems), 10 ng/ml cholera toxin (Sigma-Aldrich), 100 ng/ml hydrocortisone (Sigma-Aldrich), 100 I.U./ml penicillin-streptomycin (Life Technologies)].

For some experiments, cells were maintained for 24 hour in Starvation Media [Growth Media without serum or EGF] prior to stimulation and/or analysis. PKC α inhibitor GO6976 (Sigma-Aldrich, 2 μ M) and adenoviral particles (Ad.RFP and Ad.PKC α , Vector Biolabs) were purchased. Cells were incubated with adenoviral particles (5×10^8 particle forming units/ml) for 3-5 hours at 37°C and cells were allowed to recover for 48 hours prior to experimental analysis.

Immunofluorescence. Matrigel-embedded organoids cultured on coverslips were fixed 8 minutes in 1:1 methanol:acetone at -20°C, permeabilized in 0.5% Triton-X 100/PBS for 10 min, blocked [130 mM NaCl, 7 mM Na₂HPO₄, 3.5 mM NaH₂PO₄, 7.7 mM NaN₃, 0.1% bovine serum albumin, 0.2% Triton-X 100, 0.05% Tween-20] and stained with rabbit anti-pan-cytokeratin (Santa Cruz Biotechnology, 1:100) and AF621-goat anti-rabbit (1:100), counterstained with TO-PRO-3 Iodide (Invitrogen), and imaged using the Vanderbilt Cell Imaging Shared Resource Zeiss LSM 510 confocal microscope and LSM Image Browser software.

Western blotting. Cells and tissues were homogenized in ice-cold lysis buffer [50 mM Tris pH 7.4, 100 mM NaF, 120 mM NaCl, 0.5% NP-40, 100 μ M Na₃VO₄, 1X protease inhibitor cocktail (Roche)], sonicated 10 s, and cleared by centrifugation at 4°C, 13,000 x g for 5 min. Protein concentration was determined using BCA (Pierce).

Proteins were separated by SDS-PAGE, transferred to nitrocellulose membranes, blocked in 3% gelatin in TBS-T [Tris-buffered saline, 0.1% Tween-20], incubated in primary antibody overnight and in HRP-conjugated anti-rabbit or anti-mouse for 1 h, and developed using ECL substrate (Pierce).

Antibodies used: α -actin (Sigma-Aldrich; 1:10,000); AKT and S473 P-Akt (Cell Signaling; 1:2,000 and 1:500, respectively); S6 and P-S6 (Cell Signaling; 1:1,000); Rictor (Santa Cruz; 1:250); Raptor (Cell Signaling; 1:500); Rab11 (Cell Signaling; 1:1,000); PKC α and T638/641 P-PKC α (Cell Signaling; 1:2,000); Rac (BD Transduction; 1:200). GST-Pak-PBD effector pulldown assays were performed using reagents from Millipore as per manufacturer's protocol.

Histological analysis. Mammary glands were whole-mounted on slides, cleared of adipose, and stained with hematoxylin as described previously [82]. Sections (5- μ m) were stained with hematoxylin and eosin. *In situ* TUNEL analysis was performed on paraffin-embedded sections using the ApopTag kit (Calbiochem). IHC on paraffin-embedded sections was performed as described previously [83] using: Ki67 (Santa Cruz Biotechnologies), P-S6 (Cell Signaling Technologies); P-Akt S473 (Cell Signaling Technologies); Rictor (Santa Cruz), E-cadherin (Transduction Labs). Immunodetection was performed using the Vectastain kit (Vector Laboratories), AF488-conjugated anti-rabbit, or AF621-conjugated anti-mouse (Life Technologies), according to the manufacturer's directions.

In situ Rac-GTP assay. Methanol-fixed PMECs were probed 1 hour with GST-PBD (Millipore) diluted 1:50 in PBS. GST (lacking PBD) was used as a negative control. Samples were washed then probed with AF488-conjugated anti-GST (1:100), stained with DAPI or AF621-phalloidin, and mounted.

Transwell migration and wound closure assays. MECs (10^5) were added to upper chambers of Matrigel-coated transwells in starvation medium and incubated 5 h. Filters were swabbed and stained with 0.1 % crystal violet [84] and cells on the lower surface were counted. For wound closure, 50,000 MECs were plated on Matrigel-coated 24 well plates, grown to confluence, serum-starved for 24 hours, and wounded with a P200 pipette tip. Migration was scored by measuring the [width of the wound area at 24 hours] \div [width of the wound area at 0 hours] as described previously [85].

Microscope Image Acquisition. Mammary gland whole-mounts and transwell filters were imaged with Olympus SZX12 Inverted Microscope. Slides were imaged with Olympus BX60 Stereo Microscope. Organoids, annexin V-FITC-staining, and wound closure assays were imaged with Olympus IX71 Inverted Microscope. All images were acquired by Olympus DP 72 Digital Camera and CellSens software at ambient temperature.

Results

Rictor/mTORC2 regulates ductal branching, lengthening, and cell survival in the mammary gland in vivo

To assess the role of Rictor/mTORC2 during mammary morphogenesis in the context of the native mammary microenvironment, we bred *MMTV-Cre* mice [80] to *Rictor^{FL/FL}* mice [23], allowing mammary-specific Cre recombinase to disrupt Rictor expression at floxed (FL) *Rictor* alleles. Immunohistochemistry (IHC) for Rictor revealed expression in luminal and myoepithelial MECs in *Rictor^{+/+}MMTV-Cre (Rictor^{WT})* mice (**Figure 9A – upper panel**). Rictor expression was not seen in *Rictor^{FL/FL}MMTV-Cre (Rictor^{MGKO})* luminal MECs, and was slightly reduced in the myoepithelium, consistent with luminal but not myoepithelial Cre expression in *MMTV-Cre* mice. Akt phosphorylation at S473, the mTORC2 phosphorylation site, was decreased in MECs of *Rictor^{MGKO}* mice versus *Rictor^{WT}*, confirming decreased mTORC2 signaling upon Rictor ablation (**Figure 9A – lower panel**). Immunofluorescent (IF) staining for cytokeratin (CK)-8 and CK14, molecular markers of luminal and myoepithelial MECs, respectively, confirmed that Rictor loss did not affect the relative spatial organization of luminal and myoepithelial MECs (**Figure 9B – upper panel**), but revealed the presence of apically mis-localized nuclei in *Rictor^{MGKO}* MECs (yellow arrows), versus basally located nuclei and an organized, smooth apical border in *Rictor^{WT}* samples (white arrows).

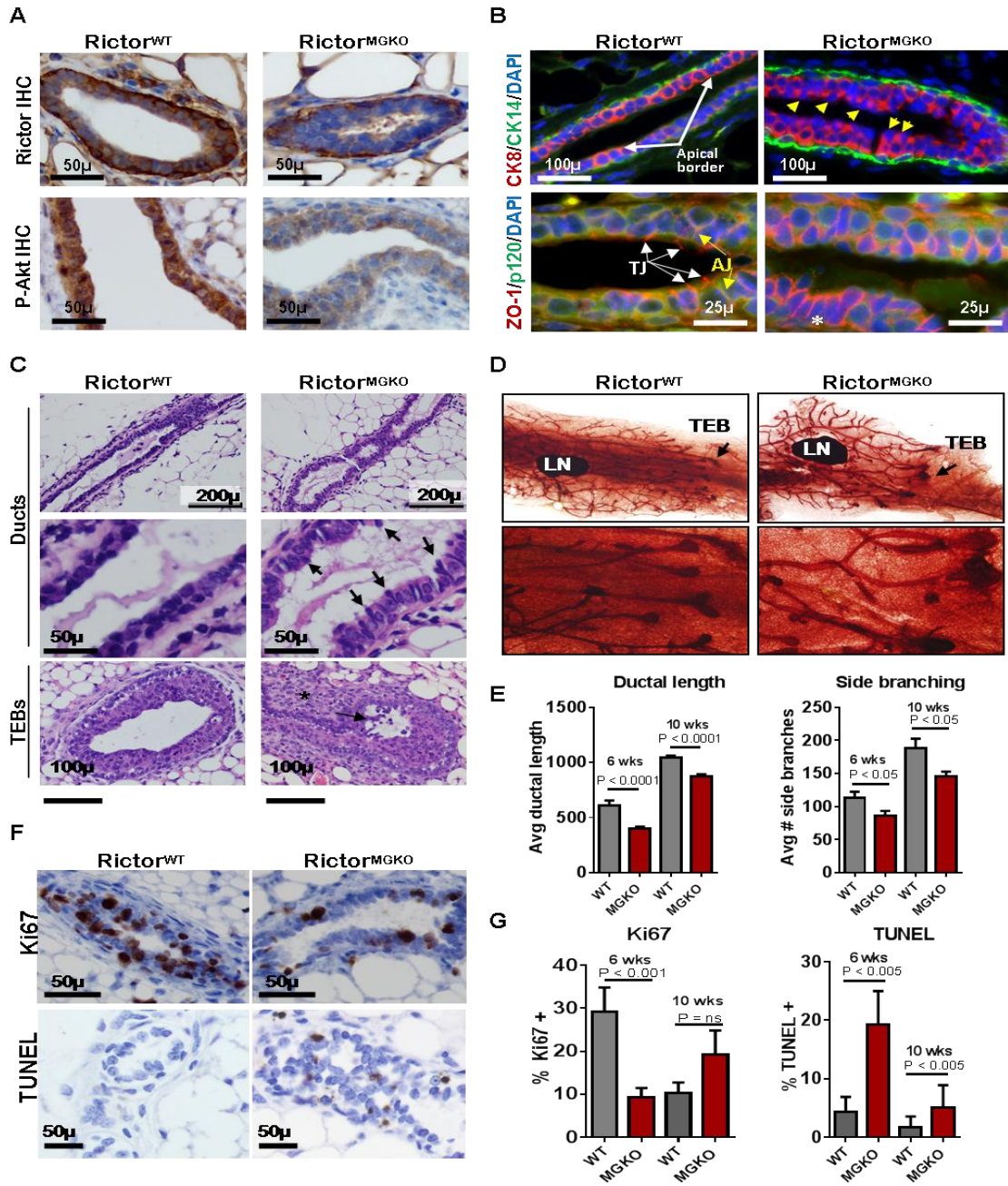


Figure 9. Loss of Rictor disrupts mammary branching morphogenesis *in vivo*. **A.** IHC for Rictor (upper panels) and P-Akt S473 (lower panels) in mammary gland sections from virgin mice. **B.** IF for CK8, CK14, ZO-1 and P120 in mammary gland sections. Yellow arrows indicate apically mis-localized nuclei in Rictor^{MGKO} tissue in upper right panel. White arrows indicate adherens junctions (AJ) in lower left panel. **C.** Hematoxylin and eosin (H&E)-stained mammary sections. Black arrows indicate irregular apical border in middle right panel. Black arrow indicates body cells sloughing in the TEM lumen and (*) indicates stromal thickening at the neck between the maturing duct and TEB. **D.** Whole mount H&E-stained mammary glands from 6-week virgin mice; lymph nodes (LN); terminal end buds (TEB's, arrows). **E.** Average ductal length (μm) beyond the mammary lymph node (left) and average number of side branches (right), \pm S.D. **F.** IHC for Ki67 (upper panels) and TUNEL (lower panels) in mammary glands from 6-week old mice. Representative images are shown. **G.** Average percent Ki67+ nuclei (left) or TUNEL+ nuclei (right) per total MEC nuclei, \pm S.D. N=10 mice for each genotype/time point. Student's T-test.

IF for the tight junction (TJ) protein Zona Occludens-1 (ZO-1) revealed apical ZO-1 localization in *Rictor*^{WT} samples. However, ZO-1 was aberrantly localized along baso-lateral membranes in *Rictor*^{MGKO} MECs (**Figure 9B – lower panel**). In contrast, the baso-lateral localization of the adherens junction (AJ) protein p120 was relatively unaltered by Rictor loss. These results suggest that Rictor loss disrupts the proper apical distribution of ZO-1 in MECs. The apically mis-localized nuclei apparent in histological mammary sections from 6-week old *Rictor*^{MGKO} female mice contributed to an irregular apical border (**Figure 9C, black arrows**). Additional structural alterations were seen in TEBs, including sloughing of body cells (the multi-layered TEB population comprised of mature and progenitor luminal MECs; **Figure 9C – lower panel, arrow**) within TEB lumens, and stromal thickening at the neck between maturing ducts and TEBs (**Figure 9C – lower panel, ***). Morphological alterations were seen throughout whole mounted, hematoxylin-stained *Rictor*^{MGKO} mammary glands (**Figure 9D, arrows, Figure 10A**). Because mammary ducts lengthen distally at a predictable rate during puberty, we measured ductal length in mammary glands from 6 week- (mid-puberty) and 10 week-old (late puberty) mice. Ductal length was significantly reduced in *Rictor*^{MGKO} mammary glands at both time points (**Figure 9E – left panel, Figure 10B**). Primary (Y-shaped) and side (T-shaped) branches were counted in each mammary gland, revealing a significant reduction in T-shaped side branches at 6 and 10 weeks of age in *Rictor*^{FL/FL}*MMTV-Cre* samples as compared to *Rictor*^{WT} (**Figure 9E – right panel**).

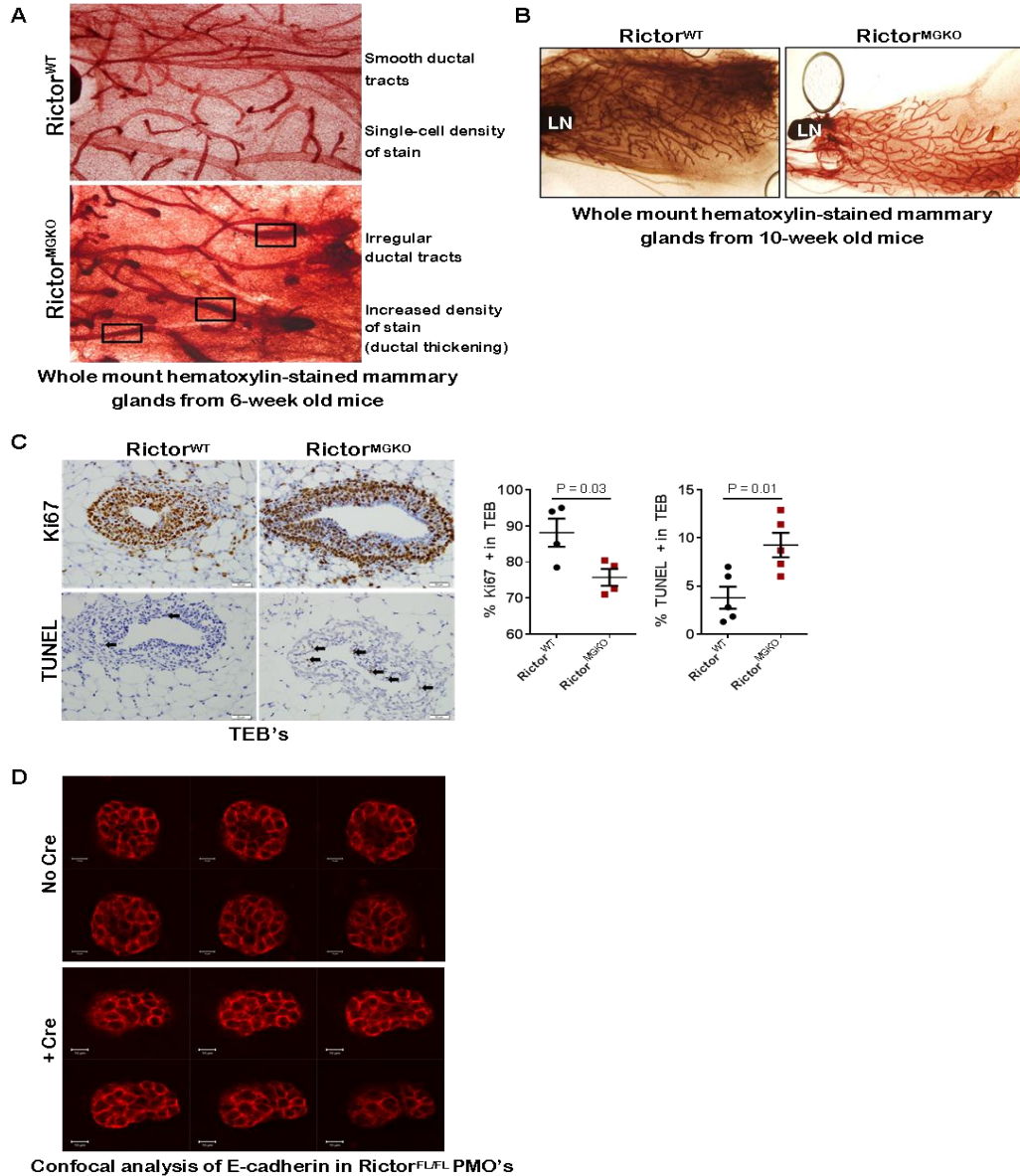


Figure 10. Loss of Rictor decreases proliferation and survival of MECs *in vivo*.
A. $Rictor^{WT}$ mice and $Rictor^{MGKO}$ mice. High magnification panels show irregular ductal tracts and increased staining density in $Rictor^{MGKO}$ samples, indicative of multiple cell layers. Data are a representation of 11 independent animals/genotype.
B. Hematoxylin stained whole mount preparations from 10-week-old wild-type $Rictor^{WT}$ mice and $Rictor^{MGKO}$ mice show sustained length defects in the ductal tracts of mammary glands lacking Rictor.
C. IHC for Ki67 or TUNEL in TEBs from 6-week-old wild-type $Rictor^{WT}$ mice and $Rictor^{MGKO}$ mice. Average percent Ki67 and TUNEL+ nuclei (\pm S.D.) was determined.
D. Confocal analysis of primary organoids (PMOs) stained for E-cadherin (red) revealed multiple cell layers in acinar structures and poor lumen formation in Rictor-deficient ($Rictor^{FL/FL}$ organoids infected with Ad.Cre) PMOs relative to control PMOs ($Rictor^{FL/FL}$ organoids infected with Ad.LacZ), consistent with the phenotype in $Rictor^{MGKO}$ epithelium *in vivo*.

IHC analysis of Ki67 in both ducts and TEBs was used as a relative measure of cellular proliferation in the mammary epithelium (**Figure 9F - upper panel, Figure 10C – upper panel**), revealing decreased Ki67+ nuclei in *Rictor*^{MGKO} samples as compared to *Rictor*^{WT} at 6 weeks of age but not at 10 weeks (**Figure 9G - left panel**). Cell death in ductal MECs or TEBs, measured using TUNEL analysis (**Figure 9F - lower panel, Figure 10C – lower panel**), demonstrated a remarkable increase in TUNEL+ MECs in *Rictor*^{MGKO} samples at 6 and 10 weeks of age (**Figure 9G - right panel**). These results demonstrate that Rictor loss impairs mTORC2 activity, P-Akt, MEC growth, and MEC survival during mammary morphogenesis.

Defects in MEC survival, branching, and motility are recapitulated by Rictor loss in an ex vivo model of mammary morphogenesis.

Western analysis of whole mammary lysates harvested from 10-week old female mice confirmed decreased P-Akt S473 in *Rictor*^{MGKO} mammary glands, and revealed increased phosphorylation of the mTORC1 effector ribosomal protein S6 [86] (**Figure 11A**) confirming that Rictor loss decreases mTORC2 activity, but not mTORC1. To dissect more precisely how Rictor signaling affects mammary morphogenesis, we used primary mammary epithelial cells (PMECs) and primary mammary organoids (PMO's) harvested from *Rictor*^{FL/FL} mice. Adenoviral infection of *Rictor*^{FL/FL} PMECs with Ad.Cre significantly reduced Rictor and P-Akt S473 levels relative to cells infected with control Ad.LacZ, and increased P-S6 levels (**Figure 11B**), similar to the impact of Rictor ablation *in vivo*.

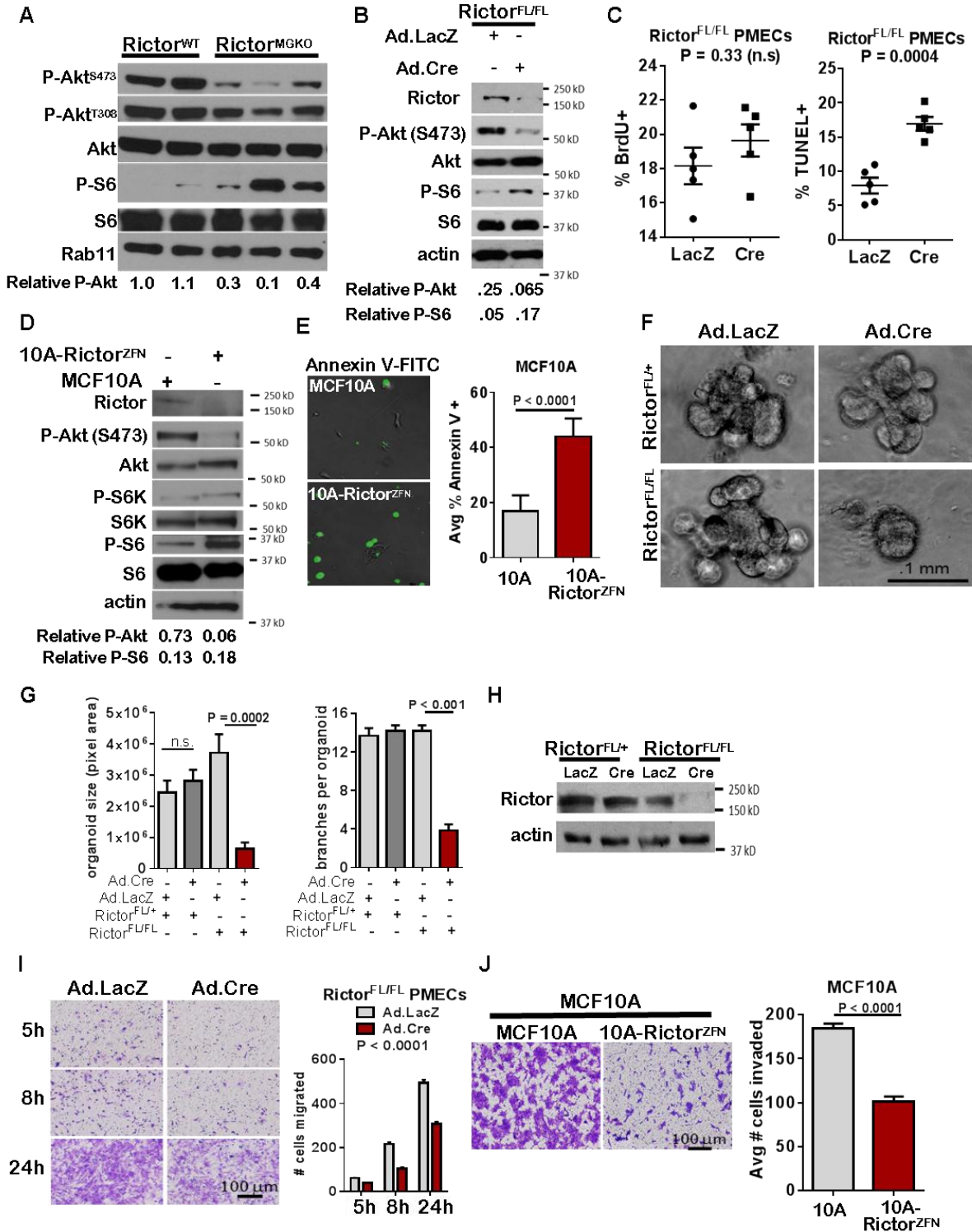


Figure 11. Impaired survival and morphogenesis of mammary epithelial structures upon loss of Rictor *ex vivo*. **A.** Western analysis of whole mammary lysates harvested from 10-week old female mice. **B-C.** *Rictor^{FL/FL}* PMECs were infected with Ad.Cre or Ad.LacZ and cultured 7 days. **B.** Western analysis of PMEC lysates under serum starved conditions. Quantitation was performed using Image J software and numbers represent P-Akt or P-S6 bands normalized to total Akt or S6 levels. **C.** BrdU+ (left) and TUNEL+ (right) nuclei relative to total nuclei were quantified. N = 5 epithelial isolates, each analyzed in triplicate. Midline values indicate average, whiskers indicate S.D., Student's T-test. **D-E.** MCF10A and MCF10A-Rictor^{ZFN} cells were analyzed. **D.** Western analysis of MCF10A lysates. **E.** Cells were labeled with Annexin V-FITC for 6 hours then photographed. Percent Annexin V+ cells versus total was quantified, average \pm S.D. shown. N = 3 independent experiments, each analyzed in quadruplicate, representative images shown, Student's T-test. **F-I.** *Rictor^{FL/FL}* PMECs and organoids were infected with Ad.Cre or Ad.LacZ. **F.** Organoids photographed after 10 days in Matrigel culture. Representative images are shown. **G.** Average organoid size, measured in pixel area using Image J software, \pm S.D. (left panel) and average number of branches/organoid \pm S.D. (right panel) are shown. N = 6 independent organoid isolates, analyzed in triplicate, Student's T-test. **H.** Western analysis of PMEC lysates. **I.** Transwell invasion of adenovirus-infected *Rictor^{FL/FL}* PMECs in response to serum at 24 hours. N = 6 PMEC isolates/condition, one-way ANOVA. **J.** Transwell invasion of MCF10A and MCF10A-Rictor^{ZFN} cells in response to serum at 24 hours is shown as average number of invading cells \pm S.D. N = 3, independent experiments, each analyzed in triplicate, Student's T-test.

Consistent with structural alterations were seen in our *Rictor*^{MGKO} model *in vivo* (e.g. sloughing of body cells in TEBs, irregular ductal tracts, multiple cell layers), confocal analysis of Rictor-deficient stained for E-cadherin revealed multiple cell layers in acinar structures and poor lumen formation relative to control PMOs infected with Ad.LacZ, which formed a well-defined lumen surrounded by a single layer of epithelial cells (**Figure 10D**). Rictor loss did not significantly impact PMEC proliferation, as measured by bromodeoxyuridine (BrdU) incorporation into genomic DNA (**Figure 11C – left panel**). However, the percentage of TUNEL+ PMEC nuclei was increased >2-fold following Ad.Cre infection (**Figure 11C – right panel**), consistent with increased cell death in Rictor-null MECs *in vivo*. Similar results were seen using MCF10A immortalized human MECs, in which *Rictor* gene targeting with *Rictor*-specific zinc finger nucleases (ZFNs) genetically impaired Rictor expression and decreased P-Akt S473 (**Figure 11D**), thus validating our findings in a human MEC model. Increased cell death was also seen in MCF10A-Rictor^{ZFN} cells as compared to parental MCF10A cells, as shown by Annexin V-FITC binding (**Figure 11E**). Therefore, Rictor is necessary for mTORC2 signaling and cell survival in human and mouse MECs.

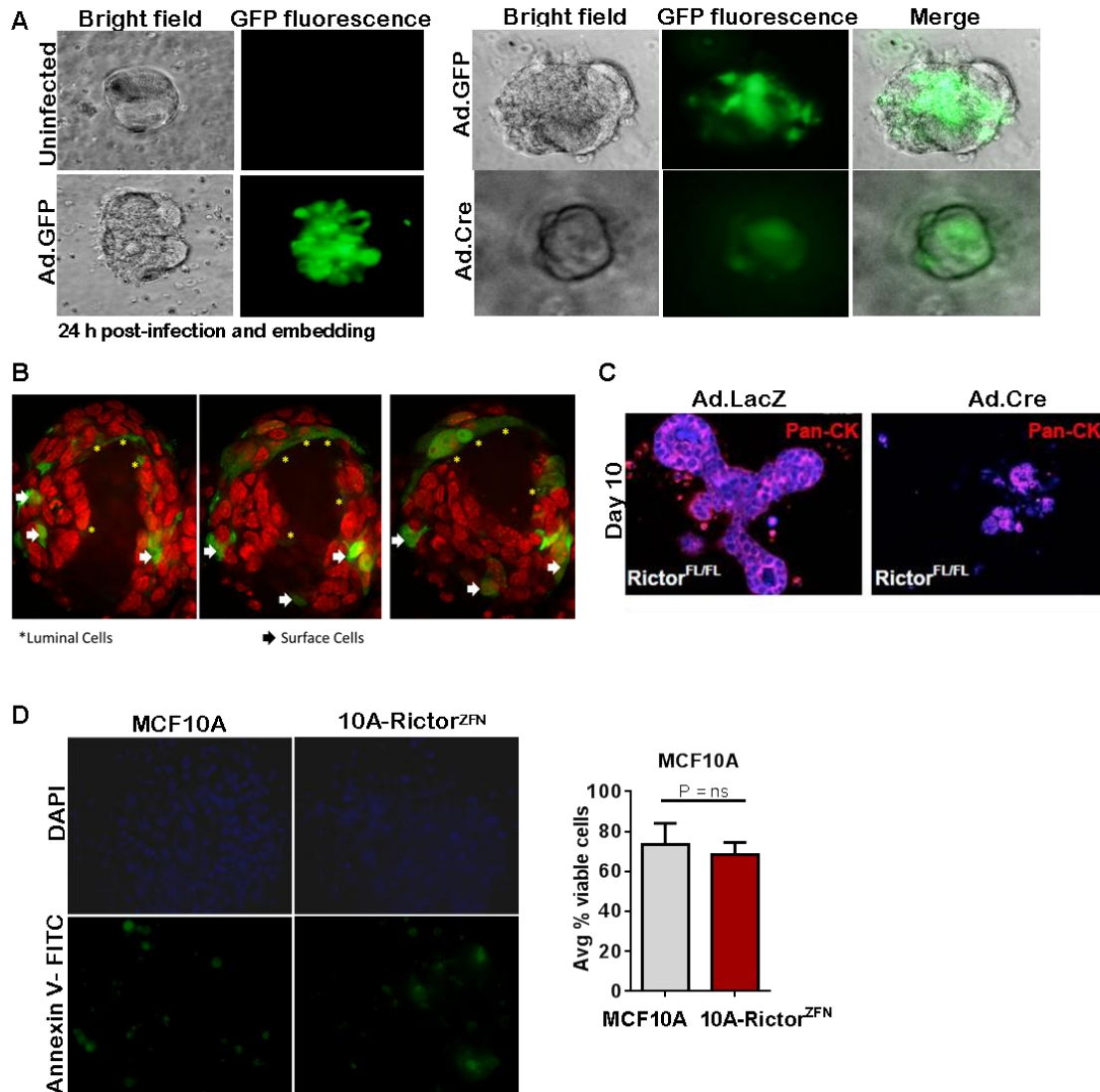


Figure 12. Loss of Rictor impairs branching and lumen formation in organoid culture. Primary organoids (PMOs) were isolated from *Rictor*^{FL/FL} mice and infected with Ad.GFP or Ad.Cre. **A.** Fluorescent imaging of organoids 24 hours post-infection. **B.** Confocal analysis of WT organoids infected with Ad.GFP. **C.** Organoids were fixed 10 days post-infection and subjected to immunofluorescent staining using a pan-cytokeratin antibody (red) to confirm epithelial identity and ToPro-3 nuclear marker (blue). While Ad.LacZ-infected *Rictor*^{FL/FL} organoids formed hollow lumens surrounded by an organized epithelial layer, Ad.Cre-infected *Rictor*^{FL/FL} organoids remained rounded and disorganized. Data are a representation of 3 independent organoid isolates. **D.** MCF10A parental or MCF10A-Rictor^{ZFN} cells were assessed for invasion through Matrigel-coated transwell filters. The cells remaining in the upper chamber after 24 hours were fixed and stained with either DAPI (blue) or Annexin V-FITC (green). The average percent viable cells (\pm S.D.) left in the upper chamber was quantitated using Image J, Student's T-test.

We cultured *Rictor*^{FL/FL} mammary organoids in three-dimensional (3D) Matrigel to assess collective epithelial morphogenesis (**Figure 11F**). Mammary organoids accurately model epithelial autonomous molecular events of mammary morphogenesis in a stroma-free environment that preserves the native relationship between luminal and myoepithelial MECs, and permits cell-cell and cell-matrix interactions in three dimensions [81]. GFP fluorescence in organoids infected with Ad.GFP or Ad.Cre-IRES-GFP confirmed efficient infection in basal and luminal cells of organoids (**Figure 12A, B**). IF staining for pan-cytokeratin confirmed that organoids were epithelial-derived (**Figure 12C**). Ad.Cre infection of *Rictor*^{FL/FL} PMECs substantially reduced organoid size and branching (**Figure 11F, G**) and reduced Rictor expression levels (**Figure 11H**). In contrast, Ad.Cre infection of *Rictor*^{FL/+} PMECs only modestly reduced Rictor expression levels (**Figure 11H**) and did not significantly affect organoid size or the number of branches formed in *Rictor*^{FL/+} organoids (**Figure 11F, G**). These data suggest that Rictor is necessary for multicellular morphogenesis of the mammary epithelium, faithfully recapitulating *ex vivo* the consequences of Rictor ablation that are seen *in vivo* and demonstrating the utility of this model to examine branching mammary gland morphogenesis.

Previous studies demonstrated that Rictor knock-down reduces migration of breast cancer cell lines [17, 55, 87]. We assessed PMEC invasion and motility through Matrigel-coated transwell filters upon Rictor ablation *ex vivo*. Fewer *Rictor*^{FL/FL} PMECs invaded through Matrigel when infected with Ad.Cre, as compared to *Rictor*^{FL/FL} PMECs infected with control Ad.LacZ (**Figure 11I**).

Similarly, invasion through Matrigel-coated transwells was profoundly reduced in MCF10A-Rictor^{ZFN} cells as compared to parental MCF10A cells (**Figure 11J**). Under these conditions, there were a similar number of viable cells remaining in the upper transwell chamber after 24 hours of culture of both MCF10A and MCF10A-Rictor^{ZFN} cells (**Figure 12D**), suggesting that cell death may not be the primary reason underlying the reduced ability of MCF10A-Rictor^{ZFN} cells to migrate/invade in these transwell assays, but rather that cell invasion, *per se*, is decreased in the absence of Rictor. Collectively, these data demonstrate that Rictor promotes MEC invasion and migration, two processes necessary for mammary ductal lengthening and branching.

Akt activation, while necessary for normal branching morphogenesis, is not sufficient to rescue morphogenesis, survival, and motility defects in the absence of Rictor

Because Rictor loss reduced P-Akt S473, we tested the hypothesis that Akt phosphorylation by Rictor-regulated mTOR complex 2 is necessary for survival and morphogenesis of MECs. Adenoviral expression of myristoylated Akt1 (Ad.Akt^{myr}) was used to express a membrane-localized (and thus, constitutively active) variant of Akt1. Indeed, expression of this Akt variant in mammary epithelium delays involution and the onset of apoptosis *in vivo* [38]. Additionally, we repeated experiments using an alternative adenoviral, constitutively active Akt construct Ad.Akt^{myr} or Ad.Akt^{DD} restored P-Akt S473 in Ad.Cre-infected *Rictor*^{FL/FL} PMECs (**Figure 13A, 14A**).

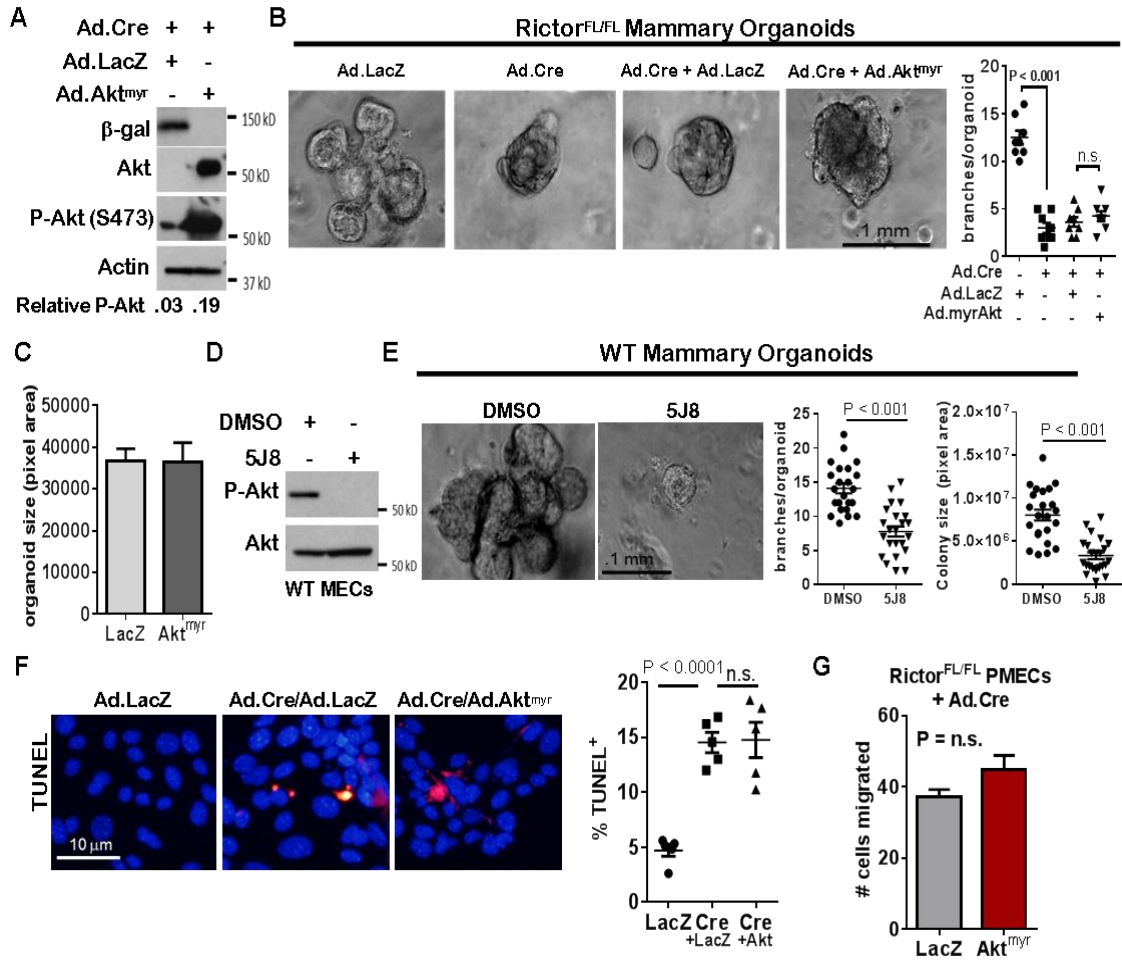


Figure 13. Akt activation is insufficient to rescue Rictor-deficient MEC survival, branch formation and invasion. A-C. PMECs and organoids from *Rictor^{FL/FL}* mice were co-infected with Ad.Cre and either Ad.LacZ or Ad.Akt^{myr}. **A.** Western analysis of PMEC lysates. **B.** Organoids photographed after 10 days in Matrigel culture. Average number of branches/organoid \pm S.D. (right panel) are shown. N = 20 independent organoids from 5 independent mice. Midline values indicate average (data points = averages from individual experiments), whiskers indicate S.D., Student's T-test. **C.** Colony size of organoids measured in pixel area. N = 20 independent organoids from 5 independent mice, average \pm S.D., Student's T-test. **D-E.** PMECs and organoids from *WT* mice treated 3-7 days with 5J8 Akt inhibitor or DMSO. **D.** Western analysis of PMECs after 3 days treatment with 5J8. **E.** Organoids photographed after 10 days in DMSO or 5J8. Average number of branches/organoid \pm S.D. (left panel) are shown. Midline values indicate average (data points = averages from individual experiments), whiskers indicate S.D., Student's T-test. Organoid size measured in pixel area shown in right panel Student's T-test. N = 23 independent organoids from 6 independent mice. **F-G.** PMECs from *Rictor^{FL/FL}* mice were co-infected with Ad.Cre and either Ad.LacZ or Ad.Akt^{myr}. **F.** PMECs were assessed by TUNEL analysis. Representative images are shown. Average percent TUNEL+ nuclei (red) per total nuclei (DAPI, blue) was calculated. Individual cell isolates (N = 5, analyzed in duplicate) are represented by each data point. Midlines values are average percentage of TUNEL+ nuclei \pm S.D., indicated by whiskers, Student's T-test. **G.** Transwell migration of PMECs at 24 hours. N = 6 independent cell isolates per condition, analyzed in duplicate, Student's T-test.

Surprisingly, *Rictor*^{FL/FL} organoids infected with Ad.Cre + Ad.Akt^{myr} or Ad.Akt^{DD} were morphologically similar, and harbored little to no statistically significant difference in the numbers of branches compared to those infected with Ad.Cre alone (**Figure 13B, 14B**). Further, size of Rictor-deficient organoids was not fully rescued by expression of Ad.Akt^{myr} or Ad.Akt^{DD} (**Figure 13C, 14C**). We found that blockade of Akt using the allosteric Akt inhibitor 5J8 blocked Akt phosphorylation at S473 (**Figure 13D**), reduced the number of branches per organoids, and reduced organoid size by nearly 50% (**Figure 13E**). These data suggest that while Akt is necessary for mammary branching and growth, restoring Akt function is not sufficient to completely rescue defects caused by loss of Rictor/mTORC2 function. Indeed, expression of Ad.Akt^{myr} did not reduce the number of Rictor-null PMECs undergoing cell death (**Figure 13F**), and did not increase the number Rictor-null PMECs invading through Matrigel-coated transwells (**Figure 13G**). Taken together, these observations suggest Rictor is necessary for Akt phosphorylation in MECs, but that Akt is not the primary effector of mTORC2 that regulates MEC survival, invasion, and side branching. Thus, while Akt is necessary for proper mammary epithelial morphogenesis, it is not sufficient to compensate for loss of Rictor/mTORC2 function.

Protein kinase C (PKC) - α activates the small GTPase Rac1 downstream of Rictor

Previous studies showed that mTORC2 phosphorylates PKC α [47]. Consistent with these findings, Rictor loss reduced P-PKC α in PMECs, as well as total PKC α (**Figure 15A**).

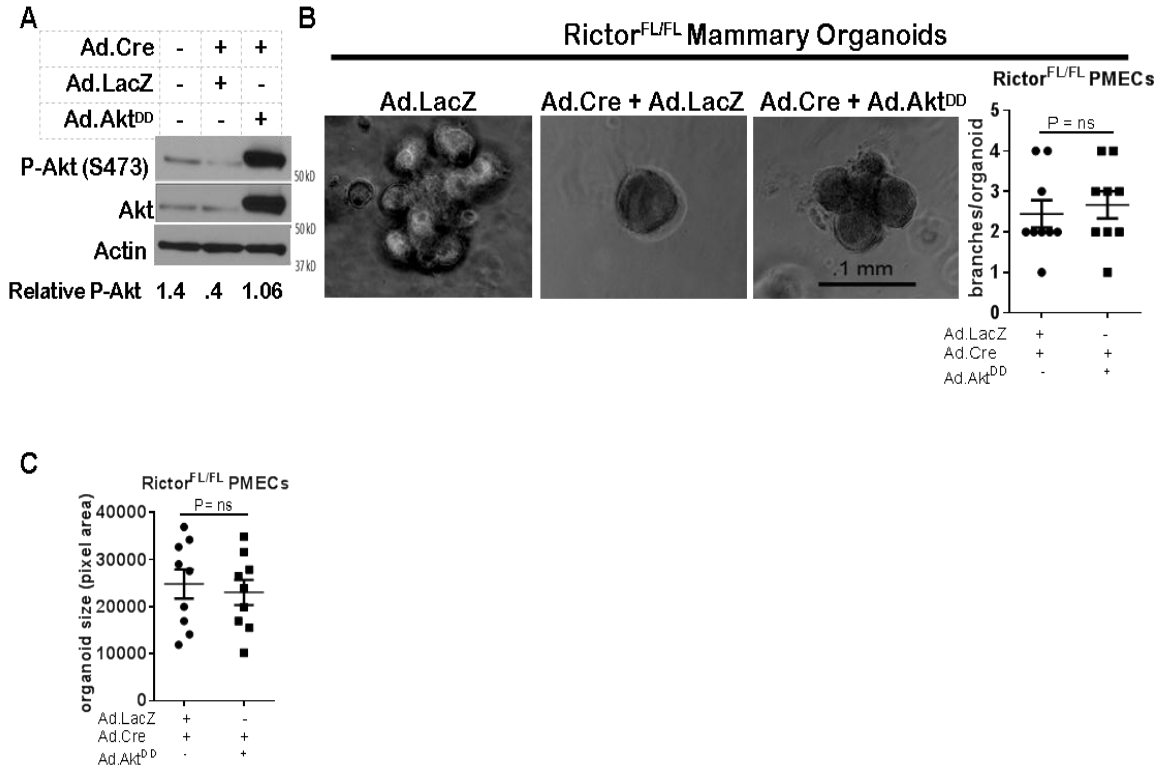


Figure 14. Akt activation is insufficient to rescue Rictor-deficient MEC branching *ex vivo*. **A-C.** PMECs and organoids from *Rictor^{FL/FL}* mice were coinfecting with Ad.Cre and either Ad.LacZ or Ad.Akt^{DD}. **A.** Western analysis of PMEC lysates. **B.** Organoids photographed after 10 days in Matrigel culture. Average number of branches/organoid \pm S.D. (right panel) is shown. N = 7 independent organoid isolates, analyzed in triplicate. Midline values indicate average, whiskers indicate S.D., Student's T-test. **C.** Colony size of organoids (\pm S.D.) measured in pixel area. N = 7 independent organoid isolates, analyzed in triplicate, Student's T-test.

We also observed decreased P-PKC α by IF in mammary gland sections from 6-week-old *Rictor*^{MGKO} mice, as compared to *Rictor*^{WT} controls (**Figure 17A**). Adenoviral PKC α expression rescued P-PKC α in Rictor-null PMECs (**Figure 15B**), rescued branching morphogenesis in Rictor-null organoids (**Figure 15C**) and increased Rictor-null organoid size (**Figure 15D**). Similar to what was seen in mouse PMECs, P-PKC α and total PKC α was diminished in MCF10A-Rictor^{ZFN} cells relative to parental MCF10A (**Figure 15E**). Restoration of PKC α by adenoviral transduction increased P-PKC α in both parental MCF10A and MCF10A-Rictor^{ZFN} cells (**Figure 15F**). Rac1, a small GTPase involved in actin cytoskeletal dynamics, is necessary for migration of many breast cancer cell lines, regulates apical polarity in MECs, and is a downstream effector of mTORC2 signaling. Importantly, Rac1 is also a known effector of PKC α in MECs [88-90], but the linear relationship between Rictor, PKC α , and Rac1 in MECs is currently unknown. We examined Rac1 activation in MCF10A cells using agarose beads conjugated to recombinant p21-activated kinase binding domain (PBD), which specifically binds to active GTP-bound Rac. Western analysis to detect Rac1 in PBD pull-downs revealed decreased Rac-GTP in MCF10A-Rictor^{ZFN} cells as compared to parental MCF10A (**Figure 15G**). However, Ad.PKC α increased Rac-GTP in Rictor-null cells, confirming that PKC α activates Rac downstream of Rictor. Additionally, Ad.PKC α increased invasion of MCF10A-Rictor^{ZFN} cells through Matrigel-coated transwells (**Figure 15H**), and significantly reduced apoptosis in MCF10A-Rictor^{ZFN}, as measured by Annexin V-FITC staining (**Figure 15I**).

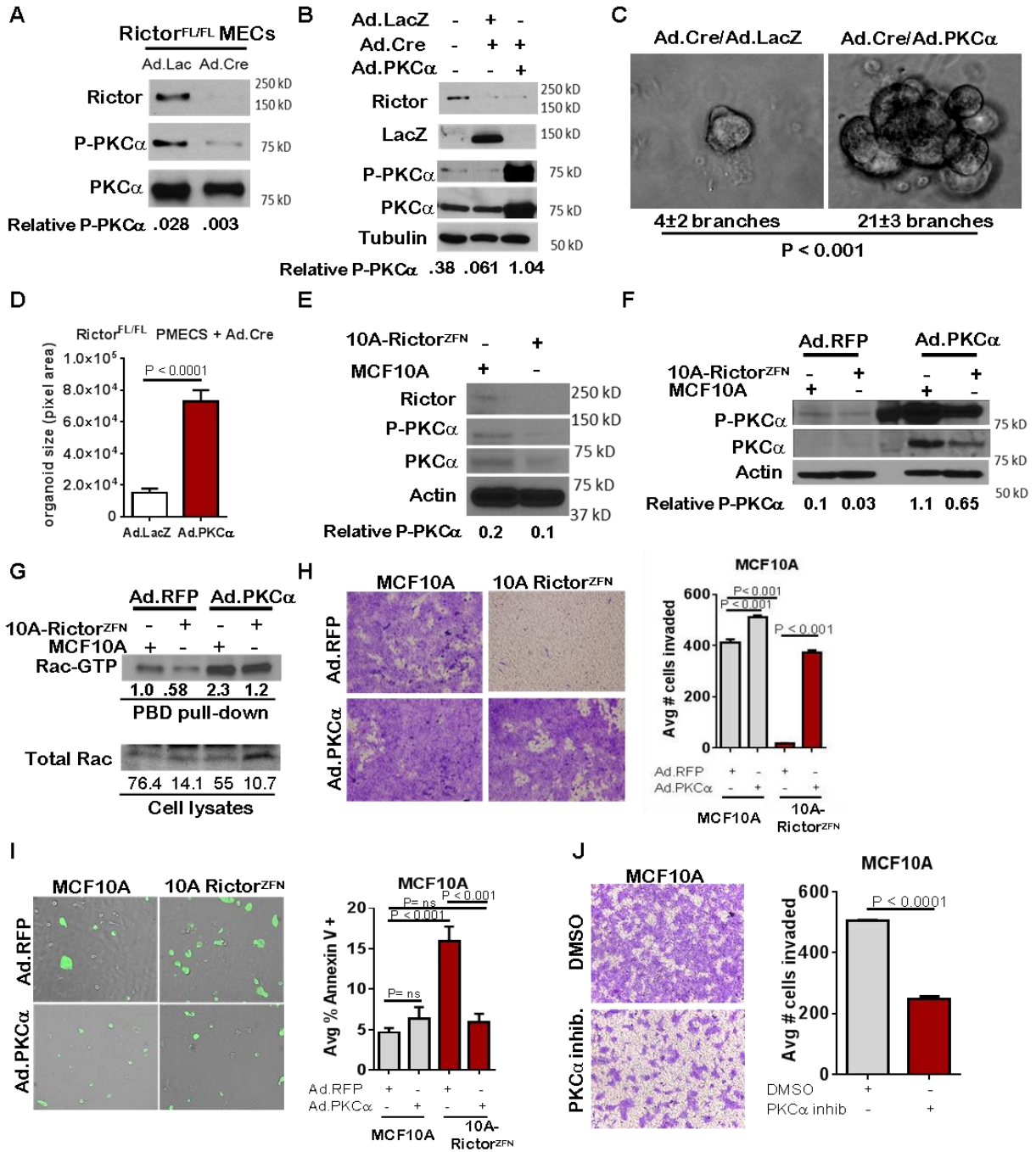


Figure 15. Loss of PKC α -mediated Rac activation in the absence of Rictor. A-D. *Rictor*^{FL/FL} PMECs and organoids were infected with the indicated adenoviruses. **A-B.** Western analysis of PMEC lysates. Quantitation was performed using Image J software and numbers represent P-PKC α bands normalized to total PKC α levels. **C.** Organoids photographed after 10 days in Matrigel culture. Average number of branches/organoid \pm S.D. indicated below panels. N = 3 independent organoid isolates/condition analyzed in triplicate, Student's T-test. **D.** Average colony size of organoids measured in pixel area \pm S.D. N = 3 independent organoid isolates/condition, analyzed in triplicate, Student's T-test. **E.** Western analysis of MCF10A parental and *Rictor*^{ZFN} lysates. Quantitation was performed using Image J software and numbers represent P-PKC α band normalized to actin for each sample. **F-I.** MCF10A parental and *Rictor*^{ZFN} cells were infected with Ad.RFP or Ad.PKC α . **F.** Western analysis of MCF10A parental and *Rictor*^{ZFN} lysates, 48 hours post-infection. Quantitation was performed using Image J software and numbers represent P-PKC α band normalized to actin for each sample. **G.** GST-Pak-PBD effector pull-downs followed by western analysis for Rac performed 48 hours post-infection. Quantitation was performed using Image J software. Numbers in upper panel represent Rac-GTP levels in MCF10A-*Rictor*^{ZFN} compared to MCF10A parental control. Lower numbers represent Rac-GTP levels normalized to total Rac for each sample. **H.** Cells were assessed for invasion through Matrigel-coated transwell filters. Cells were stained with crystal violet after 24 hours, and then imaged. Number of cells invading was quantitated in Image J. Values shown represent the average \pm S.D., Student's T-test. N = 2 independent experiments, analyzed in triplicate. **I.** Cells were assessed for Annexin V-FITC. Number of Annexin V-FITC+ per total number of cells was quantitated in Image J, Student's T-test. N = 2 independent experiments, analyzed in triplicate. **J.** MCF10A parental cells were assessed for invasion through Matrigel-coated transwell filters in the presence of PKC α inhibitor GO6976. Cells were stained with crystal violet after 24 hours, and then imaged. Number of cells invading was quantitated in Image J. Values shown represent the average \pm S.D., Student's T-test. N = 2 independent experiments, analyzed in quadruplicate.

A pharmacological PKC α inhibitor profoundly decreased invasion of parental MCF10A cells through Matrigel-coated transwells (**Figure 15J**), providing validation that PKC α is necessary for MEC motility. These data suggest Rictor-mediated PKC α signaling in MECs controls Rac1 activation, branching morphogenesis, cell survival and motility.

Restoring Rac activity rescues branching morphogenesis, survival, and motility induced by loss of Rictor

To confirm the role of Rictor in Rac1 activation *in vivo*, we examined mammary epithelium *in situ* for GTP-bound Rac1 using a glutathione-S-transferase (GST)-PBD fusion protein as a probe for Rac-GTP. IF detection of GST-PBD binding was decreased in *Rictor*^{MGKO} mammary glands compared to *Rictor*^{WT} (**Figure 16A, B, 17B**). Importantly, IF detection of GST-PBD binding in WT PMECs was abolished by a pharmacological Rac1 inhibitor (**Figure 16C, 17C**), confirming the specificity of the assay for detection of Rac1-GTP. In contrast to the abundant Rac1-GTP detected in WT PMECs, *Rictor*^{FL/FL} PMECs infected with Ad.Cre displayed a 10-fold decrease in GST-PBD binding to Rac-GTP relative to Ad.LacZ infected controls (**Figure 16C, 17C**). Phalloidin staining revealed cortical actin overlapping with GST-PBD binding in Ad.LacZ-infected *Rictor*^{FL/FL} PMECs (**Figure 17D**). However, Ad.Cre-infected *Rictor*^{FL/FL} PMECs showed increased formation of actin stress fibers, bearing no overlap with GST-PBD. Constitutively active Rac1 (Ad.caRac1) expression (**Figure 16D**) restored GST-PBD binding in Rictor-null PMECs (**Figure 16E**), suggesting that Rictor is necessary for Rac1-GTP in PMECs.

Ad.caRac1 was used to determine if restoration of Rac1-GTP could rescue invasion in Rictor-null MECs. Ad.caRac1 increased invasion 2.5-fold over Ad.LacZ in Rictor-null PMECs (**Figure 16F**). P-Akt S473 was unaffected by caRac1 (**Figure 16D**), suggesting that while Akt and Rac1 are both effectors of Rictor-dependent signaling, they exist in two separable pathways in MECs. Despite having no impact on P-Akt, Ad.caRac1 decreased cell death in Rictor-null PMECs (**Figure 16G, 17E**), suggesting that Rictor-dependent Rac1-GTP is necessary for PMEC survival. Ad.caRac1 also rescued branching morphogenesis of Rictor-deficient organoids (**Figure 16H**). Conversely, Rac inhibition using a pharmacologic Rac1 inhibitor decreased organoid size and branching in *WT* organoids (**Figure 16I**), confirming that Rac1 is necessary for mammary epithelial branching morphogenesis. Thus, Rictor is required for Rac1-GTP signaling, and restoration of Rac1 activity rescued branching morphogenesis and survival of Rictor-deficient PMECs. To determine if Rictor/mTORC2-mediated branching morphogenesis and ductal outgrowth are dependent on PKC α /Rac versus Akt, we transduced PMEC from *Rictor*^{FL/FL} mice with control Ad.GFP versus Ad.Cre in the presence or absence of Ad.PKC α , Ad.caRac, or Ad.Akt^{myr} and transplanted them into the cleared inguinal mammary fat pads of 4-week-old recipient female mice. We harvested mammary glands from these animals 6 weeks post-transplantation and assessed epithelial architecture and branching morphogenesis in whole-mount preparations. Consistent with data from *MMTV-Cre/Rictor*^{FL/FL} mice, transplanted Rictor-deficient MEC produced structures characterized by shortened ductal outgrowths with fewer branches relative to GFP controls (**Figure 16J, K**).

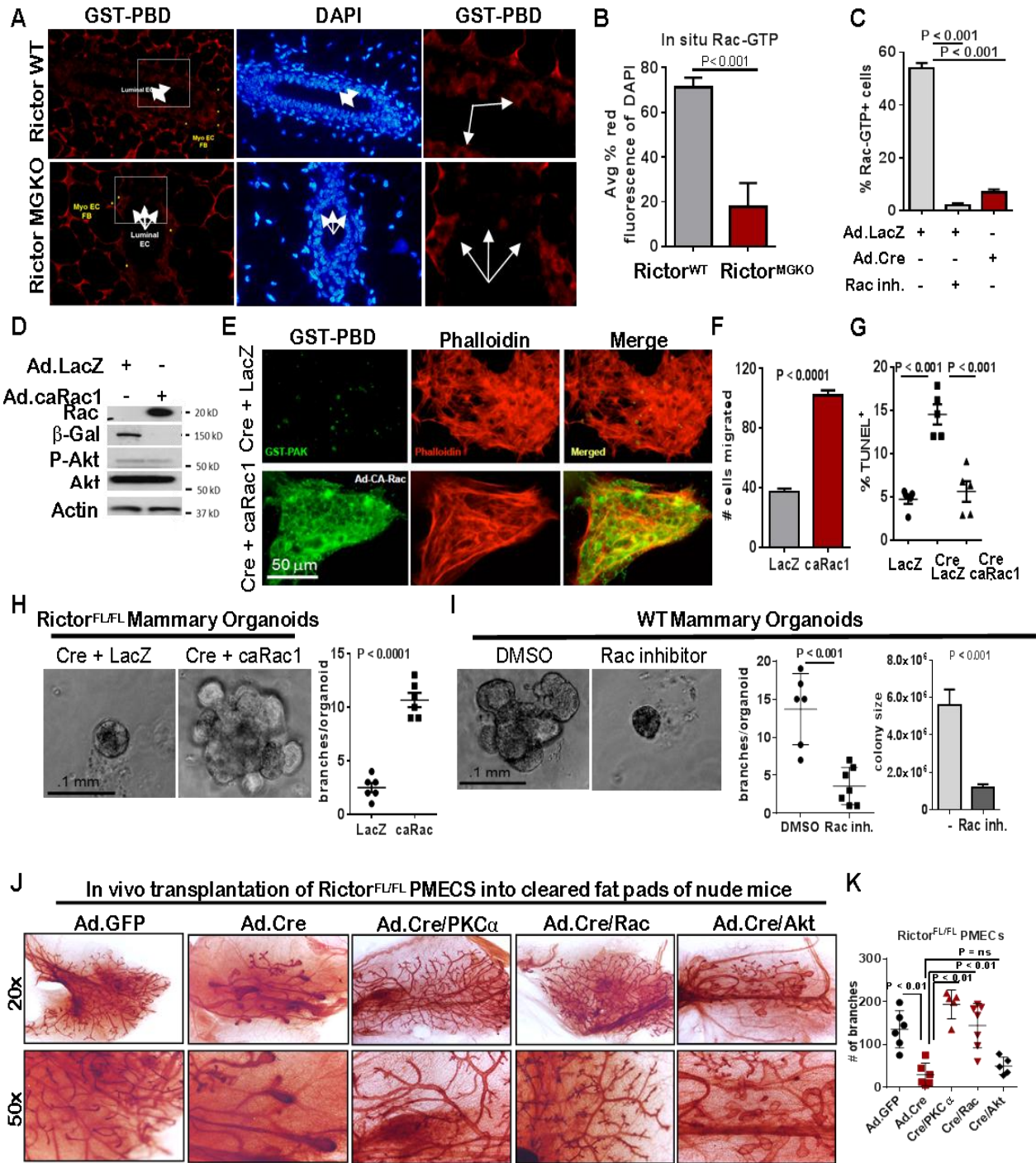


Figure 16. Rictor-mediated Rac activity is necessary and sufficient for mammary branching morphogenesis ex vivo. **A.** *In situ* detection of GTP-bound Rac via IF detection of GST-PBD (red; nuclei stained with DAPI, blue) on mammary gland sections from 6-week old mice. N = 6 independent fields analyzed in sections from 3 independent mammary gland sections/genotype. **B.** Quantitation of average percent red fluorescence (Rac-GTP) relative to blue (DAPI) on mammary gland sections from 6 week old virgin *Rictor*^{WT} and *Rictor*^{MGKO} mice, ± S.D. **C.** Cells were probed with GST-PBD (red) and counterstained with DAPI (blue). GST alone (not conjugated to PBD) was used as a negative control. GST-PBD+ fraction of total PMECs was counted and average ± S.D. shown. N = 15 fields/condition. **D-I** *Rictor*^{FL/FL} PMECs infected with Ad.Cre or Ad.LacZ (±Ad.caRac1) and analyzed. **D.** Western analysis of PMEC lysates. **E.** Cells were probed with GST-PBD (green) and counterstained with phalloidin (red). **F.** Transwell invasion assays were performed. Invading cells were visualized with crystal violet and counted ±S.D. N = 6 independent isolates, analyzed in duplicate, Student's T-test. **G.** PMECs were assessed by TUNEL analysis. N = 3 independent cell isolates, analyzed in duplicate. Representative images shown. Average percent TUNEL+ nuclei per total epithelial nuclei quantified. Midline values indicate average, whiskers indicate S.D., Student's T-test. **H.** *Rictor*^{FL/FL} organoids were infected Ad.Cre or Ad.LacZ (±Ad.caRac1) prior to embedding, and were photographed after 10 days in Matrigel culture. Right panel shows average number of branches per organoid. Each data point is the average branches per colony from individual isolates, analyzed in triplicate. Midlines are the average of all isolates, whiskers indicate S.D., Student's T-test. N = 6. **I.** WT organoids were cultured ±Rac inhibitor for 10 days. Number of branches per organoid quantified. Right panel shows average organoid size ±S.D. **J-L.** PMECs from *Rictor*^{FL/FL} mice were transduced with control Ad.GFP versus Ad.Cre in the presence or absence of Ad.PKCα, Ad.caRac, or Ad.Akt^{myr}. PMECs were transplanted into the cleared inguinal fat pads of 4-week-old recipient female mice. Mammary glands were harvested six weeks post-transplantation and epithelial architecture and branching morphogenesis in whole-mount preparations was assessed. **J.** Whole-mount preparations from indicated transplanted glands. **K.** Quantitation of average number of branches ± S.D., Student's T-test. Representative images shown from N=2 independent experiments. **L.** Western analysis of lysates from donor PMECs.

Restored PKC α or Rac activity (**Figure 16J, K**) rescued these defects and produced epithelial outgrowth that resembled endogenous epithelium in contralateral controls (**Figure 17F**). Consistent with our *ex vivo* organoid culture analyses restored Akt activity was unable to fully rescue defects produced by loss of Rictor (**Figure 16J, K**). These data suggest that Rictor/mTORC2-dependent mammary epithelial morphogenesis relies primarily upon downstream activation of PKC α and Rac-GTPase.

Rapamycin-mediated inhibition of mTORC1 and mTORC2 mimics loss of Rictor/mTORC2

Rapamycin is a pharmacologic inhibitor of mTOR originally thought to preferentially inhibit mTORC1 over mTORC2. However, sustained rapamycin treatment impairs both mTORC1 and mTORC2 in a cell type-dependent manner [66, 91-93]. Consistent with this idea, acute rapamycin treatment for 1 hour (1 h) decreased P-S6 (an mTORC1 effector) but not P-Akt (an mTORC2 effector), whereas sustained rapamycin treatment (24 h) decreased both P-S6 and P-Akt S473 (**Figure 18A**). Rapamycin treatment for 10 days significantly decreased branching morphogenesis and organoid size in *WT* organoids (**Figure 18B**). Although PMEC survival was not affected by acute rapamycin treatment, cell death increased after 24 h with rapamycin (**Figure 18C**).

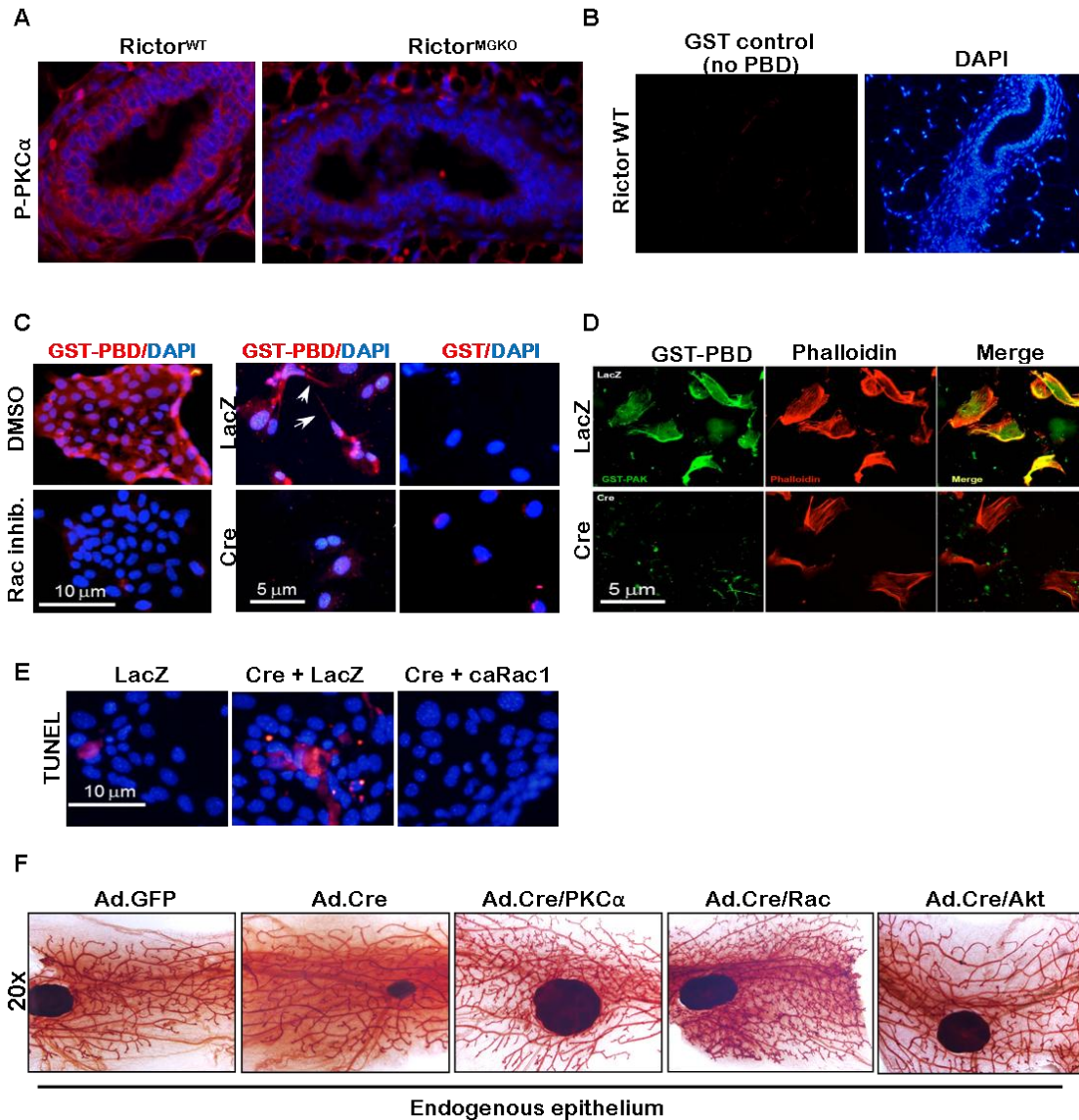


Figure 17. Rictor-mediated PKC α activation controls acinar formation and motility in human and mouse MECs. **A.** Immunofluorescent detection of P-PKC α in mammary gland sections from 6 week old virgin *Rictor*^{WT} and *Rictor*^{MGKO} mice. **B.** *In situ* detection of GTP-only control (no PBD) via IF detection of GST-PBD (red; nuclei stained with DAPI, blue) on mammary gland sections from 6-week old mice. **C.** WT PMECs cultured \pm Rac inhibitor or *Rictor*^{FL/FL} PMECs infected with Ad.LacZ or Ad.Cre were assessed for GTP-bound Rac via IF detection of GST-PBD (red; nuclei stained with DAPI, blue). **D.** *Rictor*^{FL/FL} PMECs infected with Ad.Cre or Ad.LacZ were probed with GST-PBD (green) and counterstained with phalloidin (red). Representative images are shown. **E.** *Rictor*^{FL/FL} PMECs infected with Ad.Cre or Ad.LacZ (\pm Ad.caRac1) were analyzed for TUNEL. **F.** Whole mount analysis of endogenous mammary glands harvested from WT recipient mice.

Proliferation of *WT* PMECs, as measured by BrdU incorporation, was unaffected by acute (30 min) or sustained (24 h) pre-treatment with rapamycin (**Figure 18D**). The effects of sustained rapamycin treatment, including reduced MEC survival, branching morphogenesis formation, and diminished organoid size were similar to the effects achieved by Rictor ablation in MECs. Also similar to what was seen with Rictor-deficient MECs, the phenotypic effects of rapamycin treatment were rescued by Ad.PKC α (**Figure 18E**) and Ad.caRac1 (**Figure 18F**), including rescue of branching morphogenesis and colony size. Ad.caRac1 also rescued rapamycin-mediated inhibition of cell motility (**Figure 18G**). Because the mTOR inhibitor rapamycin impairs mTORC1 and mTORC2, and recapitulates the morphological and molecular effects of Rictor ablation in MECs, these results suggest that Rictor is acting in complex with mTOR to regulate MEC survival, motility, and branching morphogenesis, supporting a role for mTORC2 in the developing mammary gland. However, these findings do not rule out the contribution of mTORC1 to mTOR-mediated mammary morphogenesis.

Raptor/mTORC1 loss produces relatively mild defects in mammary branching morphogenesis and epithelial growth in vivo and ex vivo

To understand how mTORC1 participates in mammary morphogenesis, we infected PMECs harvested from female *Raptor*^{FL/FL} mice [19] with Ad.Cre. Western analysis confirmed loss of Raptor and decreased P-S6 in serum-deprived cells (**Figure 19A**).

Figure 18. mTOR inhibition with rapamycin decreases MEC survival, motility and acinar formation, which are rescued by enforced Rac activity A-G. *WT* PMECs and organoids were cultured in DMSO vehicle or rapamycin. PMECs were cultured 0, 0.5, or 24 hours. Organoids were cultured 10 days in Matrigel in the presence of DMSO or rapamycin. **A.** Western analysis of PMEC lysates. Quantitation was performed using Image J software and numbers represent P-Akt, P-S6, or P-PKC α bands normalized to total Akt, S6, or PKC α levels. **B.** *WT* organoids photographed after 10 days in Matrigel culture. Average organoid size scored as average pixel area \pm S.D., Student's T-test, N = 6 epithelial isolates, each analyzed in triplicate. **C.** TUNEL analysis of PMECs. Average percent TUNEL+ nuclei per total PMEC nuclei \pm S.D. is shown, Student's T-test. N = 3 independent cell isolates, analyzed in duplicate. **D.** PMECs were labeled with BrdU after initial pre-treatments with rapamycin for 0.5 hours or 24 hours. Average percent BrdU+ nuclei per total nuclei \pm S.D. is shown, One-way ANOVA, N = 3 independent cell isolates, analyzed in triplicate. **E-F.** Organoids were infected with Ad.LacZ or Ad.PKC α (panel E) or Ad.caRac1 (panel F) prior to embedding in Matrigel plus rapamycin or DMSO. Average number of branches/colony is shown below each image. Average organoid size scored as average pixel area \pm S.D., Student's T-test (E) and one way ANOVA (F), N = 6 epithelial isolates, each analyzed in triplicate. **G.** Confluent PMEC monolayers were scratch-wounded, cultured in rapamycin or DMSO, and imaged at 24 hours. Total wounded area remaining after 24 h was measured. Values shown are the average wound area remaining \pm S.D. N = 3 independent cell isolates, analyzed in triplicate.

However, P-Akt S473 was unaffected by Raptor ablation, confirming that genetic ablation of Raptor causes selective inhibition of mTORC1, while Rictor ablation inhibits mTORC2. *Raptor*^{FL/FL} mammary organoids infected with Ad.LacZ formed multi-branched colonies, as expected (**Figure 19B**). Surprisingly, infection with Ad.Cre did not affect branching morphogenesis in *Raptor*^{FL/FL} organoids, the number of branches per organoid, or colony size (**Figure 19B**). Additionally, Raptor ablation had no significant impact on PMEC migration in wound healing assays (**Figure 19C**).

Raptor^{FL/FL}MMTV-Cre (*Raptor*^{MGKO}) mice were used to assess the impact of Raptor ablation on mammary morphogenesis *in vivo*. IHC detected Raptor and the mTORC1 effector P-S6 in *Raptor*^{WT} mammary glands at 10 weeks of age but did not detect P-S6 in age-matched *Raptor*^{MGKO} mice (**Figure 19D**). Immunofluorescent (IF) staining for cytokeratin (CK)-8 and CK14, molecular markers of luminal and myoepithelial MECs, respectively, confirmed that Raptor loss did not affect the relative spatial organization of luminal and myoepithelial MECs (**Figure 20A – upper panel**). Additionally, no alterations in localization or staining pattern of ZO-1 were observed (**Figure 20A – lower panel**). Proliferation, as measured by IHC for Ki67, was significantly decreased in *Raptor*^{MGKO} ducts in 6-week old mice (**Figure 19D**), but not in TEBs (**Figure 20C**). By 10 weeks, however, proliferation in ducts had recovered to levels seen in *Raptor*^{WT} (**Figure 19D**). TUNEL analysis revealed similar ratios of TUNEL+ MECs in ducts from *Raptor*^{MGKO} and *Raptor*^{WT} samples harvested from 6 and 10 week old animals (**Figure 19D**) and in TEBs from 6 week- old animals (**Figure 20B**).

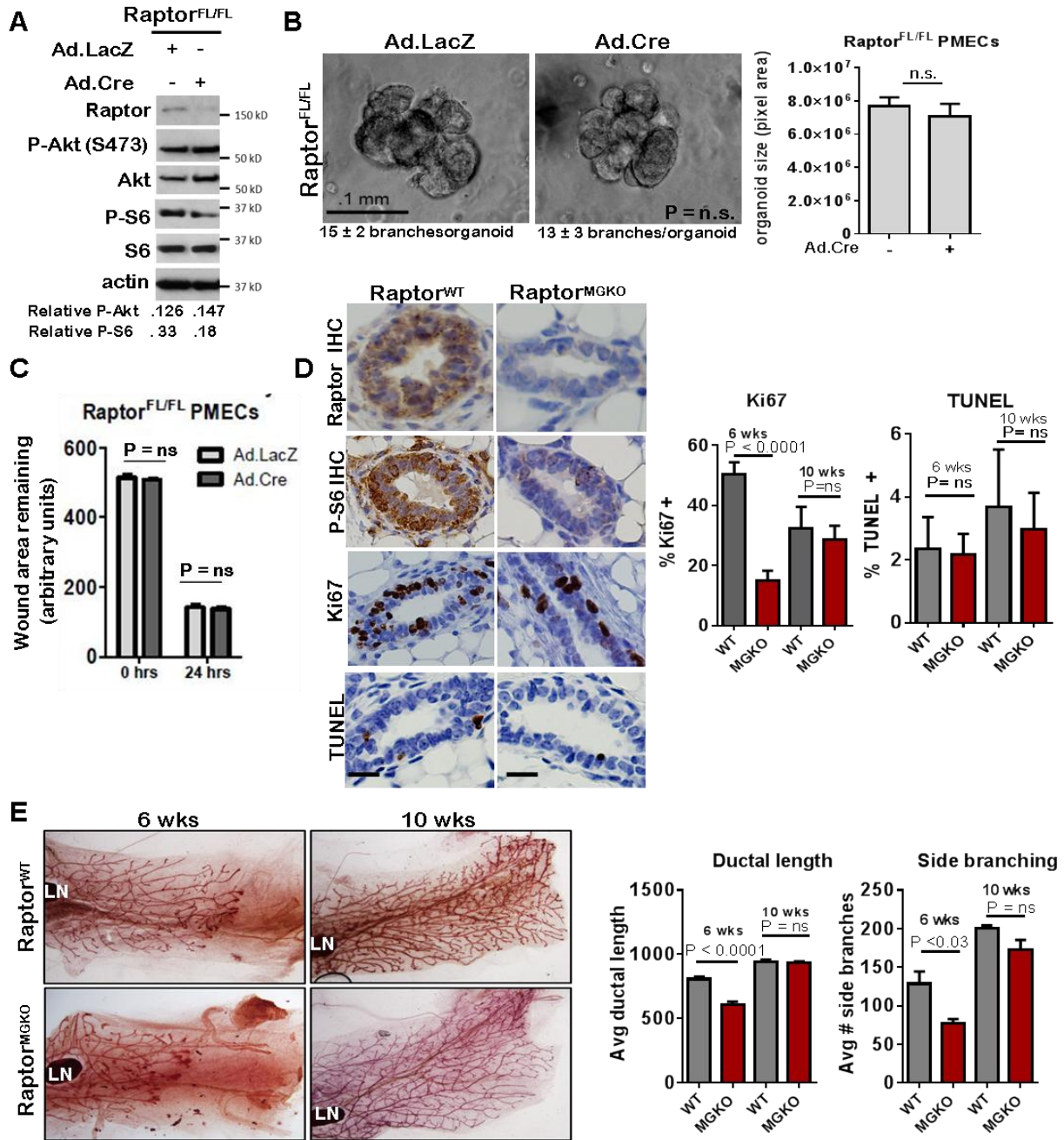


Figure 19. Unlike mTORC2, mTORC1 is dispensable for MEC survival and branching morphogenesis. **A-C.** *Raptor^{FL/FL}* PMECs and organoids were infected with Ad.Cre and Ad.LacZ, and cultured 10 days. **A.** Western analysis of PMECs cultured in the absence of serum. Quantitation was performed using Image J software and numbers represent P-Akt or P-S6 bands normalized to total Akt or S6 levels. **B.** Organoids were infected with Ad.Cre or Ad.LacZ photographed after 10 days in Matrigel culture. Representative images are shown. Average number of branches/organoid for each group is shown below the image. Average organoid size (pixels) \pm S.D. is shown, Student's T-test. N = 6 independent organoid isolates, analyzed in triplicate. **C.** PMECs from *Raptor^{FL/FL}* mice were infected with Ad.LacZ or Ad.Cre, grown to confluence and scratch-wounded. Monolayers were imaged. Total wound area remaining was measured 24 hours after wounding. Values shown are the avg \pm S.D. N=6 per time point, Student's T-test. **D-E.** Mammary glands from virgin female mice at 10 weeks of age were analyzed. N = 10 mice per genotype at each time point. Statistical analysis performed with Student's T-test. **D.** IHC for Raptor, P-S6, Ki67+, and TUNEL+ nuclei in mammary glands of 6-week old mice. Representative images are shown. Scale bars = 50 μ m. Average percent Ki67+ nuclei and TUNEL+ nuclei (\pm S.D) per total epithelial nuclei was determined **E.** Whole mount hematoxylin staining of mammary glands. Representative images are shown. LN = lymph node. The ductal length beyond the lymph node was measured. Average length (in microns) \pm S.D. is shown. The number of T-shaped side branches was enumerated. Values shown represent average number of side branches \pm S.D.

Consistent with these observations, only mild defects in side branching and ductal length were found in mammary glands from 6-week old *Raptor*^{MGKO} mice (**Figure 19E**), and these were resolved by 10 weeks of age.

Taken together, these results demonstrate that mTOR uses Rictor to activate PKC α /Rac1-dependent survival, motility, and branching morphogenesis in the mammary epithelium and that Rictor does not rely fully on Akt signaling to promote ductal morphogenesis in the breast.

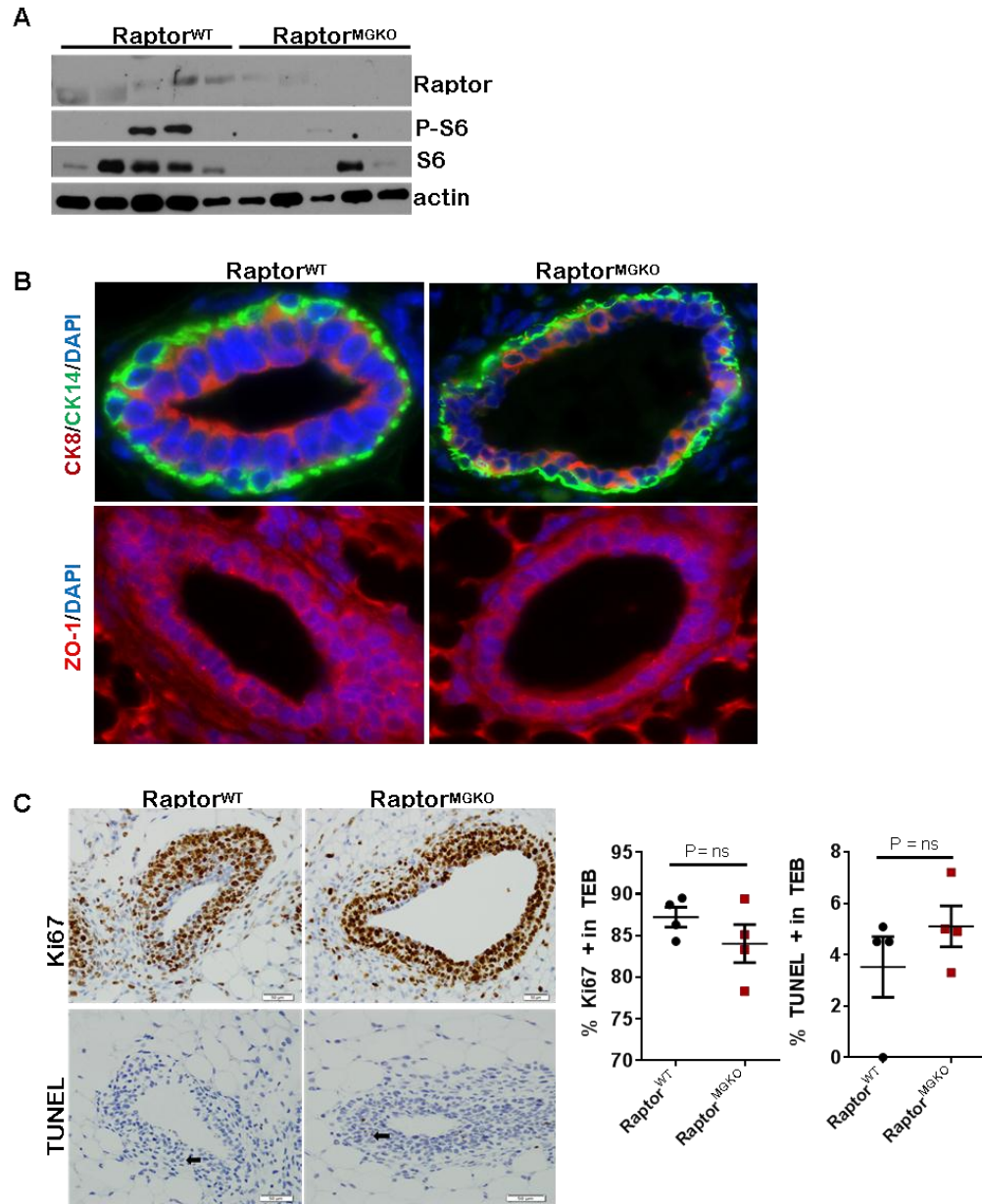


Figure 20. Unlike mTORC2, mTORC1 is dispensable for MEC survival *in vivo*. **A.** IF for CK8, CK14 and ZO-1 in mammary gland sections. **B.** IHC for Ki67 or TUNEL in TEBS from 6-week-old wild-type *Raptor*^{WT} mice and *Raptor*^{MGKO} mice. Average percent Ki67+ and TUNEL+ nuclei (\pm S.D.) was determined, Student's T-test.

Discussion

Postnatal mammary epithelial morphogenesis requires precise coordination of cell proliferation, apoptosis, differentiation, and motility in order to turn rudimentary epithelial buds into an organized, branched ductal network permeating the entire mammary fat pad by the end of puberty [34, 35]. mTOR is a central regulator of proliferation, apoptosis, differentiation, and motility, integrating numerous upstream signals to generate the desired biological outcome. Therefore, we assessed how mTOR signaling contributes to mammary morphogenesis. We found that pharmacologic mTOR inhibition reduced the size and branching complexity of mammary organoids in culture, phenotypes recapitulated by mTORC2 loss of function via *Rictor* ablation, but not upon mTORC1 inhibition through *Raptor* ablation. We also observed a disorganized epithelial architecture and stromal thickening around TEB upon tissue-specific *Rictor* ablation. The MMTV-Cre model has been reported to be leaky, leading to expression in tissues other than luminal mammary epithelium [94] thus it is possible that some of these defects may be due to loss of Rictor in stromal components. Alternatively, changes in basal epithelium may be a secondary effect of luminal cell mislocalization in the absence of Rictor, or Rictor expression in the luminal compartment may regulate expression and function of mTOR signaling intermediates in the basal cell layer through an indirect, juxtacrine signaling mechanism. We are actively investigating the role of Rictor/mTORC2 in luminal versus basal epithelium in our ongoing research.

As our epithelial branching and survival phenotypes were recapitulated in the *ex vivo* stroma-free organoid culture model, however, it is likely that the effects on stroma are, at least in part, secondary to the loss of Rictor in epithelium.

Genetic inhibition of mTORC2 also reduced ductal branching and lengthening *in vivo*, diminished P-Akt and P-PKC α , and impaired activation of the GTPase Rac1. Akt restoration only modestly enhanced branching morphogenesis in Rictor-deficient mammary organoids and was not sufficient to rescue cell survival or PMEC invasion through Matrigel. However, Akt inhibition did decrease organoid branching and colony size suggesting that Akt provides a critical signal in growth control, but is not sufficient to drive branching morphogenesis in the absence of Rictor. This is consistent with the data from our analysis of transplanted Rictor-deficient/Akt^{Myr} expressing MEC *in vivo* and with the phenotype of Akt1 deletion, which did not affect mammary epithelial cell differentiation but did impair lactation [36]. Deletion of Akt1 and one allele of Akt2 enhanced this defect [95, 96]. Moreover, Akt activation did not completely inhibit luminal apoptosis during MCF10A acinar morphogenesis in culture [97], suggesting that other factors also regulate cell survival during normal mammary epithelial development. In contrast to Akt, restoration of PKC α signaling to Rac1, or Rac1 activation independently of upstream signals, fully rescued all phenotypes resulting from Rictor loss in culture and in transplanted Rictor-deficient MEC *in vivo*, suggesting that Rictor-dependent mTORC2 is essential for PKC α -Rac1 signaling to drive mammary morphogenesis. While not directly tested here, at least one additional study has elucidated mechanisms downstream of Rac1 that can control cell survival.

One report using lymphoma cells demonstrated direct inhibition of apoptosis through Rac1-stimulated phosphorylation of the Bcl-2 family member, Bad, which occurred in an Akt-independent manner [98]. We observed a modest decrease in cell viability upon prolonged treatment with the Rac1 inhibitor in organoid culture coupled with the decreased branch extension, consistent with previous studies that also reported regulation of branching initiation and extension via PI3K-mediated Akt and Rac1, respectively [99].

Interestingly, levels of mTORC1 target P-S6 are elevated in MEC upon Rictor loss relative to controls. This could reflect shift of mTOR kinase to complex 1 in the absence of a stable mTORC2 complex. It will be of great interest to track mTOR kinase association with the two complexes over the course of mammary epithelial development to better understand its functions. Activation of the Akt signaling pathway upon mTOR inhibition via a negative feedback loop has been observed in many cell types, including breast cancer cell lines (Reviewed in [100]). In our study, rapamycin preferentially inhibited mTORC1 upon acute treatment (e.g. reduction in P-S6 without affecting P-Akt-S473 levels) and as prolonged treatment inhibited both complexes (e.g. reduction in both P-S6 and P-Akt-S473). These data are consistent with the observation that rapamycin is an effective inhibitor for activity of both complexes in many cell types [10], including MECs. The differences in response to rapamycin between normal MECs and breast cancer cell lines could be due to differences in insulin-like growth factor receptors (IGFRs), which are expressed at higher levels in cancer cells and mediate feedback to Akt upon mTOR inhibition (Reviewed in [100-102]).

Given the known roles of mTORC1 in cell growth, metabolism, and protein and lipid synthesis [76], it was surprising that Raptor loss produced only a transient delay in ductal lengthening. It is possible that other signaling pathways may compensate for loss of mTORC1 function in Raptor-deficient mammary epithelium, such as RSK-mediated activation of S6 [103, 104]. However, we observed similar decreases in cellular proliferation in the absence of Raptor and Rictor expression at 6 weeks that recovered by 10 weeks, suggesting that MEC proliferation may rely on both mTORC1 and mTORC2. Decreased MEC proliferation upon genetic mTORC1 ablation is consistent with other reports of rapamycin-mediated cell growth inhibition in lactating mouse mammary explants, in lactating mice, and in milk-producing HC11 cells. Based on these previous studies, it will be important to determine the effects of Raptor and Rictor ablation on growth, differentiation, and milk production in alveolar mammary epithelium during pregnancy and lactation *in vivo*.

The PI3-kinase (PI3K)/mTOR pathway is aberrantly activated up to 60% of clinical breast cancers, facilitating tumor cell growth, survival, metabolism, and invasion [105, 106]. Moreover, increased PI3K activity in *MMTV-Cre/PTEN^{FL/FL}* mice increases mammary epithelial branching and decreases apoptosis during pubertal development [107], suggesting that PI3K signaling is important in branching and survival in the breast. This idea is consistent with the phenotype produced by *MMTV-Cre*-driven Rictor loss, in which loss of a PI3K pathway mediator produces decreased branching and survival.

While inhibitors of mTORC1 show limited clinical efficacy as single agents, anti-PI3K agents combined with dual mTORC1/2 inhibitors appear to be more effective [67, 108-110], underscoring the clinical relevance of mTORC2 in breast cancer. Importantly, these recent clinical observations parallel the data shown here demonstrating that mTORC2 inhibition due to either sustained rapamycin treatment or to Rictor deletion profoundly affected the complex series of events driving mammary morphogenesis, and these mTORC2-dependent processes occur in a manner unique and separable from mTORC1. Interestingly, preferential targeting of mTORC2 versus mTORC1 reduced breast cancer cell motility and survival in culture and *in vivo* [55, 68], and Rictor knockdown suppressed anchorage-independent growth of MCF7 breast tumor cells [111].

Although at least one report suggests elevated Rictor levels correlate with higher overall and recurrence-free survival [112], Rictor overexpression was observed in clinical invasive breast cancer specimens relative to normal breast tissue, as well as in lymph node metastases [55], supporting the clinical relevance of mTORC2 in invasive breast cancer. Given our findings that Rictor/mTORC2 is required in the normal mammary epithelium for PKC α -Rac1 activation which drives MEC survival, motility, and invasion, it will be interesting to determine if the mTORC2-PKC α -Rac signaling axis is used by breast cancer cells to drive metastasis. If so, mTORC2-specific targeting or PKC α inhibition could represent potential therapeutic strategies to limit metastatic spread of breast tumors, and to limit survival of disseminated tumor cells.

Although data shown herein are the first demonstration of mTORC2-mediated regulation of normal MEC migration and invasion, several lines of evidence suggest that cancer cells exploit Rictor-dependent signaling pathways to facilitate invasion and metastasis. For example, siRNA-mediated Rictor knockdown inhibited MCF7 and MDA-MB-231 breast cancer cell migration [55, 68]. Rictor knockdown inhibited transforming growth factor beta (TGF β)-mediated epithelial-to-mesenchymal transition (EMT) in breast cancer lines [69]. In contrast to our findings that untransformed MECs use Rictor to activate PKC α and Rac1-mediated invasion, breast cancer cells used Rictor to drive motility through protein kinase C ζ (PKC ζ ; [55]), integrin-linked kinase (ILK; [69]) and Akt [68]. Although Akt phosphorylation at S473 required Rictor/mTORC2 in primary MECs, restoring Akt function was not sufficient to rescue survival, motility, or branching morphogenesis in the absence of Rictor. Restoration of Rac1 activity, an essential regulator of mammary epithelial branching morphogenesis [81, 113] and a downstream effector of mTORC2 and PKC α , rescued survival and migration defects induced by genetic mTORC2 inhibition. While not specifically linked to Rictor in breast cancer cells, Rac1-mediated invasion and metastasis of breast cancer cells has been reported previously [114-116]. Together, these data suggest that Rictor/mTORC2-dependent Rac signaling could promote breast cancer invasion, paralleling its function normal MEC branching morphogenesis. It is possible that breast cancer cells can engage multiple pathways (PKC ζ , ILK, Akt, Rac, and others) to regulate tumor cell metastasis, and it is interesting to speculate that Rictor may lie at the intersection of each of these pathways.

In summary, our data demonstrate distinct, non-overlapping functions of mTORC1 and mTORC2 in post-natal mammary morphogenesis. Whereas Raptor-dependent mTORC1 signaling regulates proliferation, Rictor-dependent mTORC2 is essential for cell survival, cell junctions, motility, and branching morphogenesis. These findings underscore the importance of understanding the distinct roles for mTORC1 and mTORC2 in normal physiology of the breast and in breast cancer in order to intelligently develop and administer mTOR-directed therapies.

Chapter III

RICTOR/MTORC2 DRIVES PROGRESSION AND THERAPEUTIC RESISTANCE OF *HER2*-AMPLIFIED BREAST CANCERS

Abstract

Aberrant phosphatidyl inositol-3-kinase (PI3K)/Akt signaling occurs in nearly 60% of breast cancers through *HER2* amplification, *PIK3CA* mutation, *PTEN* inactivation, or other mechanisms. The mTOR complexes mTORC1 and mTORC2 operate as activators (mTORC2) or effectors (mTORC1) of Akt, but mTORC2-specific roles in breast cancer remain elusive. Immunohistochemistry showed up-regulation of the mTORC2 obligate cofactor Rictor, but not the mTORC1 cofactor Raptor, in invasive breast tumors. Genomic gains in mTORC2 obligate cofactors correlated with decreased survival in breast cancer patients. Rictor loss in a mouse model of *HER2*-amplified breast cancer decreased tumorigenesis, tumor cell proliferation and survival, and Akt-S473 phosphorylation. Similarly, Rictor loss in human *HER2*-amplified breast cancer cells decreased Akt-dependent cell survival. mTORC2 inhibition using Rictor knockdown or dual mTORC1/2 kinase inhibition increased lapatinib-induced cell killing in *HER2*-amplified breast cancers, including those with lapatinib resistance. Raptor loss decreased tumorigenesis but did not affect cell survival or Akt-S473 phosphorylation in *HER2*-amplified breast cancer cells. Rac1-dependent cell motility, invasion, and metastasis were decreased upon loss of Rictor, but not Raptor, due to accumulation of the Rac inhibitor RhoGDI2 in Rictor-depleted cells.

Thus, *HER2*-amplified breast cancers use Rictor/mTORC2 to drive Akt and Rac signaling, warranting additional studies into mTORC2-specific inhibitors.

Introduction

Breast cancer is the most common malignancy among western women. Approximately 20% of breast cancers exhibit overexpression of human epithelial growth factor receptor 2 (*HER2*), a marker of aggressive disease [117]. While *HER2*-targeted therapies improve outcome for patients with *HER2*-amplified breast cancers, resistance to *HER2* inhibitors often occurs, underscoring the need for increased understanding of the signaling pathways required for *HER2*-mediated transformation and malignancy [118]. *HER2* activates the phosphoinositol-3 kinase (PI3K)/Akt signaling cascade, regulating tumor cell growth, survival, metabolism and motility. Targeting *HER2* using antibodies (e.g., Herceptin) or tyrosine kinase inhibitors (e.g., lapatinib, neratinib) reduces PI3K/Akt signaling, resulting in decreased tumor cell growth and survival in *HER2*-amplified breast cancers. Although *HER2*-targeted treatments have improved the outcome for patients with *HER2*-positive breast cancers, primary or acquired resistance to *HER2* inhibitors frequently occurs, accompanied by resurgent PI3K/Akt signaling. PI3K inhibitors block Akt activation and are being tested in *HER2*-amplified breast cancers. However, increasing evidence demonstrates that loss of negative feedback to PI3K, mitogen activated protein kinase (MAPK) and receptor tyrosine kinases resulting from PI3K inhibition dampens the net response to treatment [119]. Additionally, dose-limiting toxicities reported with PI3K inhibitors may limit its clinical utility.

Therefore, a greater understanding of signaling pathways both upstream and downstream of Akt is required if we are to effectively block Akt signaling in *HER2*-amplified breast cancers.

Interestingly, the intracellular serine/threonine kinase mammalian target of rapamycin (mTOR) is unique in that it functions both to activate Akt, and to respond to activated Akt [120]. This dual functionality of mTOR is possible because mTOR exists in two structurally and functionally distinct complexes, defined by the cofactors associating with mTOR, and by their relative sensitivity to rapamycin. Specifically, Raptor is a required cofactor for rapamycin-sensitive mTORC complex 1 (mTORC1), which is activated downstream of PI3K/Akt and mediates cell growth, protein translation, and metabolism [19]. Rictor is a required cofactor for mTORC2, which controls cell survival, polarity, and cytoskeletal dynamics [121]. mTORC2 lies upstream of Akt, directly phosphorylating Akt at S473, an event necessary for maximal Akt activation and substrate specificity [16, 122]. Given that mTORC1 and mTORC2 are comprised of distinct co-factors and phosphorylate distinct substrates, it is likely that mTORC1 and mTORC2 have distinct physiological roles, and their dysregulation may produce distinct pathological consequences. This notion is supported by recent findings that Rictor/mTORC2 is required during mammary gland development for ductal lengthening, secondary branching, mammary epithelial cell (MEC) motility and MEC survival, while Raptor/mTORC1 is necessary for MEC proliferation [62]

Breast cancers often hijack many signaling pathways used by normal MECs to support tumor cell growth, survival, and metastasis [123, 124].

It is possible, therefore, that the unique effects of mTORC1 and mTORC2 in MECs are paralleled in breast cancers. The clinical efficacy of rapalogues (e.g., everolimus) in luminal breast cancers suggests that mTORC1 is important [70, 125]. Preclinical studies suggest this may also be true in *HER2*-amplified breast cancer cells [126]. However, increasing evidence suggests that targeting mTORC1 alone may increase IRS1-to-PI3K signaling and mTORC2-mediated Akt phosphorylation, ultimately dampening tumor response and promoting therapeutic resistance [66]. Clinical trials are currently investigating mTOR kinase inhibitors that would block both mTORC1 and mTORC2 [67]. However relatively little is known about the distinct role of mTORC2 in breast cancer formation, progression, and therapeutic response, despite its known role in activation of Akt, a key signaling node and critical effector of RTKs, including *HER2*. Interestingly, emerging evidence from prostate [63] and glioblastoma [64] models suggest a direct link between mTORC2 and PI3K-driven cancer progression. Preliminary studies show that genetic mTORC2 inhibition reduced breast tumor cell motility and survival in breast cancer cell lines [55, 68] [111].

We used a genetically engineered mouse model of *HER2*-amplified breast cancer to determine if Rictor/mTORC2 supports spontaneous tumor formation, and human *HER2*-amplified breast cancer cell lines to determine the impact of Rictor/mTORC2 on tumor cell survival and therapeutic response to *HER2* inhibition. Our study uncovers a previously unreported role for Rictor/mTORC2 in *HER2*-amplified breast cancers.

Materials and Methods

Mice. All animals were housed under pathogen-free conditions, and experiments were performed in accordance with AAALAC guidelines and with Vanderbilt University Institutional Animal Care and Use Committee approval. *Rictor*^{FL/FL} mice (C57BL/6) were kindly provided by Dr. Mark Magnuson (Vanderbilt University) and have been previously described [23], and were inbred to FVB for >10 generations. *MMTV-NIC* mice (FVB) were purchased from the Jackson Laboratories, and have been previously described. All analyses of *Rictor*^{FL/FL} X *MMTV-NIC* mice were performed on age-matched siblings in from FVB inbred crosses. *Raptor*^{FL/FL} mice (C57BL/6) were purchased from the Jackson Laboratories (Bar Harbor, ME) and have been previously described [19]. All analyses of *Rictor*^{+/+} X *MMTV-NIC* were performed on age-matched siblings resulting from F1 (1:1, FVB:C57BL/6) intercrosses.

Cell culture. All breast cancer cell lines were purchased from ATCC and cultured in DMEM plus antibiotics and 10% serum. MCF10A and MCF10A Rictor null cells were purchased from Sigma and transduced with lentiviral HER2-RFP particles or RFP control (GenTarget) and cultured in DMEM F12 plus insulin (4 mg/mL), cholera toxin (1 mg/mL), EGF (100 ug/mL), hydrocortisone (2 mg/mL) and 5% horse serum with 10 ug/mL blasticidin. The Akt kinase inhibitor AZD5363 was purchased from SelleckChem. The in solution Rac1 inhibitor was purchased from Calbiochem/Millipore. The PKC α inhibitor, GO6976, was purchased from Tocris. Adenoviral particles Ad.caRac1, Ad.Akt^{DD}, Ad.PKC α were purchased from Vector Biolabs. Lapatinib resistant cell lines were generated as previously described [127].

Generation of stable knockdown cell lines. Rictor and Raptor lentiviral shRNA's were purchased from Addgene. Plasmid DNA was transfected into 293 FT cells plus packaging vectors and cells were allowed to produce virus for 48 hours. Target breast cancer cells were infected every 4 hours for 2 days, then fresh media was added and cells were selected with puromycin (2mg/mL) for approximately 2 weeks. Stable knockdown of Rictor and Raptor was confirmed through western analysis for each independent shRNA construct. Knockdown cells were maintained under puromycin selection at a low passage.

Reagents, siRNA and shRNA. *ARGHGDIB* siRNA's were purchased from Sigma using the following siRNA ID's: SASI_Hs01_00125904 and SASI_Hs01_00125905. Prk5-myc-Rictor plasmid was a generous gift from Dr. Sarbassov. Short hairpin RNA's for Rictor, Raptor, and scramble control were obtained from Addgene:

- Rictor shRNA #1853, 1854
- Raptor shRNA #1857, 1858
- scramble shRNA #1864

Western blotting. Cells were homogenized in ice-cold lysis buffer [50 mM Tris pH 7.4, 100 mM NaF, 120 mM NaCl, 0.5% NP-40, 100 μ M Na₃VO₄, 1X protease inhibitor cocktail (Roche)], sonicated for 10 s, and cleared by centrifugation at 4°C, 13,000 x g for 10 min. Protein concentration was determined using the BCA assay (Pierce). Proteins were separated by SDS-PAGE and transferred to nitrocellulose membranes.

Membranes were blocked in 3% gelatin in TBS-T [Tris-buffered saline, 0.1% Tween-20) for 1 h, incubated in primary antibody in 3% gelatin overnight, washed with TBS-T, incubated in HRP-conjugated anti-rabbit or anti-mouse IgG, washed with TBS-T, and then developed using ECL substrate (Pierce). The following primary antibodies were used: α -actin (Sigma-Aldrich; 1:10,000); phospho-cocktail (Cell Signaling; 1:250); AKT, S473 and T308 P-Akt (Cell Signaling; 1:1000); S6 and P-S6 (Cell Signaling; 1:1000), Rictor (Santa Cruz; 1:250), Raptor (Cell Signaling; 1:500), RhoGDI2 (Spring Biosciences; 1:200), Rac1 (BD Biosciences; 1:1000), PKC α (Cell Signaling; 1:1000) and P-PKC α (Abcam; 1:1000)

Transwell migration/invasion assays. Breast cancer cells (100,000) were serum starved overnight, counted and added to the upper chamber of uncoated (migration) or Matrigel-coated (invasion) transwells in starvation medium and incubated for 24 hours. Invasion was scored as described previously [84] by fixing cells on transwells, staining with 0.1 % crystal violet, and counting cells on the lower surface that migrated/invaded in response to growth medium plus 10% FBS or EGF (20 nm).

Annexin V-FITC staining. Cells were trypsinized, counted, 5,000 cells were plated in 96-well plates in triplicates and allowed to adhere to the plates overnight. 5 μ L Annexin V-FITC (Invitrogen 807876) in 95 μ L complete or serum-free DMEM was added to each well. Annexin V staining was monitored and images were captured at 6 hours. The number of Annexin V-FITC positive cells was quantitated using Image J and the percentage of Annexin V-FITC positive cells of total cells was calculated.

Caspase 3/7 Glo assay (Promega). 5,000 cells in 200 uL complete growth media were plated in 96-well plates and allowed to sit down overnight. The reagent and plate were allowed to equilibrate to room temperature, 175 uL media was removed (leaving 25 uL behind), 25 uL Caspase Glo 3/7 reagent was added (1:1 ratio) and plate was incubated at room temperature for 1 hour. Plate was read on a plate reader to detect luminescence.

Growth assays. For two-dimensional/monolayer growth assays, 5,000 cells were seeded in 12-well plates and allowed to grow over 14 days. Growth media (supplemented with 1 uM lapatinib, Rac inhibitor, PP242 or equal volumes of DMSO) was changed every 3 days. At 14 days, cells were washed with ice cold PBS, fixed with 10% formalin and stained with crystal violet. Plates were imaged and average colony area was quantified using the Odyssey imaging system and Odyssey software. For three-dimensional growth assay, 5,000 cells were resuspended in 100 uL Matrigel and plated in 96-well plates. After the Matrigel solidified, 100 uL growth media was added on top. Growth media (supplemented with 1 uM indicated inhibitors or equal volumes of DMSO) was changed every three days and colonies were photographed over the course of 14 days. Average colony area or average colony number was quantitated using Image J software.

Human Tissue Microarray. Human tissue microarray (breast carcinoma with normal tissue controls) was purchased from Cybrdi (#CC08-10-001).

Histological analysis. Tumors were resected and sections (5- μ m) were stained with hematoxylin and eosin. *In situ* TUNEL analysis was performed on paraffin-embedded sections using the ApopTag kit (Calbiochem).

IHC on paraffin-embedded sections or on human TMA's was performed as described previously [83] using: Rictor (Santa Cruz Biotechnologies), Raptor (Abcam), Ki67 (Santa Cruz Biotechnologies), P-S6 (Cell Signaling Technologies); P-Akt S473 (Cell Signaling Technologies); Rictor (Santa Cruz) Immunodetection was performed using the Vectastain kit (Vector Laboratories), AF488-conjugated anti-rabbit, or AF621-conjugated anti-mouse (Life Technologies), according to the manufacturer's directions.

Xenograft experiments. Estrogen pellets (14 days extended release, 0.17 mg β estradiol; Innovative Research of America) were implanted subcutaneously into 3- to 4-week-old female BALB/c athymic nude mice (Harlan Laboratories). Right and left inguinal mammary fat pads were injected with 10^6 MDA-MB-361 shScramble or shRictor cells in 100 μ l growth factor-reduced Matrigel or 2×10^6 BT474 LR cells or BT LR shRictor cells. Tumors were measured with calipers twice weekly.

Statistics. To assess statistical significance in experiments directly comparing an experimental group with a control group, Student's unpaired, 2-tailed *t* test was used. To assess statistical significance in experiments in which multiple groups were compared across a single condition, 1-way ANOVA was used. To compare the response of 2 agents combined to either single agent alone, 2-way ANOVA was used. $P < 0.05$ was considered significantly different from the null hypothesis.

Study approval. All animal experimentation was performed in AAALAC-approved facilities at Vanderbilt University Medical Center. All animal use protocols were reviewed and approved prior to experimentation by the Institutional Animal Care and Use Committee at Vanderbilt University.

Results

Rictor expression is elevated in invasive breast cancers and correlates with decreased survival of breast cancer patients.

Because mTORC2 is a potent activator of Akt, while mTORC1 is a potent effector of Akt, we examined mRNA expression levels of obligate mTORC1 and mTORC2 cofactors in clinical breast cancer specimens curated by The Cancer Genome Atlas (TCGA), specifically examining tumors with genetic alterations in PI3K pathway genes, including *HER2* gene amplification, *PIK3CA* activating mutations, and *PTEN* loss/mutation (**Figure 21A**). mRNA upregulation of mTORC2 cofactors *RICTOR* and *MAPKAP1* (the gene encoding Sin1) occurred in nearly 20% of all breast tumor samples. Specifically, upregulation of *RICTOR* and *MAPKAP1* occurred in 20/99 *HER2*-amplified tumors, 52/181 *PIK3CA* mutant tumors, and 35/149 *PTEN*-altered tumors, supporting a potential role for mTORC2 in PI3K-driven breast cancers. Interestingly, genetic mTORC2 alterations rarely overlapped with each other. *RPTOR* mRNA upregulation was not detected (**Table 2**). Additionally, genomic gains of *MAPKAP1* ($P = 0.004$) or *RICTOR* ($P = 0.093$) but not *RPTOR*, ($P = 0.630$) correlated with decreased survival in breast cancer patients (**Figure 21B**). Rictor and Raptor protein levels were assessed in clinical breast cancer tissue microarrays (TMAs) by immunohistochemistry (IHC). While Rictor was expressed below the level of detection in normal breast and ductal carcinoma in situ (DCIS) specimens (**Figure 21C**), Rictor was significantly upregulated in invasive breast carcinomas (IBCs), 37% of which scored positive for Rictor staining (**Table 3**).

In contrast, Raptor was expressed similarly in normal breast tissue, DCIS, and IBCs. Strikingly Rictor (but not Raptor) staining intensity was higher in grade II/III breast tumors as compared to what was seen in grade I/II tumors, suggesting that Rictor expression may be informative of aggressiveness and outcome in breast tumors, particularly those with PI3K pathway activating aberrations (**Figure 21D**). These data suggest that Rictor expression may be informative of aggressiveness and outcome in breast tumors, particularly those with PI3K pathway-activating aberrations. Consistent with this notion, *RICTOR* genomic gains/amplifications occurred in 37/59 (63%) of the breast cancer cell lines assessed and reported by the Cancer Cell Line Encyclopedia (CCLE), versus *RPTOR* gains which occurred in 23/59 (39%) of all samples (**Figure 21E**). Assessment of *RICTOR* and *RPTOR* mRNA levels by RT-qPCR revealed elevated expression of *RICTOR* in 8/9 (89%) of breast cancer cell lines assessed as compared to what was seen in untransformed MCF10A mammary epithelial cells, while 6/9 (66%) of breast cancer cell lines displayed increased *RPTOR* mRNA (**Figure 21F**). *RICTOR* expression was higher in *HER2*-amplified breast cancer cells as compared to luminal or basal-like. Rictor protein expression was observed in *HER2*-amplified cells, which also exhibited phosphorylation of Akt at S473, the mTORC2-specific site required for full AKT activation (**Figure 21G**). Collectively, these data indicate a potential role for Rictor and mTORC2 in human breast cancers, and suggest that *HER2*-amplified breast cancers in particular may rely on Rictor/mTORC2.

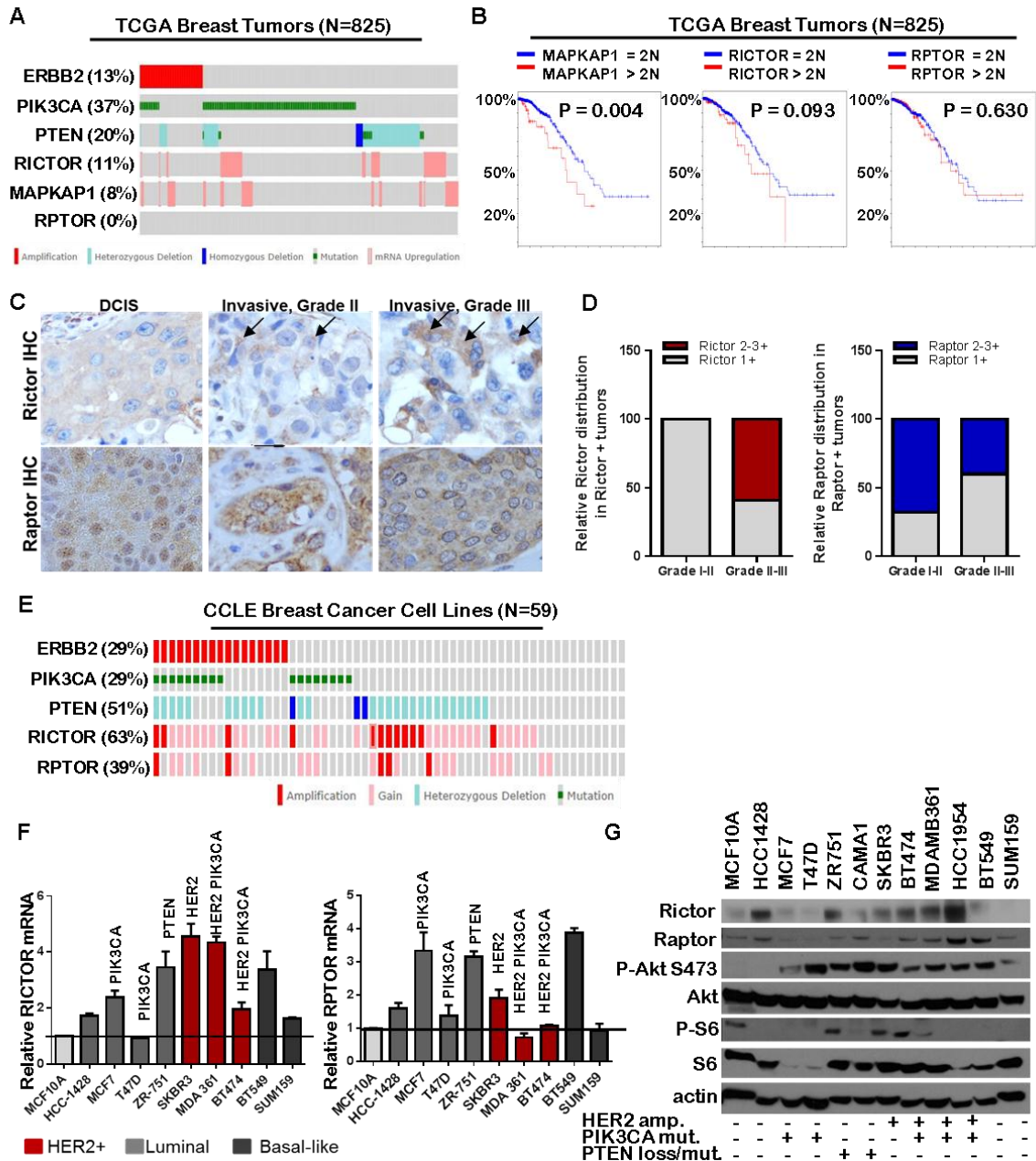


Figure 21. Rictor expression is elevated in human breast cancer. A-B TCGA-curated breast cancers were assessed. A. HER2/PI3K/mTOR pathway genetic aberrations were assessed. B. Kaplan-Meier analysis of survival in patients with 2N or > 2N copies of the indicated genes. C-D. Representative images (C) and quantitation (D) of Rictor and Raptor IHC in human breast cancers by stage and grade. Arrows in C indicate Rictor positive cells. E. Rictor, Raptor and HER2-PI3K pathway alterations in the CCLE breast cancer cells. F-G Rictor and Raptor mRNA levels (F) and protein levels (G) in breast cancer cell lines compared to untransformed MCF10A cells.

	<i>Rictor</i> mRNA upregulation	<i>MAPKAP1</i> mRNA upregulation	<i>Rptor</i> mRNA upregulation
HER2-amp	6% (6/99)	14.1% (14/99)	0%
PIK3CA mut	15% (27/181)	23.8% (25/181)	0%
PTEN loss	13.4% (20/149)	10% (15/149)	0%
Co-occurrence w/ PI3K pathway aberration (HER2-amp, PIK3CA mut, PTEN loss)	13.4%	12.3%	0%

Table 2. Upregulation of mTORC2 pathway components overlaps with HER2/PI3K pathway alterations. *Rictor* and *MAPKAP1* (the gene encoding Sin1) mRNA upregulation co-occurs with HER2/PI3K pathway alterations in TCGA-curated breast tumors (n=825). *Rptor* mRNA upregulation was not detected.

	Rictor negative	Rictor positive	Raptor negative	Raptor positive
DCIS/ normal	100% (10/10)	0% (0/10)	0%	100% (8/8)
Invasive	63% (85/134)	37% (49/134)	8% (10/123)	92% (113/123)
ER/PR+	59% (16/27)	41% (11/27))	14% (1/7)	26% (22/72)
HER2+	61% (49/80)	38% (31/80)	43% (3/7)	43% (31/72)
TNBC	49% (13//27)	51% (14//27)	43% (3/7)	31% (22/72)

Table 3. Rictor and Raptor protein expression analysis in a human tissue microarray (TMA)

Conditional loss of RICTOR delays HER2-driven tumor formation

The *MMTV-Neu-IRES-Cre (NIC)* transgenic mouse model [128] expresses a bicistronic transcript comprised of an oncogenic *Neu* (the rat *HER2* homologue) expression cassette, followed by an internal ribosomal entry site (IRES) and a Cre recombinase expression cassette. These mice develop mammary tumors with an average latency of 6 months [129]. *NIC* mice were intercrossed with mice harboring floxed *RICTOR* alleles (*Rictor^{FL/FL}*) or floxed *RPTOR* alleles (*Raptor^{FL/FL}*) to generate *Rictor^{FL/FL}NIC* mice or *Raptor^{FL/FL}NIC* mice, respectively. The coupled expression of *Neu* and Cre ensures that floxed *RICTOR* and *RPTOR* alleles in all *Neu*-transformed mammary tumor cells undergo Cre-mediated recombination, eliminating *Rictor* and *Raptor* expression. We analyzed mammary glands of tumor-free, virgin female *Rictor^{FL/FL}NIC* mice at 12 months of age by whole mount hematoxylin staining, showing that, while *Rictor^{+/+}NIC* samples harbored diffuse hyperplasia within six months (**Figure 22A, 23A**), loss of *Rictor* in *Rictor^{FL/FL}NIC* mammary glands resulted in decreased hyperplasia through 12 months of age. Importantly, focal neoplasias were reduced >3-fold in *Rictor^{FL/FL}NIC* samples as compared *Rictor^{+/+}NIC* controls (**Figure 22B**). Diffuse hyperplasia and focal neoplasias were similarly decreased in mature *Raptor^{FL/FL}NIC* mammary glands as compared to *Raptor^{+/+}NIC* siblings (**Figure 22C, 23B**).

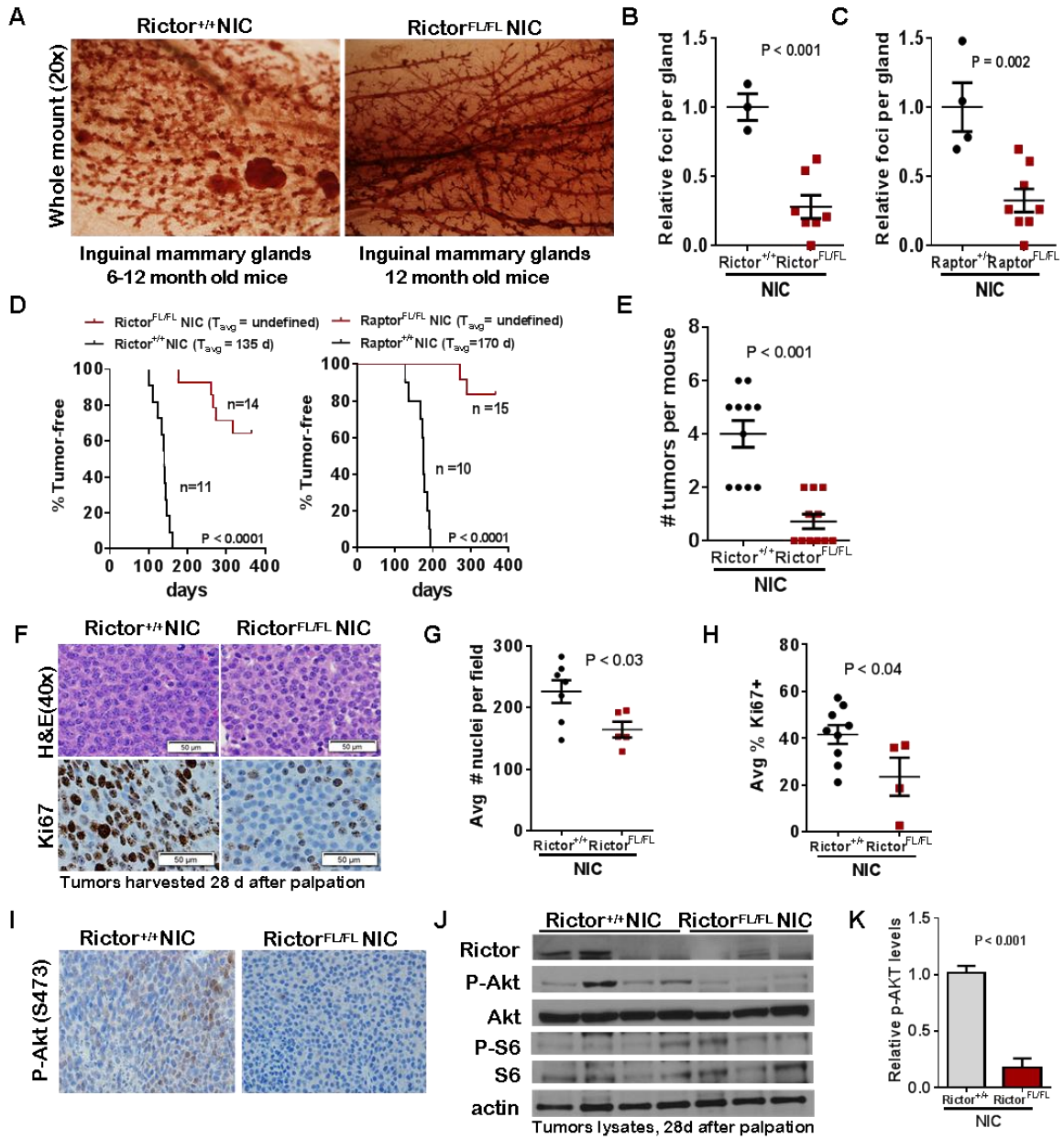


Figure 22. Loss of Rictor delays HER2-driven tumor formation. A-C. Mammary glands were assessed by whole mount hematoxylin staining. **A.** Representative images are shown. **B-C.** Average number of tumor foci per whole mounted gland was calculated for MMTV-NIC mice with floxed Rictor (**B**) or floxed Raptor (**C**) alleles. **D.** Rictor^{+/+}NIC, Rictor^{FL/FL}NIC, Raptor^{+/+}NIC and Raptor^{FL/FL}NIC mice were analyzed for tumor latency. **E.** Number of tumors per genotype was calculated. **F-K.** Tumors harvested 28 days post-tumor palpation were analyzed. **F.** Representative images of tumor sections stained for H&E (top) or Ki67 (bottom). Original magnification = 400X. **G.** Average number of nuclei per 400X field is shown. Each point represents the average value from 5 random fields/tumor. **H.** Average percentage of Ki67 cells per total number of nuclei. Each dot represents the average value from 5 random fields/tumor. **I.** IHC to detect P-Akt (S473), original magnification = 400X. **J.** Western analysis of whole tumor lysates. **K** Intensity of phosphorylated-Akt bands normalized to total Akt was quantitated using Image J software. Values represent the average of each individual tumor. N = 3-4.

Although *Rictor*^{+/+}*NIC* mice (N = 11) and *Raptor*^{+/+}*NIC* mice (N = 10) formed tumors with 100% penetrance and an average latency of 135 and 170 days, respectively, only 5/14 (35%) of *Rictor*^{FL/FL}*NIC* animals and 2/10 (18%) of *Raptor*^{FL/FL}*NIC* formed tumors, and did so with a substantially delayed latency (**Figure 22D**). These findings suggest that both Rictor and Raptor are required individually for HER2-mediated mammary tumor formation. Because only two *Raptor*^{FL/FL}*NIC* mice developed mammary tumors, further analysis of tumors was precluded in this model. However, we assessed the 5 tumor-bearing *Rictor*^{FL/FL}*NIC* mice to determine the impact of Rictor loss on tumor progression. *Rictor*^{FL/FL}*NIC* mice developed fewer tumors per mouse as compared to what was seen in *Rictor*^{+/+}*NIC* mice (**Figure 22E**). While tumor volume measured at the time of necropsy (28 days after initial tumor palpation) was similar in *Rictor*^{FL/FL}*NIC* and *Rictor*^{+/+}*NIC* mice (**Figure 23C**), *Rictor*^{FL/FL}*NIC* tumors were distinct histologically from controls, harboring a lower nuclear-to cytoplasmic ratio, more serous fluid and more acellular debris than *Rictor*^{+/+}*NIC* controls (**Figure 23D**), which were comprised largely of solid epithelial sheets (**Figure 22F – upper panel**). This trait was quantitated in terms of tumor cellularity, excluding large areas of acellular debris from analysis, revealing decreased nuclei per 400X field in *Rictor*^{FL/FL}*NIC* samples as compared to Rictor-expressing controls (**Figure 22G**). We used immunohistochemical (IHC) detection of Ki67 as a relative measure of tumor cell proliferation. For quantitation, we chose histological tumor areas where epithelial tumor cell density was similar in both *Rictor*^{FL/FL}*NIC* and *Rictor*^{+/+}*NIC* samples (**Figure 22F – lower panel**).

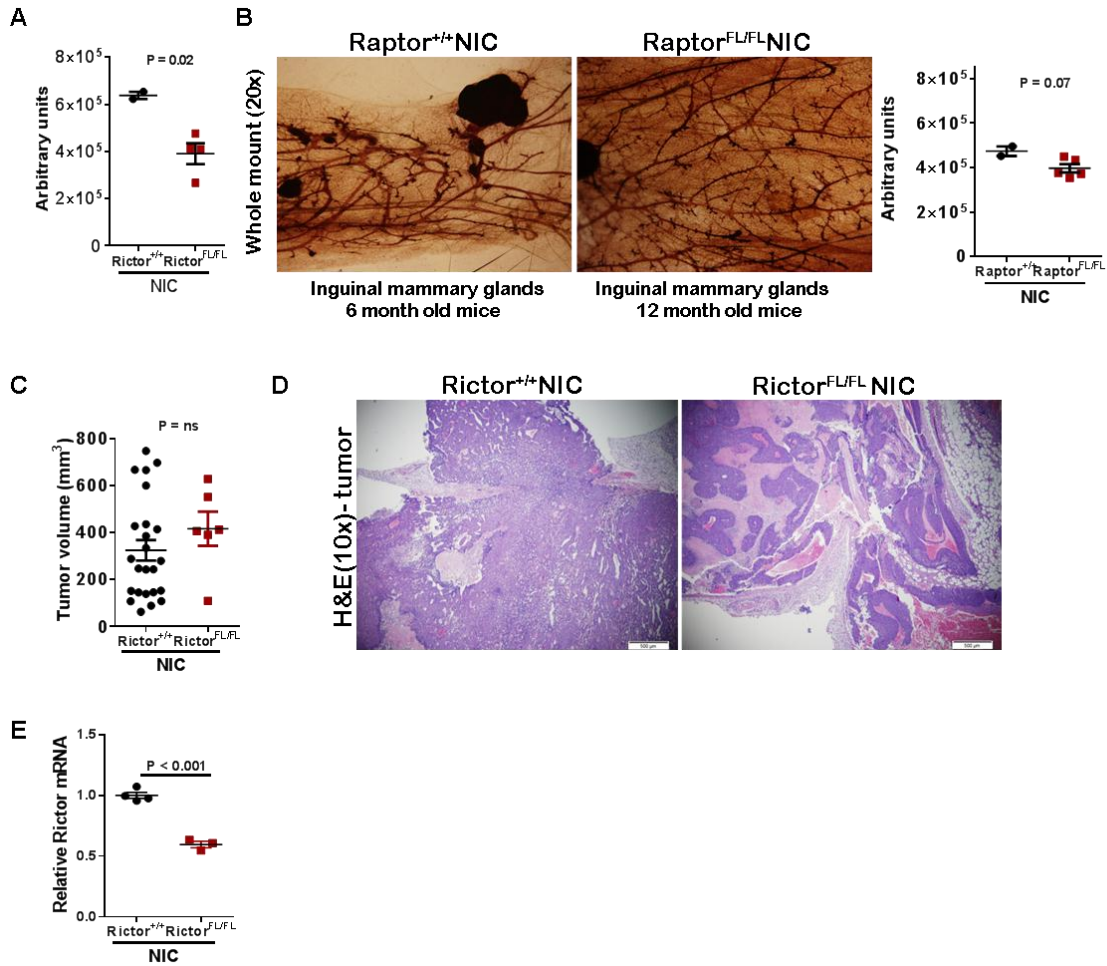


Figure 23. Loss of Rictor or Raptor decreases HER2-induced focal neoplasias. **A.** Image J was used to quantitate epithelial area from hematoxylin-stained whole mounted mammary glands isolated from the indicated mice. **B.** Mammary glands were assessed by whole mount hematoxylin staining. **C.** Final tumor volume from indicated mice was measured upon sacrifice. **D.** H&E stained tumor sections from indicated mice. **E.** RNA isolated from whole tumors from the indicated mice was used for qRT PCR analysis of Rictor mRNA levels normalized to GAPDH. Values represent the average of individual tumors. Student's T-test.

Rictor^{FL/FL}*NIC* tumors displayed a marked reduction in Ki67-positive nuclei compared to *Rictor*^{+/+}*NIC* tumors, suggesting that decreased tumor progression in *Rictor*^{FL/FL}*NIC* samples may be due, at least in part, to decreased tumor cell proliferation (**Figure 22H**). *Rictor*^{FL/FL}*NIC* tumors harvested 28 days after initial tumor palpation displayed reduced phospho AKT S473- positive cells (**Figure 22I**) and loss of Rictor expression (**Figure 22J**) as compared to what was seen in *Rictor*^{+/+}*NIC* tumors. AKT S473 phosphorylation was reduced by 80% in *Rictor*^{FL/FL}*NIC* (**Figure 22K**). These findings were confirmed by RT-qPCR analysis, demonstrating decreased *RICTOR* transcript in *Rictor*^{FL/FL}*NIC* tumors (**Figure 23E**). These data are consistent with the important role of Akt as an effector of HER2 signaling in breast tumorigenesis, and suggest that Rictor/mTORC2 is required for tumor cell growth and Akt phosphorylation in *HER2*-amplified tumor cells.

Rictor loss decreases growth and Akt S473 phosphorylation in established HER2-amplified breast cancer cells

mTORC2-specific inhibitors do not currently exist, however clinical trials are currently investigating enzymatic mTORC1/2 inhibitors. Preclinical data shows that mTOR inhibition is necessary for antitumor response following HER2 inhibition [130]. However the particular roles of mTORC1 versus mTORC2 in this regard are not entirely clear but warrant clarification since mTORC1 inhibition relieves negative feedback on oncogenic PI3K signaling, and since mTORC1/2 inhibitors are entering clinical trials in combination with HER2 inhibitors for *HER2*-amplified breast cancers.

Therefore, we tested if mTORC1/2 inhibition could enhance *HER2*-amplified breast cancer response to *HER2* inhibition. As expected, lapatinib treatment blocked P-*HER2* in three *HER2*-amplified breast cancer cell lines (SKBR3, MDA-MB-361 and BT474) and decreased P-S6 and P-Akt S473 (**Figure 24A**). Dual mTORC1/2 inhibition using PP242 inhibited P-S6 (a downstream effector of mTORC1) and reduced P-Akt S473. However, combined treatment with lapatinib and PP242 completely abolished P-Akt S473 and P-S6 in all three cell lines. Although PP242 and lapatinib each decreased growth of SKBR3, MDA-MB-361, and BT474 cells as single agents, the combination of lapatinib with PP242 blocked cell growth to a greater degree than either agent alone (**Figure 24B, 25A**). To distinguish the relative impact of mTORC1 and mTORC2 in this scenario, we transduced *HER2*-amplified breast cancer cells with lentivirus encoding two distinct Rictor shRNA sequences (shRictor), Raptor shRNA sequences (shRaptor) and a scrambled control shRNA sequence (shScr). We confirmed Rictor and Raptor depletion in MDA-MB-361 (*PIK3CA*^{E545K}*HER2*^{amp}), SKBR3 (*HER2*^{amp}), and BT474 (*PIK3CA*^{K111N}*HER2*^{amp}) cells. Cells expressing shRictor displayed a robust down-regulation of Rictor protein expression, and decreased phosphorylation of Akt S473 (**Figure 24C**), the mTORC2 substrate site. Expression of shRaptor decreased Raptor levels and phosphorylation of the mTORC1 substrates 4EBP1 and S6 (S240) (**Figure 24C**). Zinc-finger nucleases (ZFNs) with specific homology to Rictor genomic sequences (ZFN-Rictor) were used to engineer homozygous *RICTOR* genomic deletion in MCF10A-*HER2* cells, resulting in decreased levels of both Rictor and P-Akt S473 (**Figure 25B**).

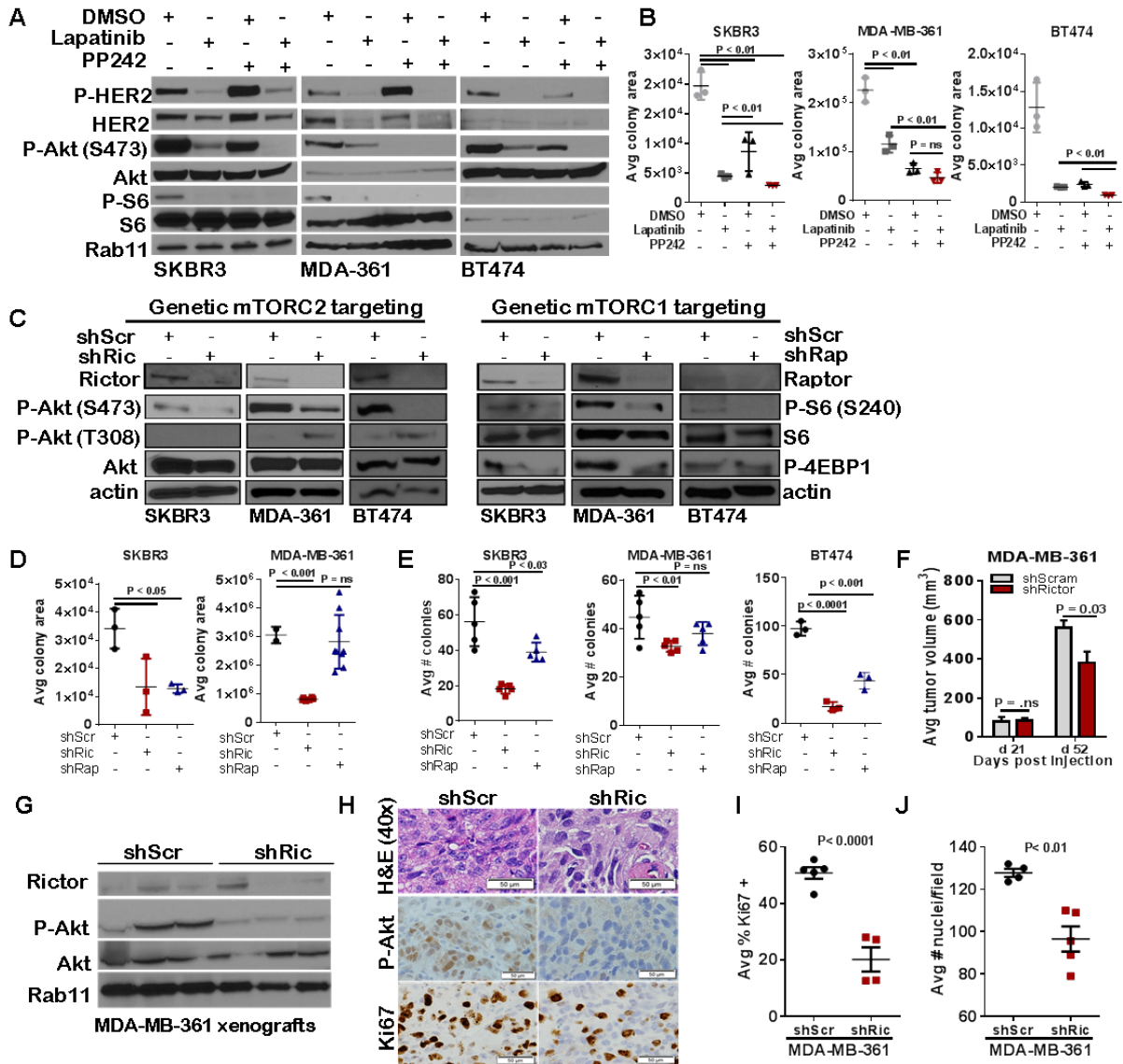


Figure 24. Rictor loss decreases growth and Akt S473 phosphorylation in established *HER2*-amplified breast cancer cells. **A.** Cells were treated with PP242 (1 μ M) or lapatinib (1 μ M) for 4 hours and analyzed by western blot. Representative blots are shown. **B.** Cells were cultured 14 days with PP242 (1 μ M) or lapatinib (1 μ M), stained with crystal violet, and scanned for fluorescent area using Odyssey. Midlines are the average colony area, individual points are the average values obtained for samples assessed in duplicate, N = 3. **C-E.** Breast cancer cells expressing shRNA for Rictor or Raptor were assessed. **C.** Whole cell lysates were assessed by western analysis. Representative blots are shown. **D.** Cells were cultured 14d, stained with crystal violet, and scanned for fluorescent area using Odyssey. Midlines are the average colony area, individual points are the average values obtained for samples assessed in duplicate, N = 3. **E.** Cells were embedded in Matrigel, cultured 14 days, and imaged. Midlines represent average number of colonies; data points represent the average value of duplicate samples. **F-J.** MDA-MB-361 shControl and shRictor xenografts were assessed. **F.** Tumors were measured and volume calculated (N = 8). **G.** Western analysis of MDA-MB-361 whole tumor lysates. **H.** Tumor sections were stained for H&E, pAkt (S473), and Ki67. Representative images are shown. Original magnification = 400X. **I.** Ki67-positive nuclei were quantitated using Image J. **J.** Data points represent the average value of 5 images per tumor, N = 4-5 tumors. **J.** Average number of nuclei per field is shown (midlines); each data point is average of 5 images/tumor.

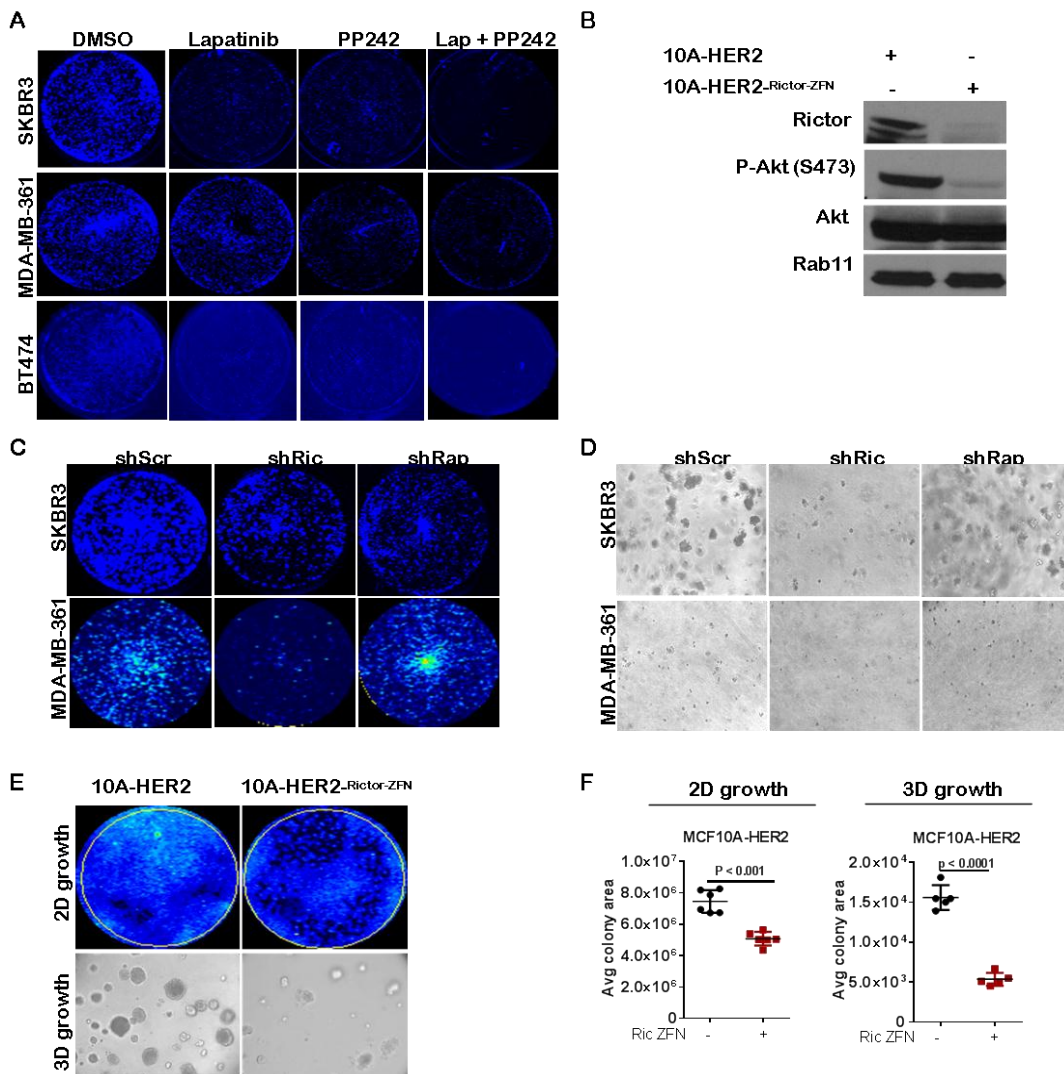


Figure 25. Genetic ablation of Rictor decreases growth and survival of HER2-positive breast cancer cells. **A.** Cells were cultured 14 days with PP242 (1 μ M) or lapatinib (1 μ M), stained with crystal violet, and scanned for fluorescent area using the Odyssey system. **B.** Western analysis of cell lysates from MCF10A-HER2 cells or MCF10A-HER2-Rictor-ZFN cells. **C.** Cells were cultured 14 days, stained with crystal violet, and scanned for fluorescent area using the Odyssey system. **D.** Cells were embedded in Matrigel, cultured 14 days and imaged. **E.** Cells were cultured 14 days, stained with crystal violet, and scanned for fluorescent area using the Odyssey system or embedded in Matrigel, cultured 14 days and imaged. Midlines represent average colony area, data points represent the average of duplicate samples. Data is representative of $n=3$ independent experiments.

Rictor knockdown decreased growth of SKBR3 and MDA-MB-361 in monolayer while Raptor depletion decreased growth of SKBR3 cells, but not MDA-MB-361 (**Figure 24D, 25C**). Similar results were found with cells embedded in three-dimensional 3D Matrigel, showing that knockdown of either Rictor or Raptor decreased cell growth in *HER2*-amplified breast cancer cells. Rictor ablation decreased cell growth to an equal or greater extent than Raptor ablation (**Figure 24E, 25D**). MCF10A-HER2 cells expressing ZFN-Rictor exhibited decreased growth in monolayer and in 3D Matrigel as compared to parental MCF10-HER2 cells (**Figure 25E**).

We assessed the impact of Rictor knockdown *in vivo* by xenografting MDA-MB-361 cells expressing shScr and shRictor into inguinal mammary fat pads of BALB/c athymic (*nu/nu*) female mice. All tumors were palpable 7–14 days after injection, suggesting that Rictor depletion did not affect tumor take rate in this model. Tumor measurements revealed similar tumor volumes in shScr and shRictor samples at 21 d post-injection (**Figure 24F**), suggesting that early tumor growth may not be affected by Rictor loss. However, by 52 d post injection, shRictor tumors were 30% smaller than what was seen in shScr tumors, suggesting that tumor progression *in vivo* requires Rictor. Western analysis of whole tumor lysates harvested at day 52 confirmed decreased Rictor and P-Akt S473 in shRictor tumors (**Figure 24G**). Decreased P-Akt S473 was similarly observed in shRictor tumors assessed by IHC (**Figure 24H**). Also, the percentage of cells expressing Ki67 was decreased in shRictor tumors (**Figure 24H, I**).

Similar to what was seen in spontaneous *Rictor*^{FL/FL}*NIC* tumors, MDA-MB-361 shRictor tumors displayed fewer nuclei per 400X field (**Figure 24H, J**). Taken together, these data suggest that Rictor depletion delays tumor growth and progression, but not tumor initiation.

Rictor-mediated Akt activation controls survival of HER2-positive breast cancer cells.

Detection of caspase 3/7 activity demonstrated that dual mTORC1/2 inhibition using PP242 increased tumor cell death in *HER2*-amplified breast cancer cells, and increased caspase-mediated cell death upon treatment with lapatinib (**Figure 26A**). Because Rictor loss reduced P-Akt S473, and because Akt is a key regulator of tumor cell survival in *HER2*-amplified breast cancers [131], we tested the hypothesis that Rictor-mediated Akt activation is necessary for survival of *HER2*-driven breast cancer cells. Using Annexin-V labeling to detect dying cells, we found that the percentage of Annexin V-positive cells was increased in MDA-MB-361, SKBR3 and BT474 cells expressing shRictor as compared to cells expressing shScr (**Figure 26B, 27A**). In contrast, shRaptor did not increase the number of Annexin V-positive cells. Further, caspase 3/7 activity, which correlates with caspase-mediated cell death, was increased in shRictor cells as compared to shScr or shRaptor cells, suggesting that Rictor, but not Raptor, controls cell death of *HER2*-positive breast cancer cells (**Figure 26C**). MDA-MB-361 xenografts were assessed for apoptotic cells using *in situ* terminal dUTP nick end labeling (TUNEL) analysis, demonstrating a nearly 10-fold increase in the percentage of tumor cells that were TUNEL+ in shRictor samples as compared to shScr controls (**Figure 26D**).

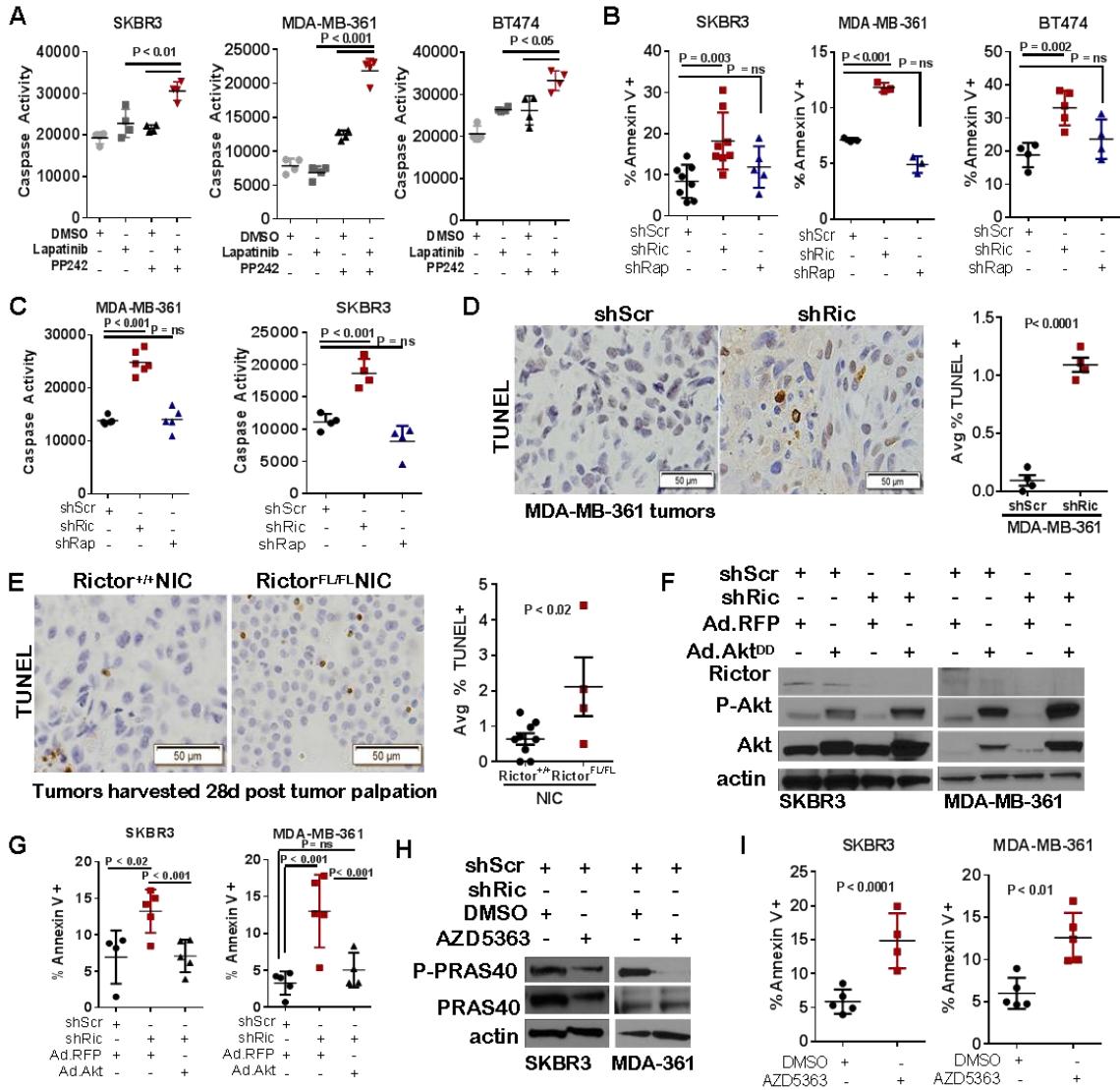


Figure 26. Rictor/mTORC2 signaling drives Akt-mediated survival of HER2-amplified breast cancers. **A.** Cells treated with PP242 (1 μ M) and lapatinib (1 μ M) were analyzed using a luminescent caspase 3/7 assay. Midlines are the average luminescence, individual points are average values obtained for samples assessed in duplicate. **B.** Cells were labeled with Annexin V-FITC for 6 hours then imaged. Midlines are the average percentage positive for Annexin V. Individual points are average values obtained for samples assessed in duplicate. **C.** Cells were analyzed for caspase 3/7 activity. Midlines are the average luminescence; individual points are average values for samples assessed in duplicate. **D-E.** TUNEL analysis of tumor sections. Representative images are shown, original magnification, 600X. Midlines are the average percentage that was TUNEL positive; individual points are the average values for 5 random fields/tumor. **F-G.** Cells expressing Akt^{DD} or RFP were assessed. **F.** Western analysis of whole cell lysates. **G.** Cells labeled with Annexin V-FITC for 6h were imaged. Midlines are the average percentage positive for Annexin V. individual points are average values obtained for samples assessed in duplicate. **H.** Western analysis of cells treated with AZD5363 (500 nM) for 24 hrs. **I.** Cells were treated with AZD5363 (500 nM) for 24 hrs, labeled with Annexin V-FITC for 6 hours were imaged. Midlines are the average percentage positive for Annexin V. individual points are the average values obtained for samples assessed in duplicate.

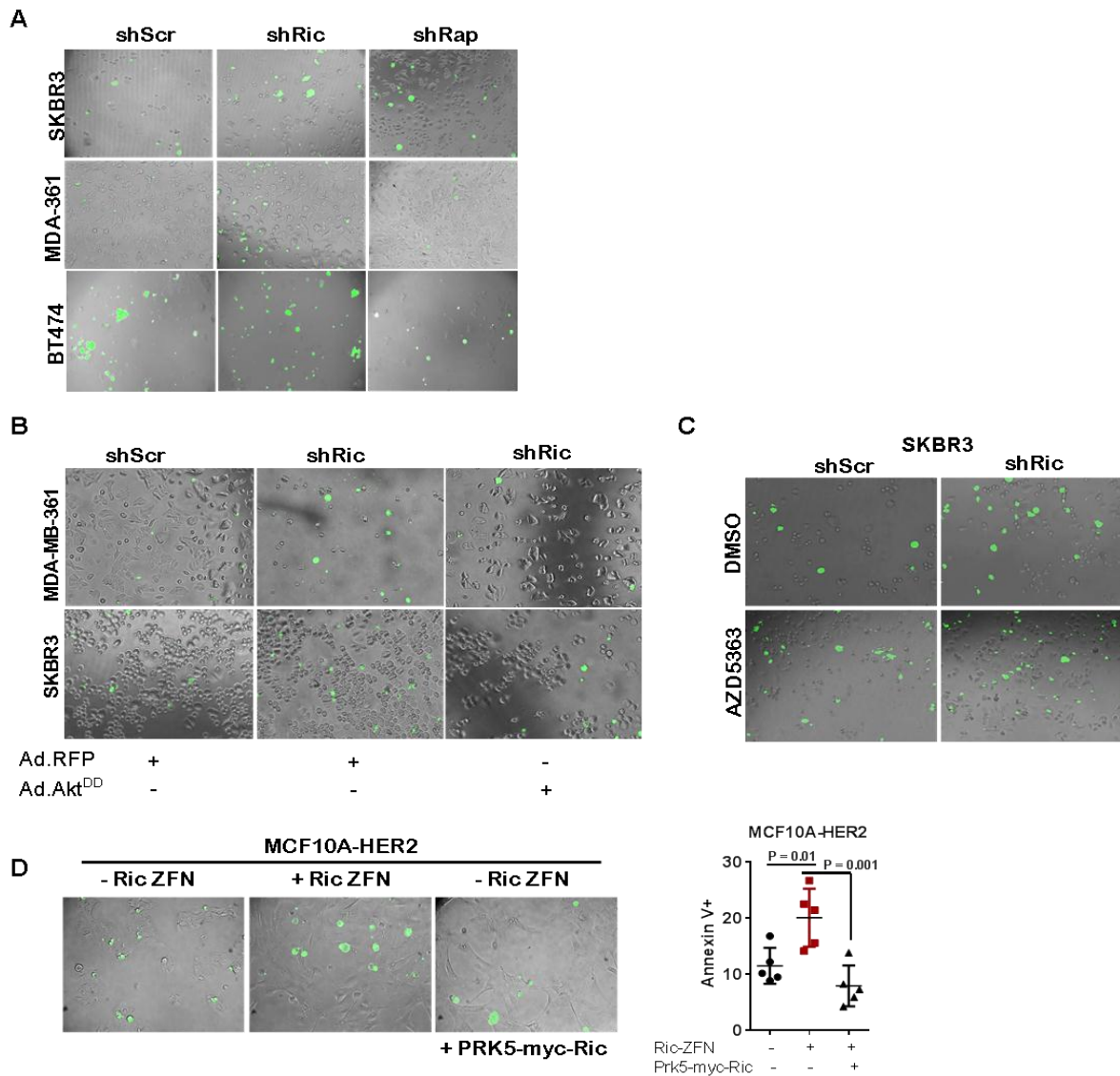


Figure 27. Rictor-mediated Akt activity is necessary and sufficient for breast cancer cell survival. **A.** Cells were labeled with Annexin V-FITC for 6 hours then imaged. **B.** shScr, shRictor or shRaptor cells were plated and infected with either Ad.RFP or Ad.Akt^{DD}. At 24 hours, cells were trypsinized and cells were plated and allowed to sit overnight. Cells were labeled with Annexin V-FITC and imaged at 6 hours. **C.** Cells were treated with AZD5363 (500 nM) for 24 hours and labeled with Annexin V-FITC for the final 6 hours, then imaged. **D.** MCF10A-HER2 cells were transduced with myc-Rictor x 48 hours, plated, labeled with Annexin V-FITC for 6 hours, then imaged. Midlines represent the average number of Annexin V-FITC positive cells of total cells. Value reflects average \pm SD, n=2 plated in quadruplicates.

Similarly, the number of TUNEL+ cells was increased nearly 4-fold in spontaneous *Rictor^{FL/FL}NIC* tumors over what was seen in *Rictor^{+/+}NIC* samples (**Figure 26E**).

We used adenoviral expression of an active Akt phospho-mimetic (Ad.Akt^{DD}) to restore Akt signaling in SKBR3 and MDA-MB-361 cells expressing shRictor, rescuing P-Akt S473 despite sustained Rictor depletion (**Figure 26F**). Restoration of Akt signaling in SKBR3 and MDA-MB-361 shRictor cells decreased the percentage of Annexin V+ cells to levels seen in shScr control cells (**Figure 26G, 27B**). Conversely, the allosteric Akt kinase inhibitor AZD5363, which decreased phosphorylation of the Akt substrate PRAS40 (**Figure 26H**), decreased survival of parental SKBR3 and MDA-MB-361 cells (**Figure 26I, 27C**). Rictor-deficient MCF10A-HER2 cells displayed an increased percentage of Annexin V+ cells. Re-expressing Rictor utilizing a myc-tagged Rictor restored levels of Annexin V+ cells to that of parental cells (**Figure 27D**). These results suggest that *HER2*-amplified breast cancer cells use Rictor-mediated Akt signaling for cell survival.

Rictor loss decreases migration/invasion of HER2-positive breast cancer cells.

Metastasis is the paramount behavior of tumor cells contributing to breast cancer mortality. Tumor-bearing *MMTV-NIC* mice develop lung metastases with nearly 100% penetrance, making it a useful model for studying metastasis *in vivo*. Using analysis of only tumor-bearing mice at 28 d after initial tumor palpation, we found that 90% (9/10) of all tumor-bearing *Rictor^{+/+}NIC* mice displayed histological evidence of lung metastases, whereas only 60% (3/5) of all *Rictor^{FL/FL}NIC* mice harbored lung metastases (**Figure 28A, B – left panel**). (Tumor-free mice were not included in the analysis of metastatic burden.)

Additionally, tumor-bearing *Rictor*^{FL/FL}*NIC* mice displayed a reduced average number of metastases per mouse as compared to *Rictor*^{+/+}*NIC* controls (**Figure 28B – right panel**). Low level expression of Rictor protein was detected in lung lesions from *Rictor*^{FL/FL}*NIC* mice, albeit in a small number of cells (**Figure 29A**), suggesting that these metastatic tumor cells may have escaped Cre-mediated Rictor loss. Metastasis is a multi-step process that requires cell motility and invasion (for intravasation and extravasation), in addition to cell survival and proliferation. We measured cellular invasion through Matrigel-coated transwell filters to determine if Rictor and/or Raptor is involved in these aspects of metastasis. Cells expressing shScr or shRaptor were capable of invasion and migration through Matrigel-coated transwells (**Figure 28C, 29B**). In contrast, few shRictor cells migrated through Matrigel-coated transwells. These results were confirmed using MCF10A-HER2 parental and Rictor-depleted cells (**Figure 29C**), again demonstrating reduced invasion and motility in the absence of Rictor. Because Rictor/mTORC2 is required for Rac1-mediated motility of untransformed MECs [62], we assessed Rac signaling in Rictor-depleted *HER2*-amplified breast cancer cells using a PAK1 binding domain (PBD)-glutathione S transferase (GST) pull-down assay, finding decreased Rac-GTP (active Rac) in SKBR3 and MDA-MB-361 cells expressing shRictor as compared to what was seen in cells expressing shScr (**Figure 28D**). We used PBD-GST to probe for *in situ* Rac-GTP in tumor sections harvested from *Rictor*^{+/+}*NIC* and *Rictor*^{FL/FL}*NIC* mice at 28 d after tumor palpation.

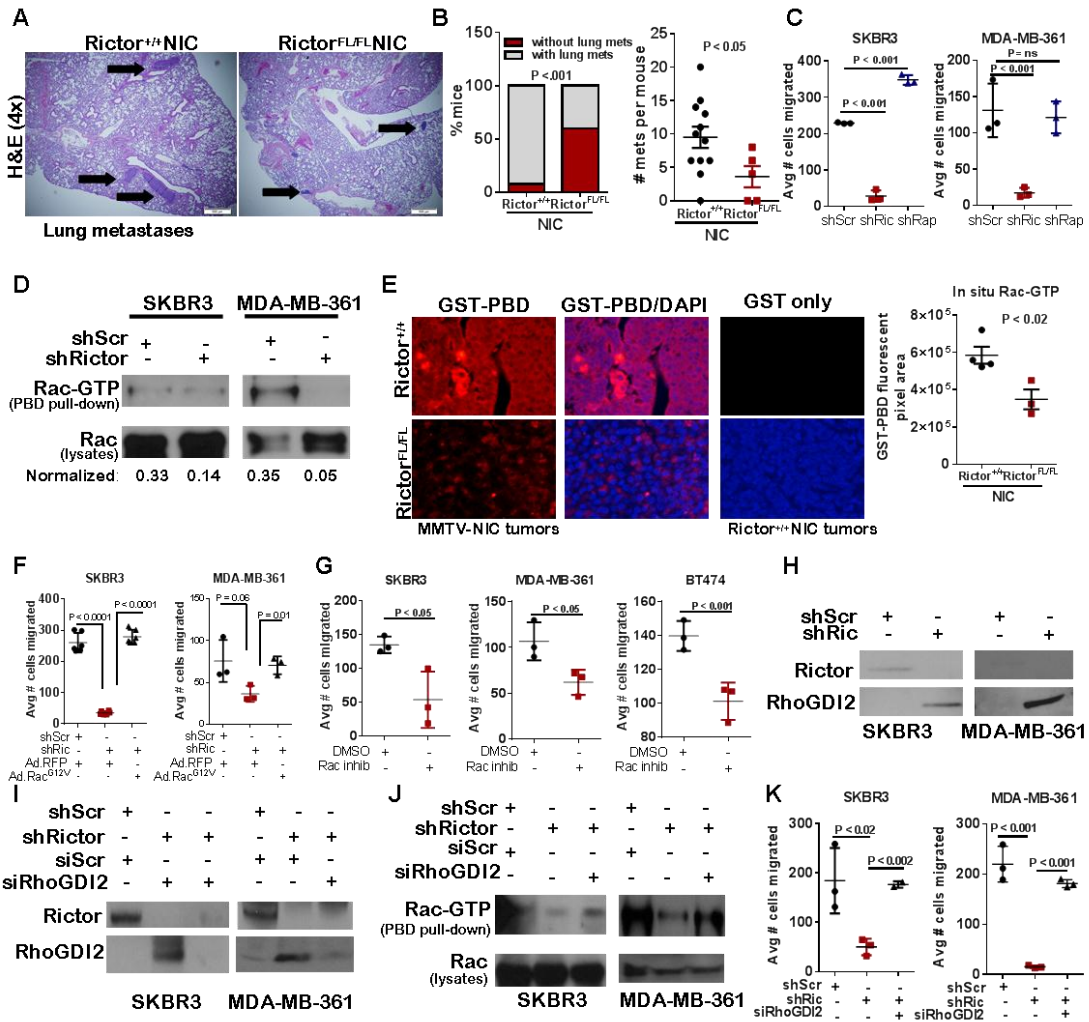


Figure 28. Rictor suppresses RhoGDI2 to activate Rac1 and control migration of HER2-positive breast cancer cells. **A.** H&E staining of lungs from the indicated mice. Representative images are shown, original magnification, 40X. **B.** Quantitation of lung metastasis in mice. Midlines in right panel represent average number of mets/mouse. Each data point represents an individual tumor-bearing mouse. **C.** Transwell migration of cells 24h after plating. Midlines represent average number of migrating cells; points represent average value of experiments performed in duplicate. **D.** PAK-PBD was used to pull down Rac-GTP in whole cell lysates, followed by immunoblot to detect Rac1. Whole cell lysates (lower panel) were assessed by western analysis. **E.** *In situ* detection of GST-PBD to assess Rac-GTP in tumor sections. Representative images are shown. Original magnification, 400X. Quantitation shows the average fluorescent pixel area/group (midlines) and the average fluorescence in 5 random fields/sample (points). **F-G.** Cells expressing Ad.RFP or Ad.Rac^{G12V} (**F**) or treated with a Rac inhibitor (**G**) were assessed for transwell migration. Midlines are the average number of migrating cells; points are the average of samples assessed in duplicate. **H-I.** Whole cell lysates were assessed by western analysis. **J.** PAK-PBD was used to pull down Rac-GTP in whole cell lysates. Pull-downs were assessed by immunoblot to detect Rac1. Rac was assessed by western analysis in whole cell lysates (lower panel). **K.** Transwell migration of cells 24h after plating. Midlines represent average number of migrating cells, points represent average value of experiments performed in duplicate.

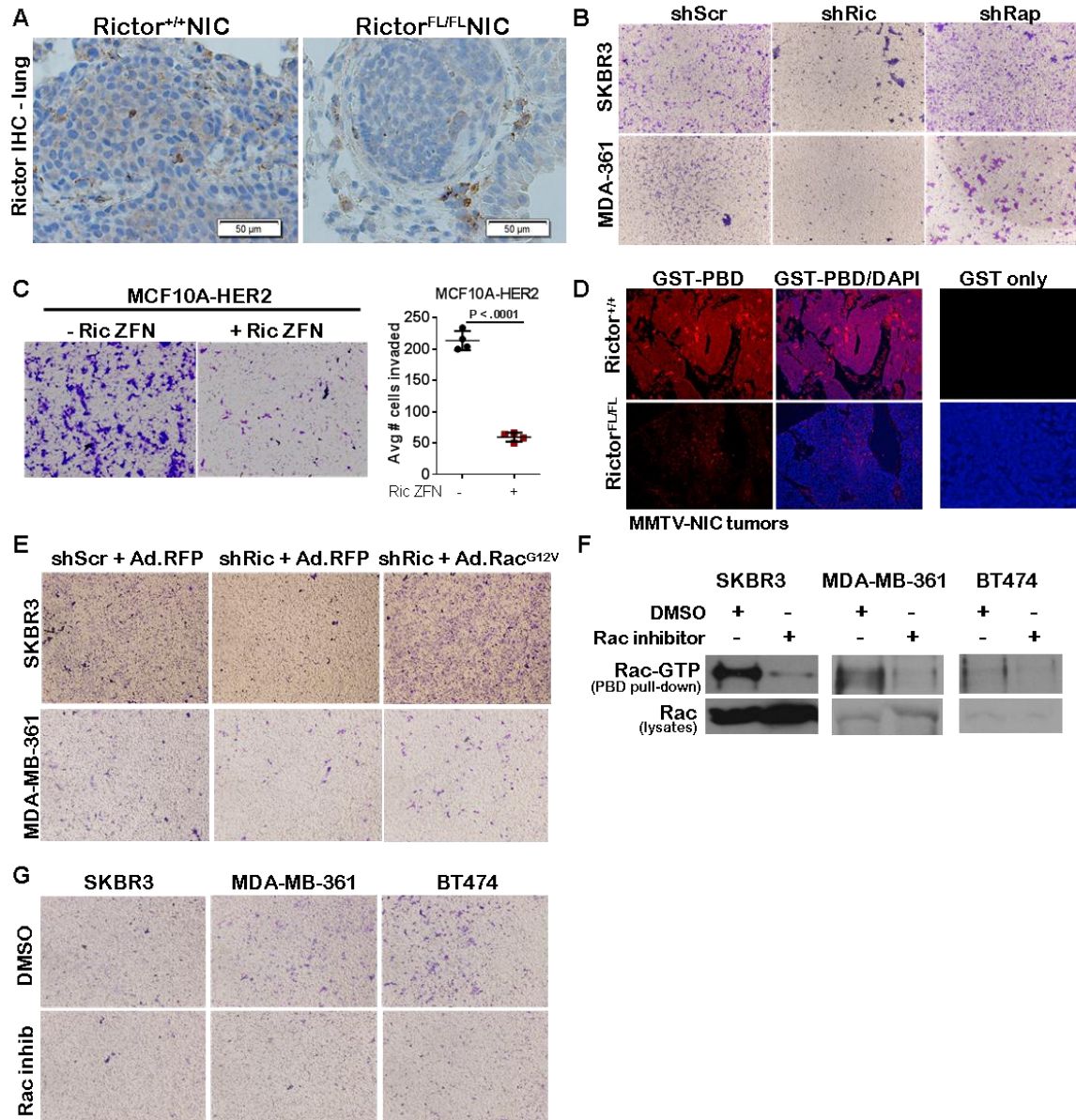


Figure 29. Rictor-mediated Rac1 activity is necessary for breast cancer cell migration. **A.** Rictor IHC was performed on lung sections from indicated mice. **B-C.** Transwell migration of cells 24 hours after plating. **D.** *In situ* detection of GST-PBD to assess Rac-GTP in tumor sections. **E.** Cells were infected with Ad.RFP or Ad.Rac^{G12V} for 24 hrs, and analyzed for their ability to migrate through transwell chambers at 24 hours. **F.** Parental breast cancer cells were treated with a Rac1 inhibitor and PAK-PBD was used to pull down Rac-GTP in whole cell lysates, followed by immunoblot to detect Rac. Whole cell lysates (lower panel) were assessed by western. **G.** Transwell migration of cells in the presence of Rac1 inhibitor at 24 hours. Data is representative of n=3 independent experiments, Student's t test. For D, n=4 tumors for Rictor^{+/+}NIC and 3 tumors for Rictor^{FL/FL}NIC.

Rictor^{+/+}*NIC* tumors showed abundant GST-PBD binding, but did not demonstrate any binding to GST lacking the PBD motif, demonstrating the specificity of the assay (**Figure 28E, 29D**). PBD-GST binding was substantially reduced in *Rictor*^{FL/FL}*NIC* tumors. We rescued Rac activity in Rictor-depleted cells using adenoviral delivery of an active Rac1 mutant, RacG12V. We found that Ad.RacG12V fully rescued motility/invasion of SKBR3 and MDA-MB-361 cells expressing shRictor (**Figure 28F, 29E**). Conversely, use of a pharmacological Rac inhibitor to inhibit Rac-GTP (**Figure 29F**) impaired motility/invasion of SKBR3, MDA-MB-361, and BT474 cells (**Figure 28G, 29G**).

Although Akt can increase cell motility in many different cell types [132], re-activation of Akt using Ad.Akt^{DD} only partially rescued cell migration in shRictor cells, despite full restoration of P-Akt S473 (**Figure 30A**). However, treatment with the Akt kinase inhibitor AZD4263 decreased migration/invasion of SKBR3 shScr cells, reducing migration to the levels seen in shRictor SKBR3 cells, but had no effect on the migration of MDA-MB-361 cells (**Figure 30B**). These data suggest that, while Akt is necessary for cell migration, it is not fully sufficient and that other signaling molecules may play a role downstream of Rictor to mediate these effects.

Rictor activates Rac1 through suppression of RhoGDI2.

Additional Rictor substrates were investigated for their role in promoting invasion/migration of HER2-positive breast cancer cells. PKC α [133] can activate Rac signaling in many circumstances, and has been linked to cell motility in normal MECs and breast cancers.

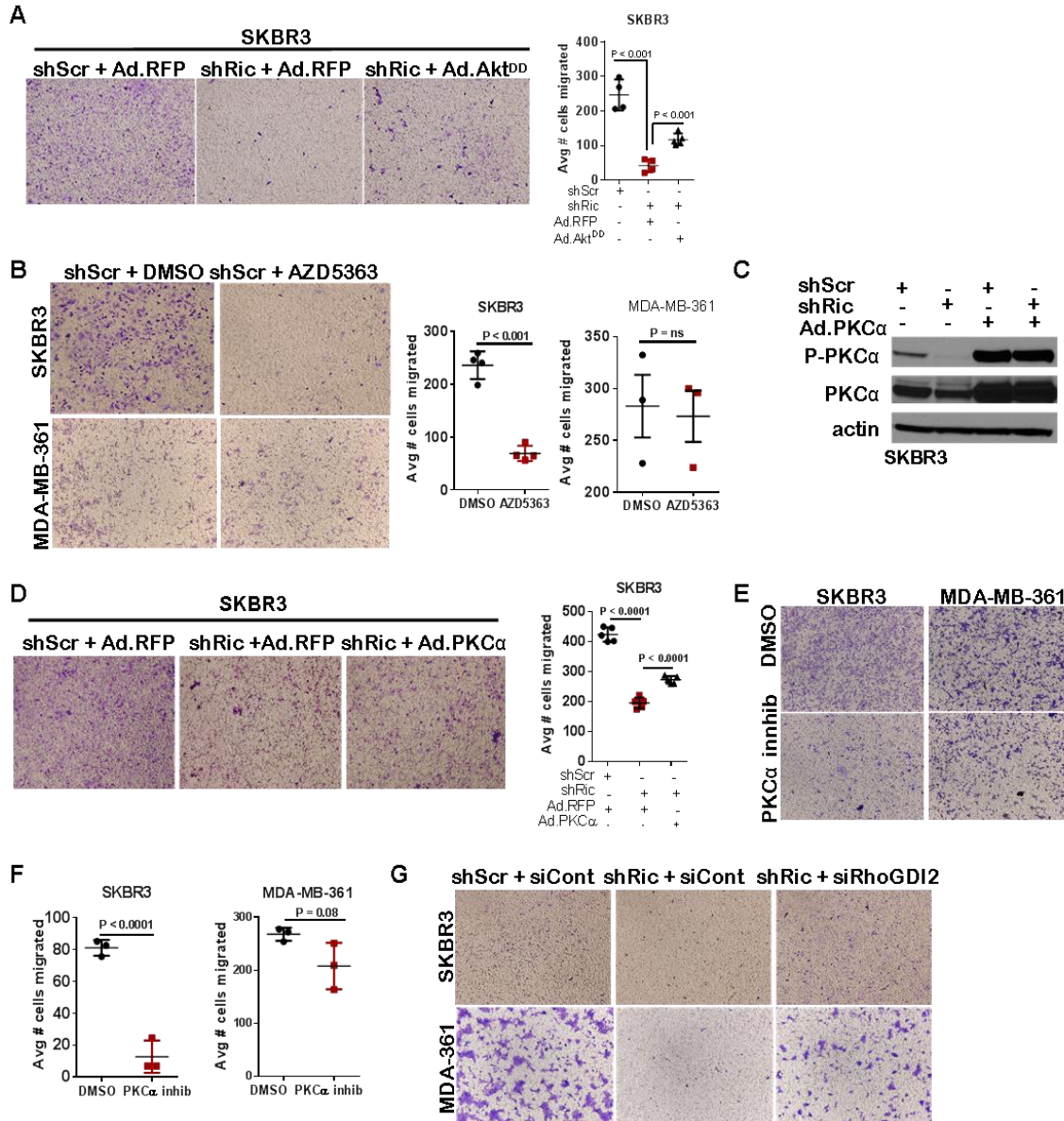


Figure 30. Akt or PKCα is insufficient to rescue Rictor-mediated defects in cell migration and invasion. **A.** Cells were infected with Ad.RFP or Ad.Akt^{DD} and analyzed for their ability to migrate through transwell chambers at 24 hours. **B.** Transwell migration of cells at 24 hour in the presence of AZD5363. **C.** Western analysis of shScr or shRictor cells treated with Ad.PKCα and **D.** analyzed for transwell migration at 24 hours. **E.** Cells were treated with PKCα inhibitor for 24 hours and analyzed for transwell migration. **E.** Transwell migration at 24 hours in the presence of a PKCα inhibitor (1μM). and **F.** quantitation. Midlines represent average number of cells migrated. Individual data points represent the average of triplicate images for each sample. **G.** Cells were treated with the indicated siRNA's for 48 hours and analyzed for their ability to migrate through transwell chambers. Data is representative of n=3 independent experiments, Student's t test. P < 0.05.

Adenoviral PKC α overexpression (**Figure 30C**) partially rescued Rictor-mediated cell migration defects in SKBR3 and MDA-MB-361 cells (**Figure 30D**). Conversely, PKC α inhibition significantly decreased transwell migration/invasion in parental SKBR3 cells but not in MDA-MB-361 (**Figure 30E, F**), suggesting that PKC α and Rictor both regulate cellular migration in *HER2*-amplified breast cancer cells, but using distinct and separable signaling pathways.

We examined expression of the Rac guanine exchange factor (GEF), RhoGDI2 in *HER2*-amplified breast cancer cells, based on previous observations that Rictor causes downregulation of RhoGDI2 levels in mouse embryonic fibroblasts to modulate Rac1 activity [87]. While RhoGDI2 remained below the level of detection by western blot in SKBR3 and MDA-MB-361 cells expressing shScr, we observed accumulation of RhoGDI2 in cells expressing shRictor (**Figure 28H**). Depletion of RhoGDI2 in Rictor-depleted cells using RhoGDI2 siRNA sequences (**Figure 28I**) restored Rac1-GTP levels to what was seen in cells expressing shScr (**Figure 28J**) and fully rescued cell migration of Rictor-depleted SKBR3 and MDA-MB-361 cells (**Figure 28K, 30G**). These data suggest that Rictor negatively regulates the Rac GEF RhoGDI2, permitting Rac1 activation and enhancing migration of *HER2*-amplified breast cancer cells.

Loss of Rictor sensitizes parental and resistant (LR) cells to lapatinib.

Since Rictor supports Akt-mediated cell survival in *HER2*-amplified breast cancer cells, we tested the impact of Rictor/mTORC2 loss on therapeutically induced tumor cell death, using lapatinib to block *HER2* kinase activity in SKBR3, MD-MB-361, and BT474 cells.

Within 0.5h, lapatinib decreased P-HER2 and P-Akt S473, as expected. However, P-Akt S473 re-emerged after 4h lapatinib treatment, despite sustained suppression of P-HER2 and P-S6. Resurgent P-Akt at 4h treatment correlated temporally with induction of Rictor protein levels (**Figure 31A**), and increased *RICTOR* mRNA (**Figure 31B**). *RPTOR* mRNA (**Figure 32A**), but not protein (**Figure 31A**), was increased at several time points but not in all cell lines and to a lesser extent than what was seen with *RICTOR* mRNA. As expected, shRictor blocked P-Akt resurgence in lapatinib-treated SKBR3 and MDA-MB-361 cells at 24 h (**Figure 31B**). SKBR3 and MDA-MB-361 cells expressing shRictor were treated with lapatinib, revealing that HER2 inhibition combined with Rictor depletion decreased P-Akt S473 to a greater extent than either agent alone (**Figure 31C**). In contrast, shRaptor had no impact on P-Akt S473. Although lapatinib decreased growth of SKBR3 and MDA-MB-361 cells expressing shScr, shRictor, and shRaptor in monolayer (**Figure 31D, 32C**) and in 3D Matrigel (**Figure 31E, 32D**), the combination of lapatinib plus shRictor produced the greatest degree of growth inhibition. Additionally, lapatinib-mediated cell death as measured by Annexin-V staining was highest in cells expressing shRictor as compared to shScr or shRaptor (**Figure 31E, 32E**). These data suggest that Rictor/mTORC2 targeting in *HER2*-amplified breast cancer cells improve tumor cell killing in response to lapatinib.

Because dual mTORC1/2 and HER2 blockade resulted in antitumor activity in breast tumor cells resistant to anti-HER2 therapies, we confirmed the requirement of mTORC1/2 in BT474 cells cultured in progressively increasing concentrations of lapatinib for greater than 6 months (BT474-LR) [127].

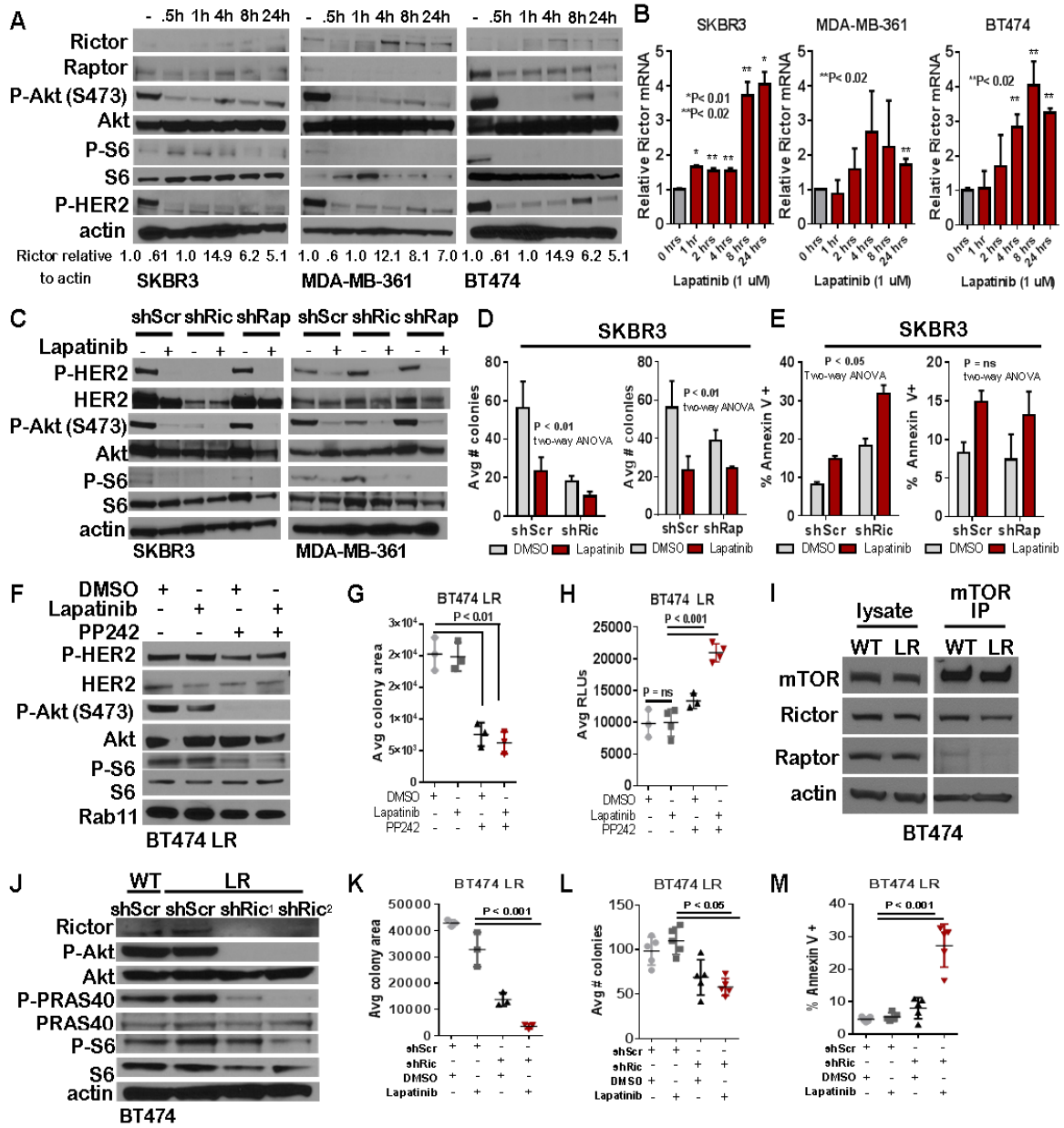


Figure 31. Rictor/mTORC2 loss sensitizes *HER2*-amplified tumor cells to lapatinib-mediated cell killing. **A-B.** Cells treated with lapatinib (1 μ M) were assessed by western blot (**A**) or qRT PCR (**B**). **C.** Western analysis of cell lysates with cells treated 4h with lapatinib (1 μ M). **D.** Cells embedded in Matrigel were cultured 14 days \pm lapatinib (1 μ M). Values shown are the average number of colonies, N =3, each assessed in duplicate. **E.** Annexin V-FITC staining of cells cultured 6h with lapatinib (1 μ M). Values shown are the average percentage of Annexin V-positive. Cells, N = 3. **F.** lapatinib-resistant BT-LR cells treated 4h \pm PP242 and \pm lapatinib were assessed by western analysis. **G.** BT-LR cells were embedded in matrigel and cultured 14 d \pm PP242 and \pm lapatinib. The average number of colonies is shown (midlines). **H.** BT-LR cells treated 24h \pm PP242 and \pm lapatinib were assessed for caspase 3/7 activity. Values shown are average luminescence per group (midline) and the average of duplicate experiments per sample (points). **I.** Immunoprecipitation of mTOR from whole cell lysates harvested from parental and lapatinib-resistant BT-474 cells, followed by immunoblot for Rictor or Raptor. **J.** Whole cell lysates were assessed by western analysis. **K-M** Parental or shRic BT LR cells were plated for growth in (**K**) 2D or (**L**) 3D Matrigel or (**M**) analysis of Annexin V –FITC staining. Values shown are the average value for each group. Points represent the average value from samples assessed in duplicate.

Lapatinib resistant BT474-LR cells treated with lapatinib in the presence or absence of PP242 revealed that, while P-AktS473 was unaffected by lapatinib treatment, PP242 abolished P-Akt S473 and reduced P-S6, consistent with mTORC1 and mTORC2 inhibition (**Figure 31F**). Further, PP242, but not lapatinib, decreased growth of BT474-LR cells cultured in monolayer (**Figure 31G, Figure 32F**), through induction of cell death as measured by detection of caspase 3/7 activity (**Figure 31H**). Interestingly, maximal growth inhibition was seen using the combination of lapatinib and PP242.

We examined mTORC2 complex assembly in parental and lapatinib-resistant BT474 cells using co-immunoprecipitation (co-IP) for mTOR with Rictor. Rictor co-precipitated with mTOR in both parental and lapatinib resistant cells (**Figure 31I**), confirming mTORC2 complex assembly. Interestingly, Raptor co-precipitated with mTOR to a lesser extent in lapatinib-resistant cells as compared to what was seen in parental BT474 cells. We next assessed the effects of Rictor/mTORC2 targeting on growth of lapatinib-resistant cells (**Figure 31J**). BT LR cells expressing shScr cultured in the presence of lapatinib expressed P-Akt S473, consistent with what has been described previously for BT474-LR cells. Rictor knock-down using shRictor resulted in blocked Akt S473 phosphorylation, even in lapatinib resistant cells (**Figure 31J**). While lapatinib reduced growth of parental BT474 cells in monolayer (**Figure 31K**), lapatinib did not affect growth of BT474-LR cells, confirming lapatinib resistance. However, shRictor decreased growth of BT474-LR cells cultured either with or without lapatinib (**Figure 33A**).

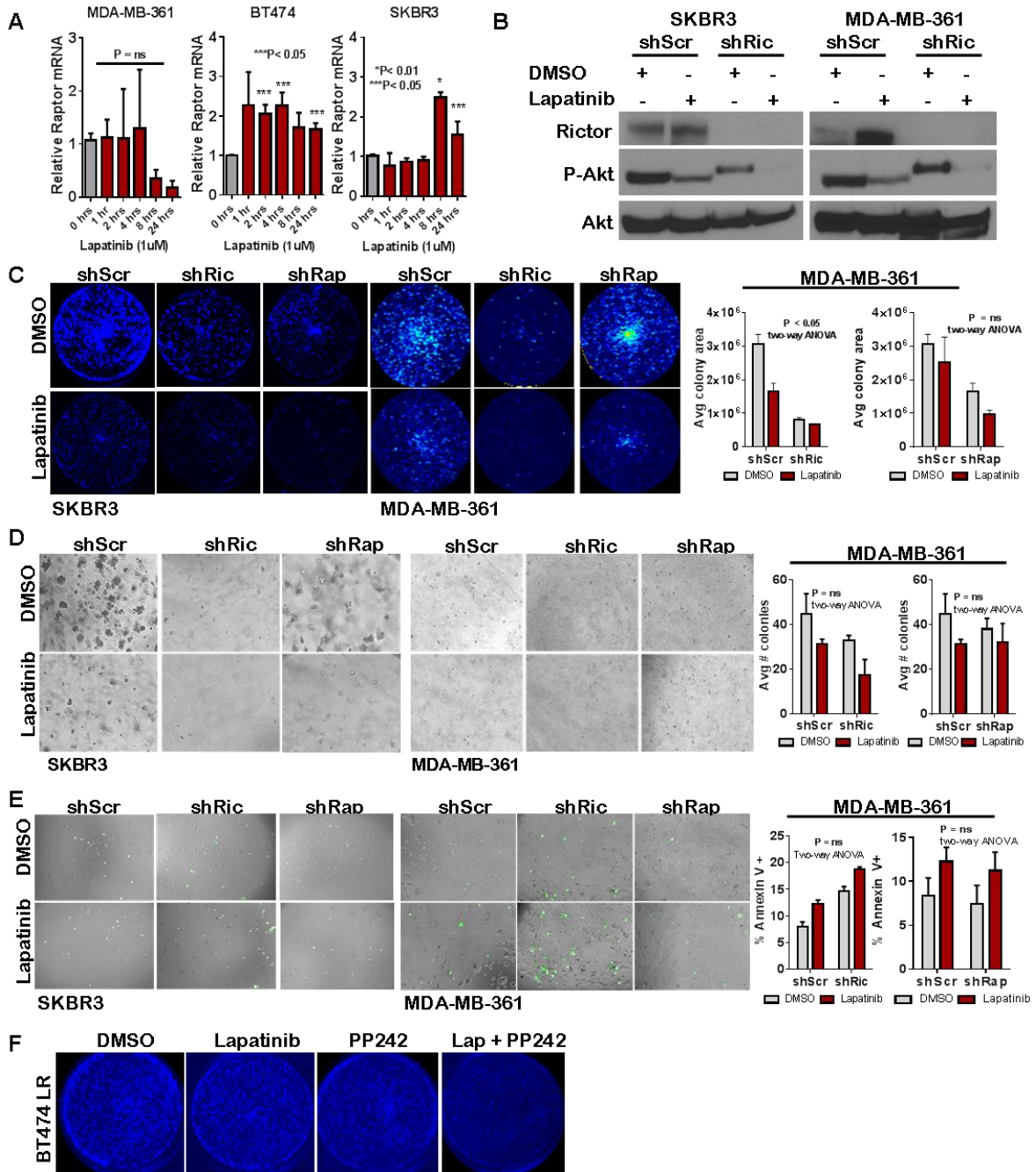
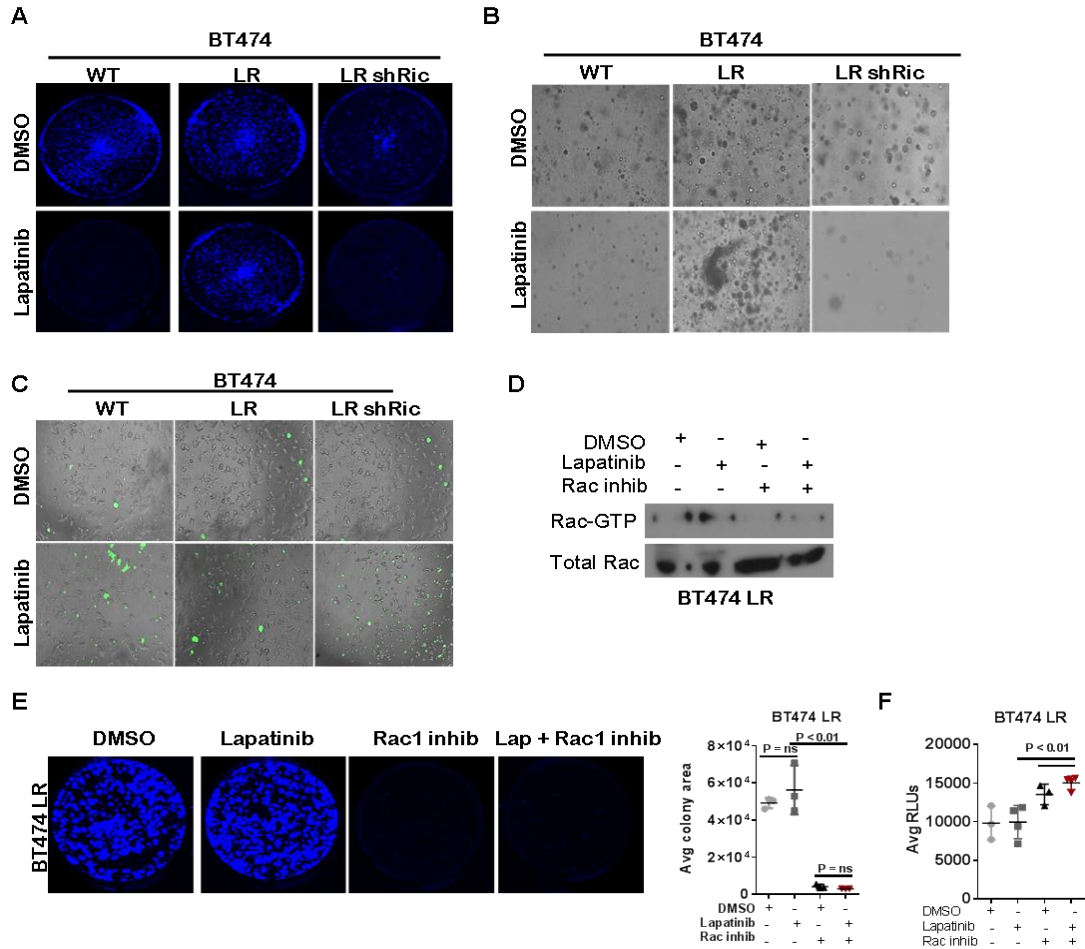


Figure 32. Loss of Rictor/mTORC2 sensitizes parental and resistant cells to lapatinib *in vitro*. **A.** Parental cells were treated with lapatinib for the indicated time and analyzed by qRT PCR to assess human Raptor mRNA levels. Values were normalized to GAPDH levels. **B.** Rictor knockdown cells were treated with lapatinib and analyzed by western blot. **C-E.** shScr, shRic or shRap cells were treated with DMSO or lapatinib and analyzed for **C.** 2D growth, **D.** 3D growth in Matrigel **E.** Annexin V-FITC staining. Representative images are shown. Quantitation was performed using ImageJ software. **F.** BT LR cells were analyzed for 2D growth in the presence of the indicated drugs.

Similar results were observed using cells cultured in 3D Matrigel, demonstrating that BT474-LR cells were insensitive to lapatinib-mediated growth inhibition, but formed fewer colonies upon depletion of Rictor (**Figure 31L, 33B**). As expected, BT474-LR expressing shScr did not display increased cell death in response to lapatinib (**Figure 31M, 33C**). However, shRictor-expressing BT474-LR cells exhibited increased cell death as compared to BT474-LR cells expressing shScr and the combination of lapatinib with shRictor loss produced >3-fold increase in BT474-LR cell death. Thus far, our data suggests that parental and LR cells use Rictor/mTORC2 for survival and growth. As Rac1 is a major downstream signaling node of mTORC2, we aimed to determine if Rac1 inhibition could decrease growth and survival of LR cells, in a similar way to mTORC1/2 inhibition. While BT474 LR cells did not respond to lapatinib with decreased growth or increased cell death, treatment with a small molecular inhibitor of Rac1 (**Figure 33D**) almost completely abolished growth in monolayer (**Figure 33E**), likely due to cell death as measured by a significant induction of caspase-mediated cell death (**Figure 33F**).

Taken together, our data uncovers a novel role for Rictor/mTORC2 in directly activating Akt and Rac to support the growth, survival and migration of *HER2*-amplified breast cancer cells. Targeting Rictor/mTORC2 or its downstream effector, Rac1, in combination with lapatinib may be clinically beneficial to patients with *HER2*-amplified tumors, including those with acquired resistance to the EGFR/*HER2* inhibitor, lapatinib.



Discussion

The studies presented here uncover the key roles played by mTORC2/Rictor in *HER2*-amplified breast cancer initiation, maintenance, progression, and metastasis. Abundant pre-clinical studies demonstrate that Akt/mTOR is a critical signaling node requiring inhibition in order to achieve a full therapeutic response in *HER2*-amplified breast cancers. However, most clinical and preclinical studies have focused primarily on mTORC1. This may be due to the fact that mTORC1 is seen as a direct downstream effector of the *HER2*/PI3K pathway, or perhaps due to the availability of pharmacological mTORC1-specific inhibitors, but not mTORC2-specific inhibitors. Increasing evidence suggests that mTORC1 inhibition promotes resurgent PI3K signaling due to loss of mTORC1-mediated negative feedback on the PI3K pathway, a potentially troublesome scenario when targeting tumors that thrive on *HER2*-activated PI3K signaling. The more recent development of mTOR kinase inhibitors, which will target both mTORC1 and mTORC2, has generated intense interest. Yet little is known about mTORC2-specific signaling in *HER2*-amplified breast cancers. Our analysis, using novel transgenic mouse models and genetic inhibition of mTORC1 versus mTORC2, reveals a vital role for Rictor/mTORC2 in the growth, survival and migration of *HER2*-amplified breast tumors and in their response to lapatinib, including those with acquired resistance to lapatinib.

Interestingly, we found increased Rictor expression in *HER2*-amplified human breast cancer cell lines and in human breast tumors. Further, Rictor intensity was highest in high-grade breast tumors, while Raptor intensity was similar across non-invasive or invasive breast cancer and adjacent normal tissue.

Interrogation of the TCGA database revealed that *RICTOR* or *MAPKAP1*, but not *RPTOR*, gains correlate with decreased patient survival. At least one additional study supports our findings that Rictor is overexpressed in human breast tumors. Zhang et al reported increased immunohistochemical detection of Rictor in primary breast tumors, correlating Rictor overexpression with lymph node metastasis [55]. Overexpression of another critical mTORC2-specific component, Sin1 (encoded by *MAPKAP1*), has been reported in aggressive papillary thyroid carcinoma and is associated with aberrantly elevated Akt phosphorylation [134]. These observations support a potential role for mTORC2 components in aggressive tumors and highlights Rictor/mTORC2 as a potential therapeutic target.

Conditional loss of either *RICTOR* or *RPTOR* in a transgenic mouse model of HER2-driven breast cancer decreased and delayed tumor formation, demonstrating that Rictor is necessary for the genesis of these tumors, and confirming a previously defined role for mTORC1 in the genesis of HER2/Neu-dependent mammary tumors [135, 136]. We found that Rictor depletion decreased Akt S473 phosphorylation (but not Akt T308 phosphorylation), decreased tumor cell growth and survival, and significantly diminished tumor cell metastasis. This strong *in vivo* data is supported by cell culture experiments showing that genetic *RICTOR*, but not *RPTOR*, loss decreased Akt activation (phospho-S473), cell survival and invasion/motility of multiple *HER2*-amplified breast cancer cell lines, including lines with activating *PIK3CA* mutations.

Abundant data highlight the key role of Akt signaling as a downstream effector of HER2 signaling in *HER2*-amplified breast cancers. Akt is phosphorylated downstream of two main pathways, the PI3K pathway (via PDK1 at T308) and the mTORC2 pathway (at S473) [137]. However, other kinases have been reported to phosphorylate Akt S473, including Inhibitor of κ B-Kinase (IKK)- α , DNA protein kinase (DNA-PK), and Integrin-Linked Kinase (ILK) [17]. Because Rictor loss decreases Akt S473 phosphorylation in these cells, and because expression of an active Akt mutant rescued cell survival in Rictor-depleted cells, it is possible that *HER2*-amplified breast cancers may be particularly reliant on mTORC2/Rictor for Akt S473 phosphorylation, revealing a potential vulnerability to mTORC2 inhibition in *HER2*-amplified cancers.

In our studies, restoration of Akt1 was sufficient to fully restore cell survival downstream of Rictor; however it could only partially rescue the invasion defects exerted by the loss of Rictor. Several lines of evidence suggest that cancer cells exploit Rictor-dependent signaling pathways to facilitate invasion and metastasis. For example, siRNA-mediated Rictor depletion decreased migration of MCF7 and MDA-MB-231 cells [55, 68]. In gliomas, Rictor overexpression promoted mTORC2 activity and tumor cell growth and motility [64]. Additionally, Rictor may interact with PKC isoforms to regulate breast cancer metastasis [55], although we found that PKC α inhibition only partially inhibited migration in *HER2*-amplified breast cancer cells, while PKC α restoration only partially rescued invasion/migration of Rictor-depleted *HER2*-amplified cells. Our Rictor-deficient *HER2*-amplified breast cancer cell lines and tumors exhibited significantly decreased Rac1 activity.

Recent studies in mouse embryonic fibroblasts show that Rictor suppresses RhoGDI2 expression, a negative regulator of Rac1 and a metastasis suppressor gene, thus allowing increased Rac1-mediated cell motility [87]. In support of these data, we show that Rictor downregulation in breast cancer cells results in accumulation of RhoGDI2 protein. Genetic ablation of RhoGDI2 in Rictor knockdown cells rescued Rac1 signaling and fully restored their migratory and invasive abilities, suggesting that Rictor negatively regulates RhoGDI2, allowing for full activation of Rac and increased cell motility. Although these data are the first (to our knowledge) linking Rictor to Rac1-mediated invasion and metastasis of breast cancer cells, Rictor-to-Rac1 signaling has been previously identified for cancers originating from other tissues [114-116], and previous studies have shown that *HER2*-amplified breast cancer cells use p120 Catenin-to-Rac1 signaling to promote breast cancer metastasis [138]

Taken together, our novel data highlight a signaling axis where Rictor relieves RhoGDI2-mediated blockade of Rac1 signaling, thus promoting dissemination of *HER2*-amplified breast cancer cells. Interestingly, this is distinct from untransformed mammary epithelial cells (MECs) which rely on an Akt-independent Rictor-PKCa-Rac1 signaling axis to control mammary morphogenesis, MEC survival and invasion [62] suggesting that untransformed mammary epithelial cells utilize pathways distinct from *HER2*-driven tumor cells, which may possess increased reliance on Akt for cell survival and may downregulate RhoGDI2 to enhance Rac1 signaling and migratory ability.

Efficient metastatic progression relies on a coordinated series of steps involving cell motility and invasion (for intravasation and extravasation), in addition to cell survival and proliferation. While we show that Rictor loss decreases metastatic ability of HER2-driven breast tumors and that Rictor/mTORC2 directly controls cell migration, we have not ruled out the potential impact Rictor loss may have on survival of disseminated tumor cells and how this may affect seeding/establishment of overt lung metastases in our model.

The PI3-kinase (PI3K)/mTOR pathway is aberrantly activated up to 60% of clinical breast cancers, facilitating tumor cell growth, survival, metabolism, and invasion [105, 106]. Although mTORC1 signaling is abundantly upregulated in *HER2*-amplified cancers, inhibitors of mTORC1 show limited clinical efficacy as single agents. In agreement with these observations, we found that Raptor/mTORC1 ablation effectively inhibited cell growth, but not cell survival or cell invasion in *HER2*-amplified breast cancer cells. In contrast, Rictor/mTORC2 ablation decreased cell growth, survival, and invasion suggesting that mTORC2 targeting may be a more efficacious approach. Our findings are supported by a recent report in which heregulin/*HER2*-driven breast cancer cell lines required mTORC2 for their cell survival [139]. Although mTORC2-specific inhibitors are not yet available, dual mTORC1/2 inhibitors are being met with some success, and are being investigated in combination with currently available inhibitors of *HER2* and PI3K.

We show here that treatment of HER2-positive breast cancer cells with the mTORC1/2 inhibitor, PP242, sensitized parental and lapatinib-resistant cells to the growth inhibitory effects of lapatinib, findings that are consistent with several recent studies combining anti-HER2 agents or anti-PI3K agents with dual mTORC1/2 inhibitors [67, 108-110] [140]. Taken together, these studies underscore the clinical relevance of mTORC2 in breast cancer.

In summary, we have used clinical breast cancer datasets along with spontaneous and cell culture-based models of breast cancer to reveal previously unreported roles for Rictor/mTORC2 in the genesis, maintenance, progression, and metastasis of HER2-driven breast cancers. We have shown that targeted inhibition of Rictor/mTORC2 is effective at each stage in the natural history of *HER2*-amplified tumors. These data support continued translation investigation of dual mTORC1/2 inhibitors to improve the outcome for patients with *HER2*-amplified breast cancers, and warrant future efforts to develop mTORC2-specific inhibitors.

Chapter IV

CONCLUSIONS AND FUTURE DIRECTIONS

Conclusions

mTOR is a well-studied kinase that plays necessary roles in both physiology and in disease. It has become increasingly apparent that mTOR influences most cellular functions including cell growth, proliferation, metabolism, survival and migration. While essential roles for mTOR have been described in brain, adipose tissue, muscle, and liver under physiological conditions the differential roles of mTORC1 and mTORC2 have not been explored in regards to post-natal mammary gland development. Bridging this knowledge gap would not only highlight the important and distinct roles of mTORC2 in the normal epithelium, but also would likely provide information regarding the mammary-specific signaling pathways that cancer cells could hijack to drive breast tumor formation, progression, and therapeutic resistance. To date, breast cancer research and to some extent, mammary gland development research, has focused particular attention on mTORC1, perhaps due to its location within its signaling pathway downstream of PI3K, and in part due to the commercial and clinical development of mTORC1 inhibitors. However, a growing body of data highlighting a key role of mTORC2 in various cancer types exists, including PI3K-driven prostate and glioblastoma. When the research project described herein was initiated, the role of mTORC2 in breast cancer was understudied.

The work presented here was the first, to our knowledge, to dissect the differential roles of mTORC1 and mTORC2 in post-natal mammary morphogenesis, to elucidate how these signaling complexes are used by cancer cells to mediate survival and migration, and to identify the novel and unique role of mTORC2 in breast development and cancer.

Rictor/mTORC2 is required for normal mammary gland development

These studies are the first to demonstrate the requirement for Rictor/mTORC2 in untransformed MECs for their survival, migration and morphogenesis. Interestingly, these processes relied fully on a PKC α -Rac1 signaling axis. Surprisingly, we found that Akt, a main downstream mTORC2 effector, was necessary but not sufficient to rescue defects caused by Rictor ablation. In contrast, Raptor/mTORC1 ablation only caused minor and transient defects in proliferation of MECs at 6 weeks.

At the onset of puberty, MECs in glands of *Rictor* wildtype mice exhibited rapid proliferation and developed complex, branched structures that fully invaded into the mammary fat pad by 10 weeks of age. In contrast, *Rictor*^{MGKO} glands exhibited reduced fat pad filling at both 6 and 10 week time points, manifested as decreased ductal length and diminished side branching in whole mounted mammary glands. These defects were due, at least in part, to reduced proliferation, as measured by Ki67 staining of luminal MECs, which was observed at 6 weeks of age, but resolved by 10 weeks of age. Additionally, cell death, as measured by TUNEL staining, was significantly increased at both 6 and 10 weeks of age in *Rictor*-deficient mammary glands. In contrast, *Raptor*-deficient mammary glands displayed only transient decreases in proliferation and ductal outgrowth at 6 weeks, which resolved by 10 weeks, and no alteration in cell death.

Thus, loss of Rictor/mTORC2 impairs survival, proliferation and branching morphogenesis *in vivo*, a phenotype distinct from that produced by loss of Raptor/mTORC1.

Subsequent studies utilizing *ex vivo* manipulation of PMECs revealed molecular pathways downstream of Rictor contributing to these processes. Loss of Rictor significantly reduced P-Akt S473 levels cell survival, cell invasion and branching morphogenesis in 3D Matrigel. In contrast Raptor loss decreased phosphorylation of S6, an mTORC1 target but did not affect Akt phosphorylation, cell survival, cell invasion, or branching morphogenesis. These results reveal that mTOR operates primarily within mTORC2 to drive cell survival and motility within the untransformed mammary epithelium. Surprisingly, Akt restoration in Rictor-deficient MECs only modestly enhanced branching morphogenesis, while Akt inhibition in wild-type MECs decreased mammary branching and colony size. These results suggest that Akt is necessary but not sufficient to drive branching morphogenesis in the absence of Rictor. Further, Akt restoration in Rictor-null MECs was not sufficient to rescue MEC invasion or survival, suggesting other factors downstream of Rictor/mTORC2 regulate these processes in normal mammary gland development. To this end, restoration of PKC α signaling to Rac1, or Rac1 activation independently of upstream signals, fully rescued all phenotypes resulting from Rictor loss in cell culture and in transplanted Rictor-deficient MECs *in vivo*. Therefore, Rictor-dependent mTORC2 is essential for PKC α -Rac1 signaling to drive mammary morphogenesis.

Rictor/mTORC2 drives progression and therapeutic resistance of HER2-amplified breast cancers

As these results show that Rictor/mTORC2 is necessary in untransformed MECs and because molecular pathways that regulate normal mammary gland development are often commandeered by cancer cells to support their growth and survival, we tested the requirement of Rictor/mTORC2 in tumor cells. We used clinical breast cancer datasets, spontaneous tumor mouse models and cell culture-based models of human breast cancer to reveal previously unreported roles for Rictor/mTORC2 in the maintenance, progression, and metastasis of HER2-driven breast cancers. We demonstrated that Rictor/mTORC2 is necessary for migration of the *HER2*-amplified breast cancer cell lines, SKBR3, MDA-MB-361 and BT474, which rely on Rictor-mediated Rac1 signaling for enhanced migration. While Rictor knockdown decreased Rac activity, a constitutively active Rac mutant fully rescued migration defects in Rictor-deficient breast tumor cells. Importantly, spontaneous HER2-dependent mammary tumors required Rictor for Rac activity and metastasis to lungs, in part due to accumulation of the Rac1 inhibitor, RhoGDI2 upon Rictor loss. These data suggest that inhibition of mTORC2-to-Rac signaling may block tumor cell metastasis.

As expected based on the role of mTORC2 in Akt phosphorylation, Rictor loss from *HER2*-amplified breast tumor cells, and from spontaneous mouse mammary tumor models of *HER2*-amplified breast cancer, resulted in decreased Akt phosphorylation and decreased cell survival.

Because Rictor supported Akt-mediated cell survival in *HER2*-amplified breast cancer cells, we tested the impact of Rictor/mTORC2 loss on therapeutically induced tumor cell death, using lapatinib to block HER2 kinase activity in *HER2*-amplified breast cancer cell lines. Lapatinib treatment induced Rictor protein expression at 8-24 hours post-treatment and this corresponded with resurgent Akt activation. Blocking Rictor in combination with lapatinib resulted in greater cell death and greater inhibition of P-Akt than either condition alone. Interestingly, Rictor loss combined with lapatinib treatment resulted in greater inhibition of cell growth than loss of Raptor and lapatinib.

Because lapatinib treatment induced Rictor protein expression which correlated with reactivation of P-Akt, we tested the requirement for Rictor in HER2-positive breast cancer cells that had been cultured in increasing concentrations of lapatinib to generate lapatinib-resistant (LR) cells. Cells with acquired resistance to the HER2 inhibitor lapatinib retained P-Akt S473 following lapatinib treatment, but lost P-Akt S473 upon Rictor ablation. Additionally, while BT LR cells did not respond to lapatinib with increased cell death, as expected, loss of Rictor in combination with lapatinib treatment resulted in significantly increased cell death compared to lapatinib or DMSO control.

Because our studies demonstrate that Rac1 is a major downstream signaling effector of mTORC2, we sought to determine if Rac1 inhibition in combination with lapatinib would recapitulate the effects we saw with Rictor loss in combination with lapatinib. Indeed, Rac1 inhibition sensitized LR cells to growth inhibitory and cell-killing effects of lapatinib.

These results suggest that mTORC2-Akt signaling remains an Achilles heel in lapatinib-resistant *HER2*-amplified breast cancers, an observation that might be exploited currently using dual mTORC1/2 inhibitors, or in the future pending the development of mTORC2-specific inhibitors.

Taken together, our data uncovers a novel role for Rictor/mTORC2 in directly activating Akt and Rac to support the growth, survival and migration of *HER2*-amplified breast cancer cells. Targeting Rictor/mTORC2 or its downstream effector, Rac1, in combination with lapatinib may be clinically beneficial to patients with *HER2*-amplified tumors, including those with acquired resistance to the EGFR/*HER2* inhibitor, lapatinib.

Future directions

The role of Rictor/mTORC2 in the alveolar epithelium during pregnancy/lactation

During pregnancy, luminal MECs rapidly proliferate and differentiate to generate milk-producing alveolar cells [2]. We have demonstrated that loss of Rictor results in decreased ductal lengthening during puberty, decreased cell motility and cell survival *ex vivo*, and decreased Akt phosphorylation at S473 *in vivo* and *ex vivo*. Based on this data, it is plausible that loss of Rictor in the alveolar epithelium will also display decreased phosphorylation of Akt at S473, due to decreased mTORC2 activity and that this will correlate with decreased survival in alveolar MECs. Cell survival in the alveolar epithelium is required to sustain lactation once pups begin nursing. Accordingly, loss of Akt1 similarly impairs survival of milk-producing alveolar cells in lactating mammary glands [40]. It is therefore possible that loss of Rictor will impair cell survival in the alveolar epithelium, resulting in a phenotype similar to that induced by loss of Akt1.

Additionally, preliminary data from our lab suggests that Rictor loss in ductal MECs impairs localization of ZO-1, a tight junction protein necessary for proper cell polarization of epithelial cells. As proper polarization is necessary for alveolar cell structure and functionality [141] it will be important to determine the effects of Rictor ablation on MEC polarization, growth, differentiation, and milk production in alveolar mammary epithelium during pregnancy and lactation *in vivo*.

Breast cancer subtype-specific roles for mTORC2

Data outlined in this dissertation reveals a necessary and previously unreported role for Rictor/mTORC2 in the growth, survival and migration of *HER2*-amplified breast cancer cells. Our results are supported by additional *in vitro* studies showing that Rictor/mTORC2 is necessary for heregulin-mediated growth of *HER2*-positive breast cancer cells [139]. While we, and others, have explored the role of Rictor/mTORC2 in *HER2*-driven breast tumors, it is probable that Rictor/mTORC2 is necessary for similar processes in additional subtypes of breast cancer. Indeed, we found that Rictor mRNA and protein levels were elevated in several human, ER-positive, luminal breast cancer cell lines, including ZR75-1 and HCC1428 cells. Intriguingly, TCGA-curated data shows a significant correlation between *RICTOR* copy number gain and decreased survival in luminal breast cancers (data not shown, TCGA, $P < 0.01$). Additional, unpublished data from our lab has shown that loss of Rictor decreases P-Akt S473, decreases growth, survival and migration in MCF7 cells, similar to our findings in *HER2*-amplified breast cancer cells.

This is supported by several published studies demonstrating that Rictor knockdown suppressed anchorage-independent growth of MCF7 breast tumor cells [111] and that Rictor controls survival and migration of MCF7 (ER-positive) [142] and MDA-MB-231 (basal-like) breast cancer cells [69]. It is also clear that mTORC2 plays a necessary role in PI3K-driven prostate [63] and glioblastomas [64]. *PIK3CA* mutations are most abundant in luminal/ER+ breast cancers, suggesting this also may be true for PI3K-driven breast tumors.

As preclinical data using everolimus, an mTORC1 inhibitor, also confirms a role for mTORC1 in luminal breast cancers, additional research is necessary to understand the specific contribution of mTORC1 versus mTORC2 in the luminal subtype of breast cancer and in response to antiestrogens.

Rictor/mTORC2 in breast tumor cell metabolism

Increasing evidence from multiple cell types has demonstrated a necessary role for Rictor/mTORC2 in control of cellular metabolism. For example, liver-specific knockout of Rictor, which impaired Akt and PKCa activation, resulted in decreased glycolysis and lipogenesis, both key processes that are necessary for rapid proliferation to support uncontrolled tumor growth [30]. In glioblastoma cells, mTORC2 plays a central role in cancer metabolic reprogramming, controlling glycolytic metabolism through direct, inactivating phosphorylation of class IIa HDACs, leading to acetylation of FOXO1 and FOXO3, which releases suppression of c-myc by miRNA's [143]. In glioblastoma patients, activated mTORC2 was highly correlated with shorter survival. Overall, these studies defined a specific, Akt-independent role for mTORC2 in regulating glycolytic metabolism in glioblastoma. Therefore, it is interesting to speculate that a direct link between mTORC2 and anabolic processes in breast cancer cells could also exist. While the role of mTORC2 in glycolytic metabolism of breast cancer cells hasn't been directly tested, a recent study demonstrated that mTORC2 controls lipogenesis in breast cancer cells through direct regulation of *SREBP1* [144].

Based on these data, it would be important to assess if loss of Rictor in breast cancer cells impairs the function of lipogenic enzymes (like fatty acid synthase, FASN), transcription factors that regulate lipogenesis downstream of Akt (SREBP), and other controllers of breast cancer cell metabolism.

Targeting Rictor/mTORC2 for treatment of breast cancer

HER2-driven breast cancers are treated with HER2-targeted therapies but nearly 100% of metastatic HER2-positive breast cancers acquire resistance to HER2 inhibitors, underscoring a desperate need for new therapeutic targets in *HER2*-amplified breast cancers. Preclinical studies demonstrated that everolimus, an mTORC1 inhibitor that can inhibit mTORC2 through indirect mechanisms in some cell types, sensitized *HER2*-amplified tumors to the HER2 monoclonal antibody, Herceptin. In these studies, everolimus inhibited both mTORC1 and mTORC2. And although ATP competitive mTORC1/2 inhibitors effectively prevent mTORC2 activity, the negative consequences of mTORC1 inhibition [compensatory activation of PI3K signaling, immunosuppression] may limit their therapeutic potential. For example, a recent study showed that inhibition of mTOR kinase caused activation of receptor tyrosine kinase signaling which re-induced PI3K signaling, Akt phosphorylation at T308 and, despite persistent inhibition of mTORC2 activity and AKT S473 phosphorylation [145]. This PI3K pathway reactivation could severely limit clinical utility of these inhibitors and prove detrimental to patients treated with these drugs. Thus, while the role of mTOR in HER2-positive breast cancer is evident, a knowledge gap remains regarding the specific role and therapeutic potential of mTORC2 inhibitors in *HER2*-amplified, PI3K-dependent breast cancers.

mTORC2-specific inhibitors do not currently exist, but one may postulate how these could be designed. For example, small molecule inhibitors could be designed that target the interaction between Sin1 and mTOR, which is necessary for proper assembly and activation of mTORC2. Additionally, XPLN, an endogenous inhibitor of mTORC2 that preferentially interacts with mTORC2, but not mTORC1, has recently been described [146]. As an N-terminal, 125-amino-acid fragment of XPLN was found to be both necessary and sufficient for the inhibition of mTORC2 and downstream signaling, it is possible that fragment could be exploited for inactivation of mTORC2 in tumor cells.

In conclusion, data outlined in this dissertation shows a necessary role for Rictor/mTORC2 in growth, survival and migration of HER2-driven tumor cells. Importantly, we also demonstrate that loss of Rictor/mTORC2 signaling sensitizes parental and resistant cells to lapatinib and that loss of Rictor/mTORC2 signaling produces a greater anti-proliferation effect when combined with lapatinib than loss of Raptor/mTORC2 combined with lapatinib. This suggests that targeting Rictor/mTORC2 in combination with lapatinib, while sparing direct inhibition of mTORC1, may be a favorable approach in breast cancer and is clear evidence that mTORC2-specific inhibitors need to be further explored.

REFERENCES

1. Lauring, J., B.H. Park, and A.C. Wolff, *The phosphoinositide-3-kinase-Akt-mTOR pathway as a therapeutic target in breast cancer*. J Natl Compr Canc Netw, 2013. **11**(6): p. 670-8.
2. Hennighausen, L. and G.W. Robinson, *Information networks in the mammary gland*. Nat Rev Mol Cell Biol, 2005. **6**(9): p. 715-25.
3. Alqurashi, N., S.M. Hashimi, and M.Q. Wei, *Chemical Inhibitors and microRNAs (miRNA) Targeting the Mammalian Target of Rapamycin (mTOR) Pathway: Potential for Novel Anticancer Therapeutics*. Int J Mol Sci, 2013. **14**(2): p. 3874-900.
4. Gajewska, M., K. Zielniok, and T. Motyl, *Autophagy in Development and Remodelling of Mammary Gland*. Autophagy - A Double-Edged Sword - Cell Survival or Death? 2013.
5. Helliwell, S.B., et al., *TOR1 and TOR2 are structurally and functionally similar but not identical phosphatidylinositol kinase homologues in yeast*. Mol Biol Cell, 1994. **5**(1): p. 105-18.
6. Jacinto, E., et al., *Mammalian TOR complex 2 controls the actin cytoskeleton and is rapamycin insensitive*. Nat Cell Biol, 2004. **6**(11): p. 1122-8.
7. Laplante, M. and D.M. Sabatini, *mTOR signaling at a glance*. J Cell Sci, 2009. **122**(Pt 20): p. 3589-94.
8. Dumont, F.J. and Q. Su, *Mechanism of action of the immunosuppressant rapamycin*. Life Sci, 1996. **58**(5): p. 373-95.
9. Sehgal, S.N., *Sirolimus: its discovery, biological properties, and mechanism of action*. Transplant Proc, 2003. **35**(3 Suppl): p. 7S-14S.
10. Sarbassov, D.D., et al., *Prolonged rapamycin treatment inhibits mTORC2 assembly and Akt/PKB*. Mol Cell, 2006. **22**(2): p. 159-68.
11. Inoki, K., et al., *TSC2 integrates Wnt and energy signals via a coordinated phosphorylation by AMPK and GSK3 to regulate cell growth*. Cell, 2006. **126**(5): p. 955-68.
12. Sengupta, S., T.R. Peterson, and D.M. Sabatini, *Regulation of the mTOR complex 1 pathway by nutrients, growth factors, and stress*. Mol Cell, 2010. **40**(2): p. 310-22.
13. Feng, Z., et al., *The coordinate regulation of the p53 and mTOR pathways in cells*. Proc Natl Acad Sci U S A, 2005. **102**(23): p. 8204-9.
14. Sancak, Y., et al., *Ragulator-Rag complex targets mTORC1 to the lysosomal surface and is necessary for its activation by amino acids*. Cell, 2010. **141**(2): p. 290-303.
15. Zoncu, R., et al., *mTORC1 senses lysosomal amino acids through an inside-out mechanism that requires the vacuolar H(+)-ATPase*. Science, 2011. **334**(6056): p. 678-83.
16. Sarbassov, D.D., et al., *Phosphorylation and regulation of Akt/PKB by the rictor-mTOR complex*. Science, 2005. **307**(5712): p. 1098-101.
17. McDonald, P.C., et al., *Rictor and integrin-linked kinase interact and regulate Akt phosphorylation and cancer cell survival*. Cancer Res, 2008. **68**(6): p. 1618-24.
18. Jacinto, E., et al., *SIN1/MIP1 maintains rictor-mTOR complex integrity and regulates Akt phosphorylation and substrate specificity*. Cell, 2006. **127**(1): p. 125-37.

19. Guertin, D.A., et al., *Ablation in mice of the mTORC components raptor, rictor, or mLST8 reveals that mTORC2 is required for signaling to Akt-FOXO and PKCalpha, but not S6K1*. Dev Cell, 2006. **11**(6): p. 859-71.
20. Zinzalla, V., et al., *Activation of mTORC2 by association with the ribosome*. Cell, 2011. **144**(5): p. 757-68.
21. Dibble, C.C., J.M. Asara, and B.D. Manning, *Characterization of Rictor phosphorylation sites reveals direct regulation of mTOR complex 2 by S6K1*. Mol Cell Biol, 2009. **29**(21): p. 5657-70.
22. Liu, P., et al., *Sin1 phosphorylation impairs mTORC2 complex integrity and inhibits downstream Akt signalling to suppress tumorigenesis*. Nat Cell Biol, 2013. **15**(11): p. 1340-50.
23. Shiota, C., et al., *Multiallelic disruption of the rictor gene in mice reveals that mTOR complex 2 is essential for fetal growth and viability*. Dev Cell, 2006. **11**(4): p. 583-9.
24. Polak, P., et al., *Adipose-specific knockout of raptor results in lean mice with enhanced mitochondrial respiration*. Cell Metab, 2008. **8**(5): p. 399-410.
25. Kumar, A., et al., *Fat cell-specific ablation of rictor in mice impairs insulin-regulated fat cell and whole-body glucose and lipid metabolism*. Diabetes, 2010. **59**(6): p. 1397-406.
26. Bentzinger, C.F., et al., *Skeletal muscle-specific ablation of raptor, but not of rictor, causes metabolic changes and results in muscle dystrophy*. Cell Metab, 2008. **8**(5): p. 411-24.
27. Sengupta, S., et al., *mTORC1 controls fasting-induced ketogenesis and its modulation by ageing*. Nature, 2010. **468**(7327): p. 1100-4.
28. Li, S., M.S. Brown, and J.L. Goldstein, *Bifurcation of insulin signaling pathway in rat liver: mTORC1 required for stimulation of lipogenesis, but not inhibition of gluconeogenesis*. Proc Natl Acad Sci U S A, 2010. **107**(8): p. 3441-6.
29. Yecies, J.L., et al., *Akt stimulates hepatic SREBP1c and lipogenesis through parallel mTORC1-dependent and independent pathways*. Cell Metab, 2011. **14**(1): p. 21-32.
30. Hagiwara, A., et al., *Hepatic mTORC2 activates glycolysis and lipogenesis through Akt, glucokinase, and SREBP1c*. Cell Metab, 2012. **15**(5): p. 725-38.
31. Gu, Y., et al., *Rictor/mTORC2 is essential for maintaining a balance between beta-cell proliferation and cell size*. Diabetes, 2011. **60**(3): p. 827-37.
32. Rachdi, L., et al., *Disruption of Tsc2 in pancreatic beta cells induces beta cell mass expansion and improved glucose tolerance in a TORC1-dependent manner*. Proc Natl Acad Sci U S A, 2008. **105**(27): p. 9250-5.
33. Blouet, C., H. Ono, and G.J. Schwartz, *Mediobasal hypothalamic p70 S6 kinase 1 modulates the control of energy homeostasis*. Cell Metab, 2008. **8**(6): p. 459-67.
34. Gjorevski, N. and C.M. Nelson, *Integrated morphodynamic signalling of the mammary gland*. Nat Rev Mol Cell Biol, 2011. **12**(9): p. 581-93.
35. McNally, S. and F. Martin, *Molecular regulators of pubertal mammary gland development*. Ann Med, 2011. **43**(3): p. 212-34.
36. Boxer, R.B., et al., *Isoform-specific requirement for Akt1 in the developmental regulation of cellular metabolism during lactation*. Cell Metab, 2006. **4**(6): p. 475-90.
37. Hutchinson, J., et al., *Activation of Akt (protein kinase B) in mammary epithelium provides a critical cell survival signal required for tumor progression*. Mol Cell Biol, 2001. **21**(6): p. 2203-12.

38. Schwertfeger, K.L., M.M. Richert, and S.M. Anderson, *Mammary gland involution is delayed by activated Akt in transgenic mice*. Mol Endocrinol, 2001. **15**(6): p. 867-81.
39. Schwertfeger, K.L., et al., *Expression of constitutively activated Akt in the mammary gland leads to excess lipid synthesis during pregnancy and lactation*. J Lipid Res, 2003. **44**(6): p. 1100-12.
40. Maroulakou, I.G., et al., *Distinct roles of the three Akt isoforms in lactogenic differentiation and involution*. J Cell Physiol, 2008. **217**(2): p. 468-77.
41. Jankiewicz, M., B. Groner, and S. Desrivieres, *Mammalian target of rapamycin regulates the growth of mammary epithelial cells through the inhibitor of deoxyribonucleic acid binding Id1 and their functional differentiation through Id2*. Mol Endocrinol, 2006. **20**(10): p. 2369-81.
42. Kim, S.H., K. Zukowski, and R.F. Novak, *Rapamycin effects on mTOR signaling in benign, premalignant and malignant human breast epithelial cells*. Anticancer Res, 2009. **29**(4): p. 1143-50.
43. Galbaugh, T., et al., *EGF-induced activation of Akt results in mTOR-dependent p70S6 kinase phosphorylation and inhibition of HC11 cell lactogenic differentiation*. BMC Cell Biol, 2006. **7**: p. 34.
44. Moriya, H., et al., *Secretion of three enzymes for fatty acid synthesis into mouse milk in association with fat globules, and rapid decrease of the secreted enzymes by treatment with rapamycin*. Arch Biochem Biophys, 2011. **508**(1): p. 87-92.
45. Pauloin, A. and E. Chanat, *Prolactin and epidermal growth factor stimulate adipophilin synthesis in HC11 mouse mammary epithelial cells via the PI3-kinase/Akt/mTOR pathway*. Biochim Biophys Acta, 2012. **1823**(5): p. 987-96.
46. Sarbassov, D.D., et al., *Rictor, a novel binding partner of mTOR, defines a rapamycin-insensitive and raptor-independent pathway that regulates the cytoskeleton*. Curr Biol, 2004. **14**(14): p. 1296-302.
47. Ikenoue, T., et al., *Essential function of TORC2 in PKC and Akt turn motif phosphorylation, maturation and signalling*. EMBO J, 2008. **27**(14): p. 1919-31.
48. Sun, M., et al., *AKT1/PKBalpha kinase is frequently elevated in human cancers and its constitutive activation is required for oncogenic transformation in NIH3T3 cells*. Am J Pathol, 2001. **159**(2): p. 431-7.
49. Li, D.M. and H. Sun, *PTEN/MMAC1/TEP1 suppresses the tumorigenicity and induces G1 cell cycle arrest in human glioblastoma cells*. Proc Natl Acad Sci U S A, 1998. **95**(26): p. 15406-11.
50. Arboleda, M.J., et al., *Overexpression of AKT2/protein kinase Bbeta leads to up-regulation of beta1 integrins, increased invasion, and metastasis of human breast and ovarian cancer cells*. Cancer Res, 2003. **63**(1): p. 196-206.
51. Stiles, B., et al., *Essential role of AKT-1/protein kinase B alpha in PTEN-controlled tumorigenesis*. Mol Cell Biol, 2002. **22**(11): p. 3842-51.
52. Steinberg, S.F., *Structural basis of protein kinase C isoform function*. Physiol Rev, 2008. **88**(4): p. 1341-78.
53. Ways, D.K., et al., *MCF-7 breast cancer cells transfected with protein kinase C-alpha exhibit altered expression of other protein kinase C isoforms and display a more aggressive neoplastic phenotype*. J Clin Invest, 1995. **95**(4): p. 1906-15.
54. Lonne, G.K., et al., *PKCalpha expression is a marker for breast cancer aggressiveness*. Mol Cancer, 2010. **9**: p. 76.

55. Zhang, F., et al., *mTOR complex component Rictor interacts with PKCzeta and regulates cancer cell metastasis*. *Cancer Res*, 2010. **70**(22): p. 9360-70.
56. Garcia-Martinez, J.M. and D.R. Alessi, *mTOR complex 2 (mTORC2) controls hydrophobic motif phosphorylation and activation of serum- and glucocorticoid-induced protein kinase 1 (SGK1)*. *Biochem J*, 2008. **416**(3): p. 375-85.
57. Kobayashi, T. and P. Cohen, *Activation of serum- and glucocorticoid-regulated protein kinase by agonists that activate phosphatidylinositide 3-kinase is mediated by 3-phosphoinositide-dependent protein kinase-1 (PDK1) and PDK2*. *Biochem J*, 1999. **339** (Pt 2): p. 319-28.
58. Sahoo, S., et al., *Coordinate expression of the PI3-kinase downstream effectors serum and glucocorticoid-induced kinase (SGK-1) and Akt-1 in human breast cancer*. *Eur J Cancer*, 2005. **41**(17): p. 2754-9.
59. Sommer, E.M., et al., *Elevated SGK1 predicts resistance of breast cancer cells to Akt inhibitors*. *Biochem J*, 2013. **452**(3): p. 499-508.
60. He, Y., et al., *Mammalian target of rapamycin and Rictor control neutrophil chemotaxis by regulating Rac/Cdc42 activity and the actin cytoskeleton*. *Mol Biol Cell*, 2013. **24**(21): p. 3369-80.
61. Dada, S., N. Demartines, and O. Dormond, *mTORC2 regulates PGE2-mediated endothelial cell survival and migration*. *Biochem Biophys Res Commun*, 2008. **372**(4): p. 875-9.
62. Morrison, M.M., et al., *mTOR Directs Breast Morphogenesis through the PKC-alpha-Rac1 Signaling Axis*. *PLoS Genet*, 2015. **11**(7): p. e1005291.
63. Guertin, D.A., et al., *mTOR complex 2 is required for the development of prostate cancer induced by Pten loss in mice*. *Cancer Cell*, 2009. **15**(2): p. 148-59.
64. Masri, J., et al., *mTORC2 activity is elevated in gliomas and promotes growth and cell motility via overexpression of rictor*. *Cancer Res*, 2007. **67**(24): p. 11712-20.
65. Roulin, D., et al., *Targeting mTORC2 inhibits colon cancer cell proliferation in vitro and tumor formation in vivo*. *Mol Cancer*, 2010. **9**: p. 57.
66. O'Reilly, K.E., et al., *mTOR inhibition induces upstream receptor tyrosine kinase signaling and activates Akt*. *Cancer Res*, 2006. **66**(3): p. 1500-8.
67. Wander, S.A., B.T. Hennessy, and J.M. Slingerland, *Next-generation mTOR inhibitors in clinical oncology: how pathway complexity informs therapeutic strategy*. *J Clin Invest*, 2011. **121**(4): p. 1231-41.
68. Li, H., et al., *Targeting of mTORC2 prevents cell migration and promotes apoptosis in breast cancer*. *Breast Cancer Res Treat*, 2012. **134**(3): p. 1057-66.
69. Serrano, I., et al., *Role of the integrin-linked kinase (ILK)/Rictor complex in TGFbeta-1-induced epithelial-mesenchymal transition (EMT)*. *Oncogene*, 2013. **32**(1): p. 50-60.
70. Baselga, J., et al., *Everolimus in postmenopausal hormone-receptor-positive advanced breast cancer*. *N Engl J Med*, 2012. **366**(6): p. 520-9.
71. Dowsett, M., et al., *Mechanisms of resistance to aromatase inhibitors*. *J Steroid Biochem Mol Biol*, 2005. **95**(1-5): p. 167-72.
72. Bachelot, T., et al., *Randomized phase II trial of everolimus in combination with tamoxifen in patients with hormone receptor-positive, human epidermal growth factor receptor 2-negative metastatic breast cancer with prior exposure to aromatase inhibitors: a GINECO study*. *J Clin Oncol*, 2012. **30**(22): p. 2718-24.

73. André, F., et al., *Everolimus for women with trastuzumab-resistant, HER2-positive, advanced breast cancer (BOLERO-3): a randomised, double-blind, placebo-controlled phase 3 trial*. *The Lancet Oncology*. **15**(6): p. 580-591.
74. Taberero, J., et al., *Abstract CT-02: A phase I, open label, dose escalation study of oral mammalian target of rapamycin inhibitor INK128 administered by intermittent dosing regimens in patients with advanced malignancies*. *Cancer Research*, 2012. **72**(8 Supplement): p. CT-02.
75. Paplomata, E. and R. O'Regan, *The PI3K/AKT/mTOR pathway in breast cancer: targets, trials and biomarkers*. *Ther Adv Med Oncol*, 2014. **6**(4): p. 154-66.
76. Laplante, M. and D.M. Sabatini, *mTOR signaling in growth control and disease*. *Cell*, 2012. **149**(2): p. 274-93.
77. Phung, T.L., et al., *Pathological angiogenesis is induced by sustained Akt signaling and inhibited by rapamycin*. *Cancer Cell*, 2006. **10**(2): p. 159-70.
78. Rosner, M. and M. Hengstschlager, *Cytoplasmic and nuclear distribution of the protein complexes mTORC1 and mTORC2: rapamycin triggers dephosphorylation and delocalization of the mTORC2 components rictor and sin1*. *Hum Mol Genet*, 2008. **17**(19): p. 2934-48.
79. Hong, S.M., et al., *Rapamycin inhibits both motility through down-regulation of p-STAT3 (S727) by disrupting the mTORC2 assembly and peritoneal dissemination in sarcomatoid cholangiocarcinoma*. *Clin Exp Metastasis*, 2012.
80. Andrechek, E.R., et al., *Amplification of the neu/erbB-2 oncogene in a mouse model of mammary tumorigenesis*. *Proc Natl Acad Sci U S A*, 2000. **97**(7): p. 3444-9.
81. Ewald, A.J., et al., *Collective epithelial migration and cell rearrangements drive mammary branching morphogenesis*. *Dev Cell*, 2008. **14**(4): p. 570-81.
82. Brantley-Sieders, D.M., et al., *The receptor tyrosine kinase EphA2 promotes mammary adenocarcinoma tumorigenesis and metastatic progression in mice by amplifying ErbB2 signaling*. *J Clin Invest*, 2008. **118**(1): p. 64-78.
83. Qu, S., et al., *Gene targeting of ErbB3 using a Cre-mediated unidirectional DNA inversion strategy*. *Genesis*, 2006. **44**(10): p. 477-86.
84. Brantley-Sieders, D.M., et al., *EphA2 receptor tyrosine kinase regulates endothelial cell migration and vascular assembly through phosphoinositide 3-kinase-mediated Rac1 GTPase activation*. *J Cell Sci*, 2004. **117**(Pt 10): p. 2037-49.
85. Liang, C.C., A.Y. Park, and J.L. Guan, *In vitro scratch assay: a convenient and inexpensive method for analysis of cell migration in vitro*. *Nat Protoc*, 2007. **2**(2): p. 329-33.
86. Burnett, P.E., et al., *RAFT1 phosphorylation of the translational regulators p70 S6 kinase and 4E-BP1*. *Proc Natl Acad Sci U S A*, 1998. **95**(4): p. 1432-7.
87. Agarwal, N.K., et al., *Rictor regulates cell migration by suppressing RhoGDI2*. *Oncogene*, 2013. **32**(20): p. 2521-6.
88. Wullschleger, S., R. Loewith, and M.N. Hall, *TOR signaling in growth and metabolism*. *Cell*, 2006. **124**(3): p. 471-84.
89. Iden, S. and J.G. Collard, *Crosstalk between small GTPases and polarity proteins in cell polarization*. *Nat Rev Mol Cell Biol*, 2008. **9**(11): p. 846-59.
90. Muthuswamy, S.K. and B. Xue, *Cell polarity as a regulator of cancer cell behavior plasticity*. *Annu Rev Cell Dev Biol*, 2012. **28**: p. 599-625.

91. Sun, S.Y., et al., *Activation of Akt and eIF4E survival pathways by rapamycin-mediated mammalian target of rapamycin inhibition*. *Cancer Res*, 2005. **65**(16): p. 7052-8.
92. Wang, X., et al., *Enhancing mammalian target of rapamycin (mTOR)-targeted cancer therapy by preventing mTOR/raptor inhibition-initiated, mTOR/ricor- independent Akt activation*. *Cancer Res*, 2008. **68**(18): p. 7409-18.
93. Li, Y., et al., *Protein phosphatase 2A and DNA-dependent protein kinase are involved in mediating rapamycin-induced Akt phosphorylation*. *J Biol Chem*, 2013.
94. Meyer, D.S., et al., *Luminal expression of PIK3CA mutant H1047R in the mammary gland induces heterogeneous tumors*. *Cancer Res*, 2011. **71**(13): p. 4344-51.
95. Chen, C.C., et al., *Akt is required for Stat5 activation and mammary differentiation*. *Breast Cancer Res*, 2010. **12**(5): p. R72.
96. Chen, C.C., et al., *Autocrine prolactin induced by the Pten-Akt pathway is required for lactation initiation and provides a direct link between the Akt and Stat5 pathways*. *Genes Dev*, 2012. **26**(19): p. 2154-68.
97. Debnath, J., S.J. Walker, and J.S. Brugge, *Akt activation disrupts mammary acinar architecture and enhances proliferation in an mTOR-dependent manner*. *J Cell Biol*, 2003. **163**(2): p. 315-26.
98. Zhang, B., Y. Zhang, and E. Shacter, *Rac1 inhibits apoptosis in human lymphoma cells by stimulating Bad phosphorylation on Ser-75*. *Mol Cell Biol*, 2004. **24**(14): p. 6205-14.
99. Zhu, W. and C.M. Nelson, *PI3K regulates branch initiation and extension of cultured mammary epithelia via Akt and Rac1 respectively*. *Dev Biol*, 2013. **379**(2): p. 235-45.
100. Baselga, J., *Targeting the phosphoinositide-3 (PI3) kinase pathway in breast cancer*. *Oncologist*, 2011. **16 Suppl 1**: p. 12-9.
101. Pollack, M.N., *Insulin, insulin-like growth factors, insulin resistance, and neoplasia*. *Am J Clin Nutr*, 2007. **86**(3): p. s820-2.
102. Sachdev, D. and D. Yee, *The IGF system and breast cancer*. *Endocr Relat Cancer*, 2001. **8**(3): p. 197-209.
103. Fenton, T.R. and I.T. Gout, *Functions and regulation of the 70kDa ribosomal S6 kinases*. *Int J Biochem Cell Biol*, 2011. **43**(1): p. 47-59.
104. Serra, V., et al., *RSK3/4 mediate resistance to PI3K pathway inhibitors in breast cancer*. *J Clin Invest*, 2013.
105. Miller, T.W., J.M. Balko, and C.L. Arteaga, *Phosphatidylinositol 3-kinase and antiestrogen resistance in breast cancer*. *J Clin Oncol*, 2011. **29**(33): p. 4452-61.
106. Miller, T.W., et al., *Mutations in the phosphatidylinositol 3-kinase pathway: role in tumor progression and therapeutic implications in breast cancer*. *Breast Cancer Res*, 2011. **13**(6): p. 224.
107. Li, G., et al., *Conditional loss of PTEN leads to precocious development and neoplasia in the mammary gland*. *Development*, 2002. **129**(17): p. 4159-70.
108. Janku, F., et al., *PIK3CA mutations in patients with advanced cancers treated with PI3K/AKT/mTOR axis inhibitors*. *Mol Cancer Ther*, 2011. **10**(3): p. 558-65.
109. Janku, F., et al., *PI3K/AKT/mTOR inhibitors in patients with breast and gynecologic malignancies harboring PIK3CA mutations*. *J Clin Oncol*, 2012. **30**(8): p. 777-82.
110. Janku, F., et al., *PIK3CA mutation H1047R is associated with response to PI3K/AKT/mTOR signaling pathway inhibitors in early-phase clinical trials*. *Cancer Res*, 2013. **73**(1): p. 276-84.

111. Hietakangas, V. and S.M. Cohen, *TOR complex 2 is needed for cell cycle progression and anchorage-independent growth of MCF7 and PC3 tumor cells*. BMC Cancer, 2008. **8**: p. 282.
112. Wazir, U., et al., *Prognostic and therapeutic implications of mTORC1 and Rictor expression in human breast cancer*. Oncol Rep, 2013. **29**(5): p. 1969-74.
113. Kim, H.Y. and C.M. Nelson, *Extracellular matrix and cytoskeletal dynamics during branching morphogenesis*. Organogenesis, 2012. **8**(2): p. 56-64.
114. Schnelzer, A., et al., *Rac1 in human breast cancer: overexpression, mutation analysis, and characterization of a new isoform, Rac1b*. Oncogene, 2000. **19**(26): p. 3013-20.
115. Fritz, G., et al., *Rho GTPases in human breast tumours: expression and mutation analyses and correlation with clinical parameters*. Br J Cancer, 2002. **87**(6): p. 635-44.
116. Katz, E., et al., *Targeting of Rac GTPases blocks the spread of intact human breast cancer*. Oncotarget, 2012. **3**(6): p. 608-19.
117. Ross, J.S. and J.A. Fletcher, *The HER-2/neu Oncogene in Breast Cancer: Prognostic Factor, Predictive Factor, and Target for Therapy*. Oncologist, 1998. **3**(4): p. 237-252.
118. Arteaga, C.L., et al., *Treatment of HER2-positive breast cancer: current status and future perspectives*. Nat Rev Clin Oncol, 2012. **9**(1): p. 16-32.
119. Engelman, J.A., *Targeting PI3K signalling in cancer: opportunities, challenges and limitations*. Nat Rev Cancer, 2009. **9**(8): p. 550-62.
120. Kim, D.H., et al., *mTOR interacts with raptor to form a nutrient-sensitive complex that signals to the cell growth machinery*. Cell, 2002. **110**(2): p. 163-75.
121. Oh, W.J. and E. Jacinto, *mTOR complex 2 signaling and functions*. Cell Cycle, 2011. **10**(14): p. 2305-16.
122. Zhang, Z., et al., *mTOR-rictor is the Ser473 kinase for AKT1 in mouse one-cell stage embryos*. Mol Cell Biochem, 2012. **361**(1-2): p. 249-57.
123. Balko, J.M., et al., *The receptor tyrosine kinase ErbB3 maintains the balance between luminal and basal breast epithelium*. Proc Natl Acad Sci U S A, 2012. **109**(1): p. 221-6.
124. Morrison, M.M., et al., *ErbB3 downregulation enhances luminal breast tumor response to antiestrogens*. J Clin Invest, 2013. **123**(10): p. 4329-43.
125. Baselga, J., et al., *Phase II randomized study of neoadjuvant everolimus plus letrozole compared with placebo plus letrozole in patients with estrogen receptor-positive breast cancer*. J Clin Oncol, 2009. **27**(16): p. 2630-7.
126. Lu, C.H., et al., *Preclinical testing of clinically applicable strategies for overcoming trastuzumab resistance caused by PTEN deficiency*. Clin Cancer Res, 2007. **13**(19): p. 5883-8.
127. Rexer, B.N., et al., *Phosphoproteomic mass spectrometry profiling links Src family kinases to escape from HER2 tyrosine kinase inhibition*. Oncogene, 2011. **30**(40): p. 4163-74.
128. Finkle, D., et al., *HER2-targeted therapy reduces incidence and progression of midlife mammary tumors in female murine mammary tumor virus huHER2-transgenic mice*. Clin Cancer Res, 2004. **10**(7): p. 2499-511.
129. Northey, J.J., et al., *Signaling through ShcA is required for transforming growth factor beta- and Neu/ErbB-2-induced breast cancer cell motility and invasion*. Mol Cell Biol, 2008. **28**(10): p. 3162-76.

130. Miller, T.W., et al., *Inhibition of mammalian target of rapamycin is required for optimal antitumor effect of HER2 inhibitors against HER2-overexpressing cancer cells.* Clin Cancer Res, 2009. **15**(23): p. 7266-76.
131. She, Q.B., et al., *Breast tumor cells with PI3K mutation or HER2 amplification are selectively addicted to Akt signaling.* PLoS One, 2008. **3**(8): p. e3065.
132. Enomoto, A., et al., *Akt/PKB regulates actin organization and cell motility via Girdin/APE.* Dev Cell, 2005. **9**(3): p. 389-402.
133. Tan, M., et al., *Upregulation and activation of PKC alpha by ErbB2 through Src promotes breast cancer cell invasion that can be blocked by combined treatment with PKC alpha and Src inhibitors.* Oncogene, 2006. **25**(23): p. 3286-95.
134. Moraitis, D., et al., *SIN1, a critical component of the mTOR-Rictor complex, is overexpressed and associated with AKT activation in medullary and aggressive papillary thyroid carcinomas.* Surgery, 2014. **156**(6): p. 1542-9.
135. Anisimov, V.N., et al., *Rapamycin extends maximal lifespan in cancer-prone mice.* Am J Pathol, 2010. **176**(5): p. 2092-7.
136. Popovich, I.G., et al., *Lifespan extension and cancer prevention in HER-2/neu transgenic mice treated with low intermittent doses of rapamycin.* Cancer Biol Ther, 2014. **15**(5): p. 586-92.
137. Tandon, M., Z. Chen, and J. Pratap, *Runx2 activates PI3K/Akt signaling via mTORC2 regulation in invasive breast cancer cells.* Breast Cancer Res, 2014. **16**(1): p. R16.
138. Johnson, E., et al., *HER2/ErbB2-induced breast cancer cell migration and invasion require p120 catenin activation of Rac1 and Cdc42.* J Biol Chem, 2010. **285**(38): p. 29491-501.
139. Lin, M.C., et al., *Identification of mTORC2 as a Necessary Component of HRG/ErbB2-Dependent Cellular Transformation.* Mol Cancer Res, 2014. **12**(6): p. 940-52.
140. Garcia-Garcia, C., et al., *Dual mTORC1/2 and HER2 blockade results in antitumor activity in preclinical models of breast cancer resistant to anti-HER2 therapy.* Clin Cancer Res, 2012. **18**(9): p. 2603-12.
141. Richert, M.M., et al., *An atlas of mouse mammary gland development.* J Mammary Gland Biol Neoplasia, 2000. **5**(2): p. 227-41.
142. Haiyan, L., *Targeting of mTORC2 prevents cell migration and promotes apoptosis in breast cancer.* Breast Cancer Research Treatment, 2012.
143. Masui, K., et al., *mTOR complex 2 controls glycolytic metabolism in glioblastoma through FoxO acetylation and upregulation of c-Myc.* Cell Metab, 2013. **18**(5): p. 726-39.
144. Li, S., et al., *Inhibition of mTOR complex 2 induces GSK3/FBXW7-dependent degradation of sterol regulatory element-binding protein 1 (SREBP1) and suppresses lipogenesis in cancer cells.* Oncogene, 2015.
145. Rodrik-Outmezguine, V.S., et al., *mTOR kinase inhibition causes feedback-dependent biphasic regulation of AKT signaling.* Cancer Discov, 2011. **1**(3): p. 248-59.
146. Khanna, N., et al., *XPLN is an endogenous inhibitor of mTORC2.* Proc Natl Acad Sci U S A, 2013. **110**(40): p. 15979-84.